Investigation on Role of Fillers on Viscoelastic properties of Tire Tread Compounds

A thesis submitted
to
The Maharaja Sayajirao University of Baroda
for the award of the degree

Doctor of Philosophy
in
Chemical Engineering

By
Sarat Ghosh

Guided by
Prof. R. Sengupta

Chemical Engineering Department
Faculty of Technology & Engineering
The Maharaja Sayajirao University of Baroda
Vadodara - 390 001.
October 2011

CERTIFICATE

This is to certify that this thesis entitled "Investigation on role of fillers on viscoelastic properties of tire tread compounds" submitted by Mr. Sarat Ghosh in fulfillment of the requirements of the degree of Doctor of Philosophy in Chemical Engineering is a bonafide record of the investigations carried out by him in the Department of Chemical Engineering, The Maharaja Sayajirao University of Baroda under my supervision and guidance. In my opinion this thesis has attained the standard fulfilling the requirements of the Ph.D. degree as prescribed in the regulations of the university.

R.SENGUPTA
Professor,
Department of Chemical Engineering,
The M.S. University of Baroda,
Vadodara.
(Guiding Teacher)

Head,
Department of Chemical Engineering,
Faculty of Technology & Engineering,
The M.S. University of Baroda,
Vadodara.

Dean,
Faculty of Technology & Engineering,
The M.S. University of Baroda,
Vadodara.

This thesis is dedicated to my late parents

ACKNOWLEDGEMENT

I offer my heartfelt gratitude and deep sense of obligation to my research guide, **Prof. Ranjan Sengupta**, Head of the department, Chemical Engineering, Faculty of Technology & Engineering, The M.S. University of Baroda. I extend my heartiest thanks to **Dr. Bina Sengupta** for her constant support during the whole period of research work.

My sincere thanks to the management of **Apollo Tyres Limited, India** who has not only given permission to carry out my research work but also allowed me to fully utilise research facility at Apollo Tyres R&D Centre; provided all necessary raw materials and full support to complete my research work.

My work would have been uncompleted without offering thanks to **Mr.P.K.Mohamed**, Chief Advisor, Research & Development, Apollo Tyres Ltd. for his constant encouragement, support and guidance to carry out this research work. I have received his blessing at all the time during the tenure of research work.

I offer my sincere thanks to **Mr**. **Peter Becker,** Chief (Research & Development) of Apollo Tyres Ltd. for his support and encouragement for this research work.

I would like to thank **Prof. (Dr.) Michael Kaliske**, Director, Institute of Structural Analysis, Technical University Dresden, Germany and **Bastin Naiser**, Research scholar, Leipzig University, Germany for their assistance to establish internal programme to predict tire rolling resistance.

I extend my heartiest thanks to **Prof. (Dr.) Gert Heinrich,** Director of Leibniz-Institut für Polymerforschung Dresden, Dresden, Germany for his great assistance in my research work.

I like to remember and thanks to **Prof. Dhanesh Patel**, Applied Mathematics Department, The M.S.University of Baroda who has inspired to start research work.

It my pleasure to extend my thanks to my colleagues **S.K.P. Amarnath**, **J.P.Rath, P.Shankarganesh** and **Bharat Makwana** who have really extended their whole hearted support to me to complete my research work.

My sincere thanks to **Dr. Amit Das** of Leibniz-Institut für Polymerforschung Dresden e.V.for his support in getting the TEM pictures and technical literature whenever required. I would like to extend my sincere thanks to **Dr. Santanu Chattopadhya**, Associate professor, Indian Institute of Technology, Kharagpur for his help to do the XRD study.

I would like to thanks **Dr. Samar Bandopadhya,** Head (R&D), Pedilite Industries Ltd. for his help for carrying out compound mixing.

I would like to acknowledge the help received from Rubber Technology Centre IIT, Kharagpur; Department of Polymer Science & Technology, Calcutta University; Leipzgig University, Germany and Leibniz-Institut für Polymerforschung Dresden, Germany;

I would like to thanks all the Professors, Assistant Professors, Lecturers of Chemical Engineering Department, The M.S.University of Baroda for their whole hearted support during the tenure of my research work.

My sincere thanks to my family members **Ratan Chandra Saha**, **Amrita Saha**, **Payal Saha** and **Arpita Saha** who have constantly supported me to complete my research.

Finally, I would like to thanks my wife **Sumitra** for her unforgettable sacrifice & constant support and my son **Arnab** for his help in computer work and my daughter **Aditi** for her pure love & naughtiness to overcome strain and get relaxation.

SARAT GHOSH

CONTENTS

LIST OF TABLES

LIST OF FIGURES

LIST OF SYMBOLS

Symbols	Explanation
ω	Angular velocity
γ	Camber angle of tire with respect to its axis
θ_l	Contact angle between solid and liquid
Ψ^{diss}	Dissipated energy in one full rotation
ξ	Factor in temperature equation (6.4)
λ	Principle stretch used in Material model
δ	Phase lag between stress and strain in dynamic properties
σ	Stress
ε	Strain
Ψ	Strain (elastic) energy in Tire simulation
α	Slip angle of tire with respect to its axis
γ_l	Surface energy of liquid
γ_s	Surface energy of solid
γ_F	Surface energy of filler
γ_P	Surface energy of polymer
φ	Volume fraction of the filler

LIST OF ABBREVIATIONS

Abbreviation	Explanation
M_Z	Aligning torque
BIRC	Brazil, India, Russia and China
BE	Breaking energy
TESPT	Bis(triethoxysilylpropyl)-tetrasulfan (TESPT)
CAD	Computer aided design software
CAE	Computer aided engineering software
Tc50	Cure time (50%) in rheometer
Tc90	Cure time (90%) - optimum cure time
CB	Carbon Black
F_G	Contact force
XNBR	Carboxylated nitrile rubber
F_D	Driving force
EB	Elongation at break
ESBR	Emulsion styrene butadiene rubber
FSSBR	Functionalized solution styrene butadiene rubber
FEA	Finite element analysis
ΔG_i	Free Energy
T_g	Glass transition temperature of rubber
H_t	Heat development rate
P_{in}	Input power
F_y	Lateral force
E''	Loss modulus
J''	Loss compliance
MES	Mild extract solvent

M100	Modulus at 100% strain
M200	Modulus at 200% strain
M300	Modulus at 300% strain
ML	Min. rheometric torque
MH	Max. rheometric torque
MMT	Montmorillonite clay
G	Modulus of the filled system
Go	Modulus of unfilled system
F_Z	Normal force
NR	Natural rubber
P_{out}	Out put power
M_X	Overturning moment
OLS	Organic layer silicate
BR	Polybutadiene rubber
PCR	Passenger car Radial
P_R	Power Loss
RAE	Residual aromatic extract
RR	Rolling Resistance
F_{RR}	Rolling resistance force
C_R	Rolling resistance coefficient
M_X	Rolling resistance moment
Ts2	Scorch time (process safety) in rheometer
W	Strain energy function
I	Strain Invariant
SBR	Styrene butadiene rubber
SSBR	Solution styrene butadiene rubber
G'_o	Shear Modulus at very low strain

E’	Storage modulus
G'_{∞}	Shear Modulus at very high strain
V	Speed
TBR	Truck Bus Radial
TEM	Transmission Electron Microscopy
F_x	Tractive force
TDAE	Triple distillate aromatic extract
TS	Tensile strength
Tan δ	Tangent delta [Loss Modulus (E’’)/Storage Modulus (E’)]
R	Universal Gas Constant
WXRD	Wide angle X-ray diffraction
W_a	Work of adhesion
X	X -axis
XRD	X-ray diffraction
Y	Y-axis
Z	Z-axis

CHAPTER 1

INTRODUCTION

1.1 GENERAL INTRODUCTION

Transportation system is the backbone of modern civilization. From animal drawn carts to airplane, wheel is the key component. In the modern era, we can not imagine wheel without tire. Hence role of tire for road as well as air transport is very important. Ever since it was invented by John Boyd Dunlop in 1888, pneumatic tires have gained immense importance in modern civilization. A modern pneumatic radial tire is made up with composite materials where besides rubber that is the main constituent, fabric and steel are also used. The use of rubber in tires is because of its unique viscoelastic characteristics due to which it can not only absorb substantial amount of energy but also provide cushioning effect. The major limitation of rubber is that it cannot be used alone; several other chemicals and pigments need to be added to make it useful. Rubber has to be cross-linked with sulphur and accelerators to get elasticity and dimensional stability. The organic and/or inorganic materials called fillers are added to reinforce rubber for the improvement of its mechanical properties. Antioxidants and antiozonenants are added to protect rubber from oxidative and thermo-mechanical degradation.

Fillers are among the most important ingredients used in rubber compound formulation. Carbon black continues to be the most important reinforcing filler in the rubber industry followed by silica. About 5 million metric tons of carbon black is globally consumed each year while ~250,000 tons of the different silica grades are used each year. Incorporation of fillers improves mechanical and fracture properties of rubber; but at the same time it influences the hysteresis loss. The major reason of hysteresis loss in rubber is due to filler-filler interaction that is influenced by the nature of filler, its quantity and the polymeric material used.

Rolling resistance is the force acting in the opposite direction to the driving force and to over come this, a good amount of fuel is burnt. The energy consumed by the tire is converted into heat. ***Glaeser (2005) of Federal Highway Research Institute, Germany*** reports that at a constant speed of 100 km/h a passenger car needs ~50% of its fuel to overcome rolling

resistance and the rest of the fuel is used to overcome air drag and in all driving conditions an average of 25% of the fuel consumption of a passenger car is due to rolling resistance (75% air drag and acceleration). He also reported that at a constant speed of 80 km/h a truck needs ~40% of its fuel to overcome rolling resistance. Energy efficient tires having 20% less rolling resistance in comparison to conventional tires reduces the fuel consumption of a car by ~5%. Improvement of 10 % rolling resistance will lead to ≈ 2 g/km less CO_2 emission.

Tire rolling resistance is greatly influenced by viscoelastic behaviour (hysteresis loss) of rubber. Approximate 90% of tire rolling loss may be attributed to hysteresis loss of rubber components. The different rubber components in a tire have their own contribution for tire rolling resistance; tread rubber alone is responsible for 39% of total tire rolling resistance (Willet 1973, 1974). In the past 20 years considerable attention has been paid to reduction of tire rolling resistance in order to reduce fuel consumption and environmental pollution, but lower rolling resistance with higher traction and better abrasion resistance are contradictory requirements from a single tire tread compound for passenger car tire.

The development of silica/silane and solution styrene butadiene rubber based passenger car tread provided a balanced approach to reduce of rolling resistance without sacrificing traction and tread wear. By using this technology tire industry has been able to cut down rolling resistance by almost 20% (Bridgestone 2002) without sacrificing traction.

Tire hysteresis loss is primary reason for tire rolling resistance which is greatly influenced by nature and volume of filler present in the compound. Carbon black has been the main filler since 1905 and only recently in the past two decades it has been partially substituted by silica. Investigation of reinforcing mechanism, filler-filler interaction and filler-polymer interactions of different fillers such as carbon black, silica and/or nanoclay are the key to understanding the role of fillers on viscoelastic properties of rubber for the reduction of tire rolling resistance.

New generation fillers like organoclay; (organic layer silicate-OLS) is gaining potential to substitute conventional fillers because of its extremely high reinforcing capability. A small quantity of nanoclay due to its very high surface area offers reinforcement similar to that by 40-50 phr of conventional fillers like carbon black and silica. As the total amount of filler is much lower in case of nanocomposite, there is a possibility of reduction of hysteresis losses. Therefore, nanocomposite based tread compounds are likely to be future candidates for low

rolling resistance tires. Modified nanoclay are very interesting and potential materials for rubber reinforcement because a very small quantity (3-4 %) gives very good mechanical properties and lowers hysteresis losses too if it is well dispersed in rubber. The exfoliation of organic layer silicate (organoclay) in rubber matrix is a difficult task and reinforcement depends on the extent of intercalation and exfoliation of clay in the rubber matrix, hence success of clay is largely depends on its dispersion.

Increased vehicle population world wide especially in the emerging economics like Brazil, Russia, India and China, (BRIC) has increased fuel consumption and creating more pollutant and hence demands a renewed focus to the tire rolling resistance. Scientists and engineers are continuously working with materials and design to bring down tire rolling resistance.

The hysteresis loss of rubber can be measured by dynamic mechanical analysis in the laboratory, but measurement of its effect on tire during developmental stage is a big challenge. Finite element (FE) simulation technique is being used to predict the rolling resistance of tire in the design stage, but there are limitations too, all simulation methods use linear viscoelastic model of rubber but in reality rubber exhibits non linear viscoelastic behaviour therefore the real challenge is the non-linear viscoelastic analysis of rubber to predict the tire rolling resistance with greater precision. Hence there is scope to study the role of fillers especially organoclay on the viscoelastic properties of rubber for the reduction of hysteresis losses i.e. rolling resistance of tire and develop a suitable simulation technique to study the rolling resistance of nanocomposite based tire tread in the design stage itself.

1.2 RESEARCH OBJECTIVE

The primary objective of this study was to develop low rolling resistance passenger car radial (PCR) and truck bus radial (TBR) tire tread compounds based on nanocomposites so as to improve the fuel efficiency and reduce carbon emission. To achieve the said objective, understanding the influence of various fillers especially organoclay and combination of organoclay and conventional fillers on rubber viscoelastic properties (hysteresis properties) is of utmost importance. The properties of nanocomposites largely depend on intercalation and exfoliation of organoclay in the rubber matrix. The investigation on the influence of compatibilizer and different mixing techniques on the clay dispersion was another important aspect of this study.

The final objective was to predict the tire rolling resistance using nanocomposite based tread compounds and compare with the commercially used standard tire tread compounds based on conventional fillers like carbon black (CB) and silica. Linear viscoelastic simulation of rubber using commercial finite element software requires complex material properties and is computationally expensive. To predict tire rolling resistance accurately requires non linear viscoelastic material properties and finite element software to compute the energy loss in tire. Suitable commercial software is not available that can perform non linear viscoelastic simulation; hence a software was developed to predict rolling resistance that can very well accommodate non linear viscoelastic properties of rubber.

1.3 OUTLINE OF THE THESIS

In this investigation the major focus was given into main three areas (a) preparation and characterization of styrene butadiene rubber/Polybutadiene-organoclay nanocomposites for passenger car radial tire (PCR) tread application (b) preparation and characterization of natural rubber/Polybutadiene-organoclay nanocomposites for truck bus radial (TBR) tire tread application and (c) investigations on the rolling resistance of nanocomposite based tread compounds using finite element simulation.

The thesis is presented in eight Chapters, ***Chapter 1:*** Introduction deals with the ideas presented above. ***Chapter 2:*** presents the Literature Survey and Scope of present investigation. ***Chapter 3:*** Materials and Methods describe Experimental methods, Analytical techniques and Materials. In ***Chapter 4:*** Development and characterization of SBR/BR nanocomposites for passenger car radial (PCR) tire tread application is elaborated. ***Chapter 5*** covers Preparation and characterization of NR/BR nanocomposites for truck bus radial (TBR) tire tread application. In ***Chapter 6*** Tire finite element simulation methods, development of rolling resistance software, *"RR Code"*, temperature equation and tire temperature distribution are elaborated. In ***Chapter 7*** Investigations on the rolling resistance of nanocomposite based tread compounds using FE simulation is described. The simulated results are compared with experimental data for commercial tires. ***Chapter 8*** describes summarizes the main conclusions and highlights the scope of future work.

CHAPTER 2

LITERATURE SURVEY

2.1 BACKGROUND

Tires are the most prominent rubber articles both with respect to importance as well as volume of production. Tire acts as a rubber spring that provides riding comfort, steering response, traction and braking. More than half of the natural and synthetic rubbers and 90% of the worldwide productions of carbon black are used in the tire industry.

Reduction of green house gas emission is a major challenge to all vehicle manufacturers in the world and to address this concern, they are designing their automobiles to make them more fuel efficient. Tire industries are also working on new compounds and tire design to bring down tire rolling resistance for greater fuel efficiency. A global effort is on the way to put legislations on critical tire performance related to environment and safety. European Union proposed tire labeling from 2012 where tire would be given rating based on wet traction, rolling resistance and noise.

It is well established that fillers influence the hysteresis loss in the rubber which is mainly responsible for tire rolling resistance. In the last 20 years, almost 20% reduction of rolling resistance has been achieved by introducing silica technology in passenger car tire. However, only silica technology is not sufficient to meet the present tire labeling requirement that demands 20-30% reduction in rolling resistance from the present level. New technology is the need of the day that will be able to provide such a decline of the rolling resistance (20 to 30%) without affecting wet grip and wear.

There is a continuous search for new fillers and new materials to reduce the hysteresis loss of tread rubber, which accounts for ~40% rolling loss. In this journey, scientists have identified nanoclay as potential filler for rubber reinforcement and modified the clay to make it compatible with rubber. Rubber nanocomposites showed remarkable improvement of properties like strength and elongation but is still far behind to meet the properties required for tire tread application.

This investigation is aimed to continue this search with the target of development of low rolling resistance nanocomposite based tread compounds for passenger car radial (PCR) tires as well as truck bus radial (TBR) tires. Further it was aimed to develop software for the prediction of rolling resistance of tire with nanocomposite tread using finite element simulation.

2.2 TIRE TECHNOLOGY

2.2.1 History

Sumerians invented the wheel 5000 years ago. The world's first pneumatic tire was invented by Scottish engineer, Robert William Thomson in 1845. Forty years later, in 1888 John Boyd Dunlop revived the pneumatic tire. The first commercially available pneumatic tire consisted of an inner-tube surrounded by a "cover" made up of several layers of rubber coated woven canvas-type fabric which was much thicker in the area that touches the ground this rubber mass that comes in contact with the surface is called tread. The first application of this invention was in bicycle tires (Blow 1986). The present radial tire was first developed and patented by Michelin in 1948.

2.2.2 Definition

A tire is a much more complex object than it looks. Actually a tire is many things: geometrically, it is a torus; mechanically, a flexible-membrane pressure container; structurally, a high-performance composite; and chemically, a tire consists of materials made up from long chain macromolecules (Mark 1994).

2.2.3 Functions

The functions of a tire can be considered in relation to three basic roles: (a) vehicle mobility, (b) performance and integrity, and (c) comfort. Performance, including driving and braking torque and rolling resistance, exerts or transfers forces or moments in forward direction. Vehicle mobility, including cornering, steering response, and abrasion, acts in the lateral direction, and the forces involved in comfort act vertically (Mark 1994).

To describe the characteristics of a tire and the forces and moments acting on it, it is necessary to define an axis system that serves as a reference for the definition of various parameters as shown in Fig. 2.1.

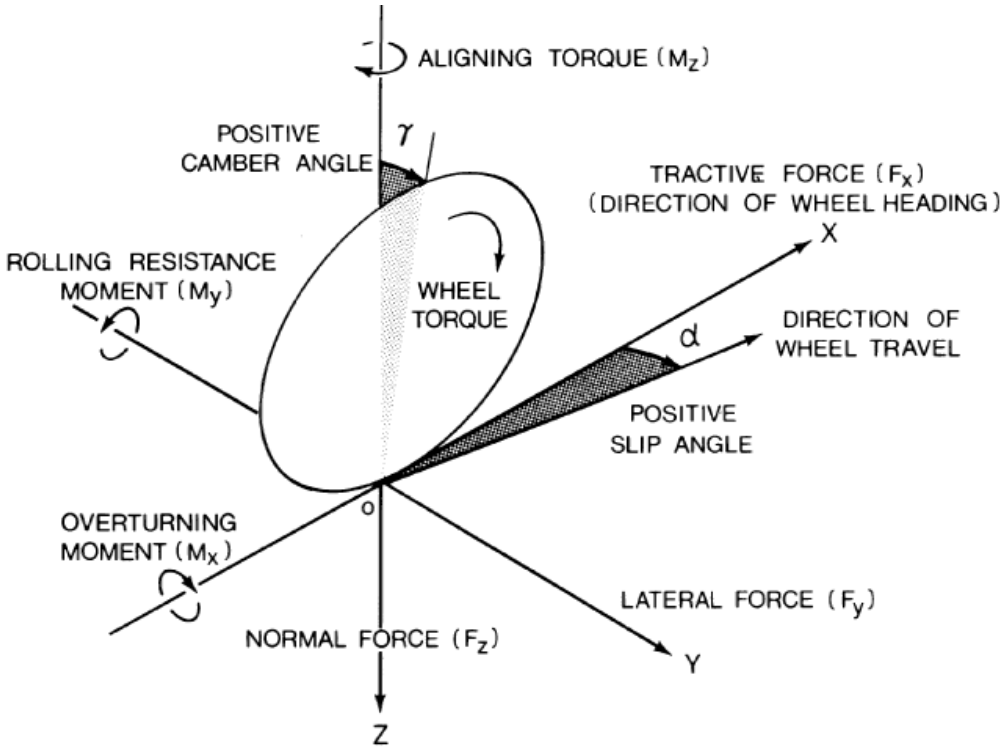

Fig. 2.1-Tire axis system and characteristics

2.2.4 Tire components

Typically a passenger car radial tire comprises of different components which includes tread, sidewall, steel belts, fabric body ply, apex, rim strip, inner liner, fabric cap ply and metal bead as shown in the Fig. 2.2. While in truck bus radial tires fabric body is replaced by steel body and additionally, shoulder cushions and belt edge filler are also included and as shown in Fig. 2.3.

Tread is the top most abrasion resistant rubber component of tire with different pattern which comes in contact with road; it forms the protective coating for the carcass. It is the most important component responsible for the main tire performance indicators like traction, breaking, handling, wear and rolling resistance.

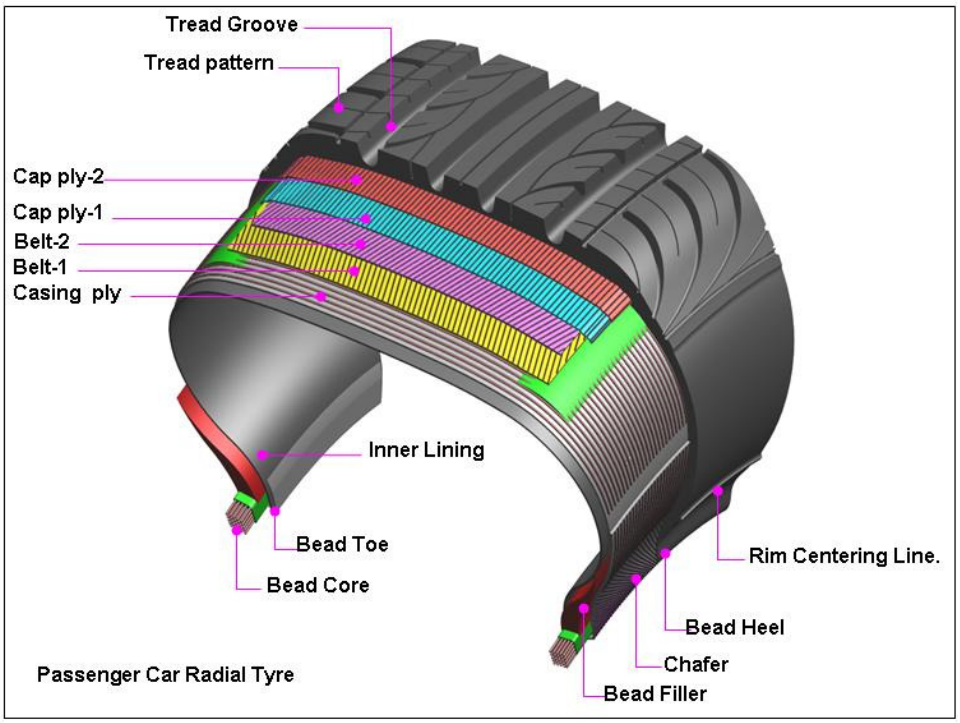

Fig. 2.2- Passenger car radial (PCR) tire construction

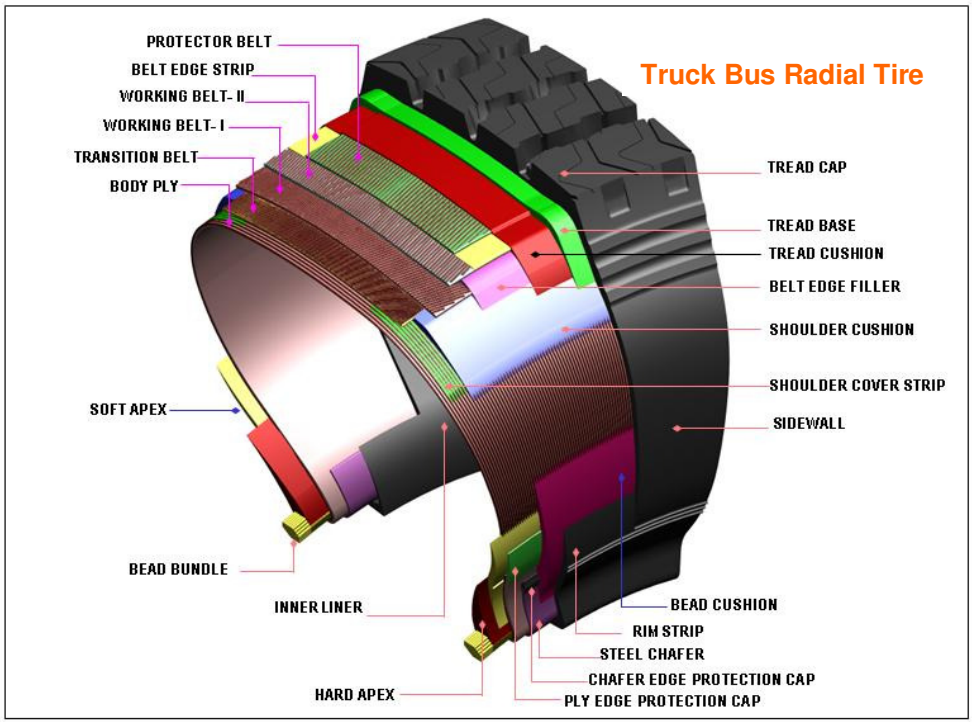

Fig. 2.3- Truck bus radial (TBR) tire construction

2.2.5 Tire nomenclature

The tire designation system is written on the tire sidewall, it is as described below. If the marking reads 205/65R15 V it implies the following

- 205 is section width in mm
- 65 is the tire aspect ration (Aspect ratio= Section height/section width)
- R represents radial construction
- 15 is nominal rim diameter in inch
- V denote speed rating of the tire

2.2.6 Application of tire

The different types of tire applications are shown below (Fig. 2.4);

Fig. 2.4- Tire applications in different areas

2.3 TIRE ROLLING RESISTANCE

Tire rolling resistance is defined as the energy consumed per unit distance of travel as a tire rolls under load. The energy consumed by the tire is converted into heat. The proper unit of rolling resistance is J/m, which equals to N, the unit of force.

Thus, the rolling resistance, F_{RR} is given by the equation:

$$\mathbf{F_{RR} = H_t/V} \text{ ……..…..} \mathbf{(2.1)}$$

Where the rate of heat development and $\mathbf{H_t}$ (≡ dH/dt) is often termed power loss P_R and V is the road speed of the tire,

$$\mathbf{F_{RR} = P_R/V = [P_{in} - P_{out}] / V} \text{ ……} \mathbf{(2.2)}$$

Where, P_{in} is the tire input power provided by the motor, and P_{out} is the tire output power supplied to traction of the car.

Rolling resistance is force acting in the opposite direction to the driving force (Fig. 2.5).

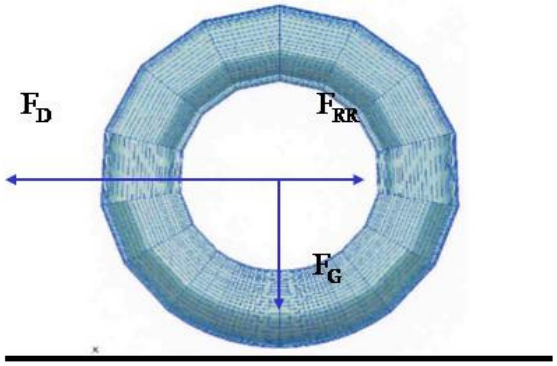

Fig. 2.5- forces acting on tires

Where; F_D - Driving force

F_G - Contact force

F_{RR} – Rolling Resistance force

The rolling resistance coefficient (C_R) of a tire is expressed by;

$$\mathbf{C_R\,[\%] = [Rolling\ Resistance\ (N) / Wheel\ Load\ (kg) \times g\ (m/s^2)]\ X\ 100} \text{ ……..} \mathbf{(2.3)}$$

2.4 TIRE TREAD

2.4.1 Performance

Tire tread is top most circumferential rubber layer with pattern that touches the ground. The characteristics of a good tire are (a) it should generate the highest possible traction force between tire and road (b) the steering characteristics should be exact and predictable under all handling situations (c) it should have the lowest possible rolling resistance and (d) give the highest possible mileage. In all these requirements the tire tread compound plays a major role viz.

a) The tire traction is determined by the friction properties of the tread compound.
b) The steering characteristics depend, apart from constructional features, on the stiffness of the tread compound, i.e. on its dynamic modulus and again on the friction properties.
c) The rolling resistance of the tire depends largely on the loss modulus of the tread compound
d) The mileage a tire depends on the abrasion resistance of the tread compound (Grosch,1996).

2.4.2 Tread compound design

The three important properties such as rolling resistance tread wear and wet grip form the so called “magic triangle” of tire properties, which means that a balance must be found between these properties. These requirements are conflicting, as it is impossible to improve all three characteristics at the same time. A compromise between these characteristics should always be achieved.

The "magic triangle of tire technology" is a principle in the tire world that says improvement to rolling resistance has to come at the expense of wet-road grip and durability (Fig. 2.6). Introduction of silica/silane technology coupled with invention of high vinyl solution styrene butadiene rubber (SSBR), made it possible to enhance the magic triangle thereby reducing the rolling resistance without sacrificing grip and wear. This technology was used to develop the “GREEN TIRE” i.e. energy efficient tire.

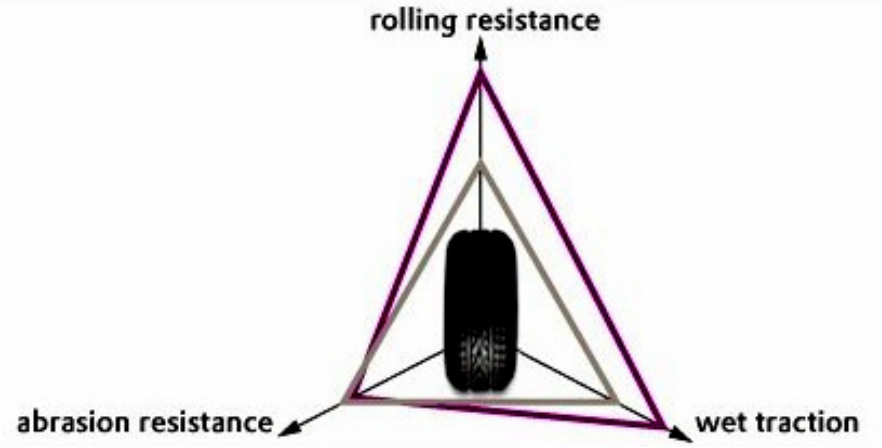

Fig. 2.6- Magic triangle of PCR tread compound

[Tire Technology 2008, Rhodia]

2.4.3 Requirements

The contributions of different tire components on rolling resistance of a passenger car are shown in Fig. 2.7. The contribution of tread rubber on rolling resistance is the highest and accounts for 39% of the total losses in PCR tire. While in TBR tires the tread alone accounts for 40% of the losses as shown Fig. 2.8.

A major problem facing tire designers has traditionally been to achieve a compromise between low rolling resistance, high wet grip and high wear resistance in passenger car tire. The lower is the rolling resistance; the less fuel is required to propel the vehicle forward. Lowering the rolling resistance, however, commonly results in a reduction in wet grip performance, which of course is unacceptable (Freund, 1998; Brinke, 2002).

A major step in solving this problem can be achieved by the replacement of (part or all) carbon black by silica in the tire's tread compound. This has enabled manufacturers to produce tires which provide improved wet grip properties, better winter performance and lower rolling resistance all at the same time (Freund, 1998; Brinke, 2002). Therefore silica based tread is considered to be a revolutionary in tire technology.

Grip is best served by rubber compounds, which absorb high levels of energy. Rolling resistance, on the other hand, is affected by low frequency distortion – the deflection of the tire

as it revolves, low rolling resistance requires compounds that absorb low quantities of energy. With the addition of silica, it was possible to produce compounds, which provide higher hysteresis at high frequencies (higher traction) as well as lower hysteresis at low frequencies (lower RR) than what was achievable with carbon black (Meneghetti, 2005).

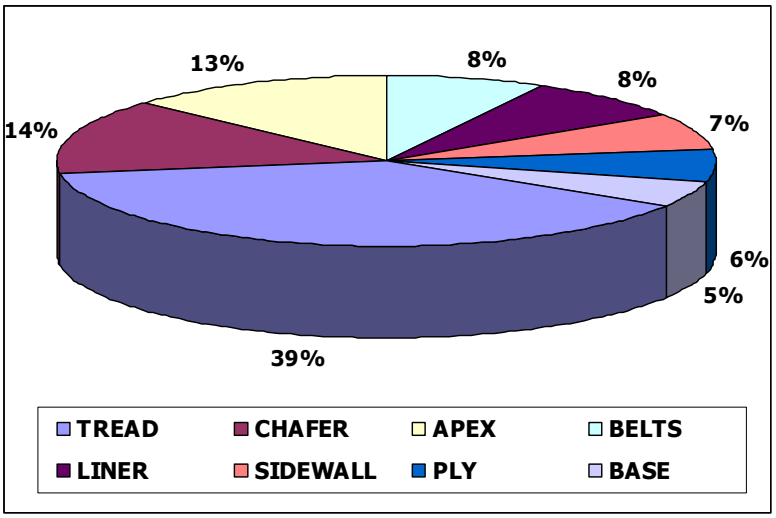

Fig. 2.7- Contribution of tire components towards rolling resistance in PCR tire

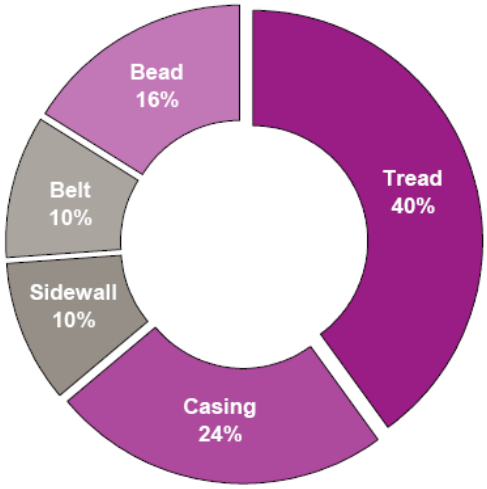

Fig. 2.8- Contribution of tire components towards rolling resistance in TBR tire

The increased concern of protecting the environment gives rise to a demand for tires which can combine a long service life, driving safety and low fuel consumption. World wide vehicle manufacturers and tire industries are working on to reduce rolling resistance to increase fuel efficiency of vehicle and reduce green house gas emission. European Union (EU) has made

legislation on tire labeling implementable by 2012 where tire will be rated based on tire rolling resistance, wet traction and noise (Fig. 2.9 to 2.11)

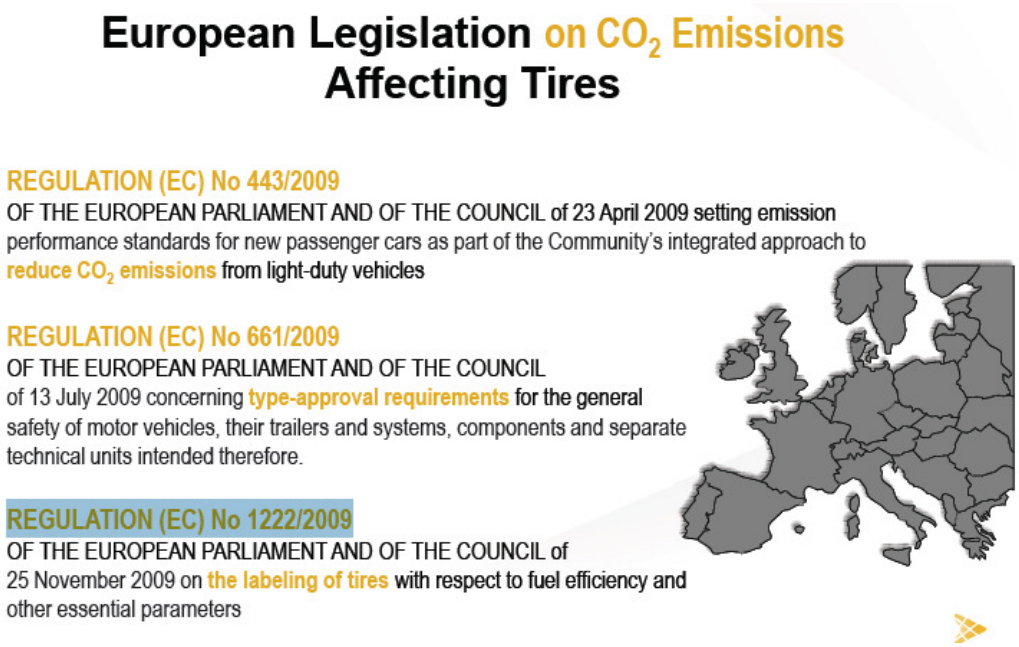

Fig. 2.9- EU legislation on tire labeling

[4th Dresden Tire Workshop (2011) on Green Tire Materials-Dr. Seven Thiele]

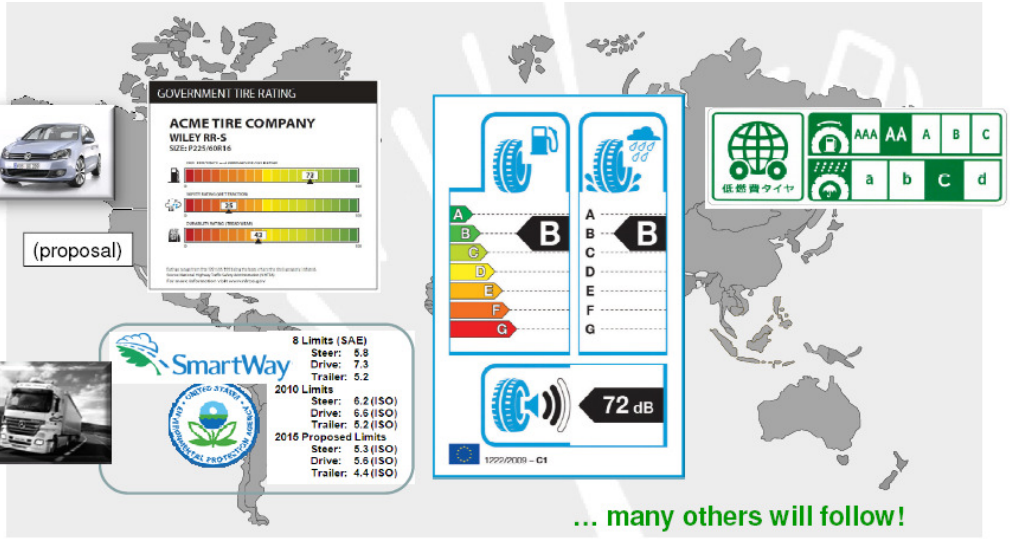

Fig. 2.10- The world wide tire labeling

[4th Dresden Tire Workshop (2011) on Green Tire Materials-Dr. Holger Lange]

Rolling Resistance Coefficient

単位(N/kN)

転がり抵抗係数 (RRC) ISO28580	等級 Grade	EU Classifi -cation
RRC≦6.5	AAA	A
6.6≦RRC≦7.7	AA	B
7.8≦RRC≦9.0	A	C
9.1≦RRC≦10.5	B	E
10.6≦RRC≦12.0	C	F

Fig. 2.11- EU classification for PCR tire rolling resistance

2.4.4 Tread compound formulations

The general raw materials used in a tire tread compound formulations are Rubber (Natural Rubber; Emulsion and Solution Styrene Butadiene rubber; Polybutadiene rubber), fillers (carbon black and silica), petroleum oils (TDAE, RAE, MES and Naphthenic), sulpfur, accelerator (Sulphenamide; thiuram; guanidine), accelerator activator (zinc oxide and stearic acid), antidegradants (diphenyl diamines; substituted phenols), wax, resins and zinc salt of fatty acids as process aids.

The rubbers used in a typical passenger car radial (PCR) tire tread compound are emulsion SBR / solution SBR blended with BR. Filler used are silica, carbon black and silica and carbon black combination with higher dosages of process oil (10 – 15%).

In truck bus tire (TBR) tread, blend of Natural rubber and Polybutadiene rubber is widely used. The main filler for TBR tread is highly reinforcing carbon black and generally no process oil is used.

2.5 FILLERS AND REINFORCEMENT

2.5.1 Reinforcement

The reinforcement improves the critical properties of rubber compounds like hardness, modulus, tensile strength, elongation, tear strength and abrasion resistance. Carbon black and silica are mainly used as reinforcing filler in tire tread compounds. The reinforcing effect depends on several parameters such as filler particle size and its structure, surface energy and morphology; and volume fraction of filler. Lower filler-filler interaction and better filler-rubber interaction are desirable for lower hysteresis loss in rubber compounds.

The filler-filler interaction was first measured by Payne and is termed as Payne's effect. The Payne effect is the drop of the shear modulus (G') with increasing strain amplitude. It corresponds to a gel-sol transition of the filler network at moderate strain and a breakdown of remaining sub-clusters at large strain. The dependence of the shear modulus (G') on strain for a reinforced rubber vulcanizate is shown in Fig. 2.12. The Shear modulus (G') of a filled rubber compound is built-up of the following:

i. A strain-independent contribution of the rubber network, which is the result of the proportionality of the G'-modulus to νRT, where ν is the number of moles of elastically effective network chains per unit volume (cross-link density).

ii. A strain-independent hydrodynamic effect of the filler, which was first derived by Albert Einstein and later exemplified for rubber by Guth and Gold (1938) and Smallwood (1944) and presented in Equ.2.4.

$$G = G_o (1 + 2.5\varphi + 14.1\varphi^2) \quad \text{..... (2.4)}$$

Where, G and Go are the moduli of the filled and unfilled system respectively and φ is the volume fraction of the filler

iii. A strain-independent effect due to chemical/physical rubber to filler interactions

iv. A strain-dependent contribution of the filler (Payne 1965, 1971)

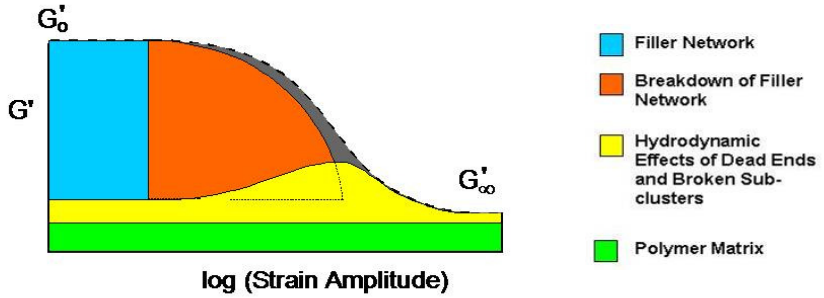

[Gert Henrich, IRC 2010]

Fig. 2.12- Payne's effect: the shear modulus (G) as a function of strain for a reinforced rubber compound

2.5.2 Characterization of rubber filler systems- surface, inter phase and interface.

In elastomeric nano-composite, interfacial interactions between filler particles and polymer matrix affect the following parameters;

- dispersibility of the nano-fillers in the polymer
- adhesion properties of fillers and polymer and
- Flocculation (re-agglomeration) of fillers in polymer matrix.

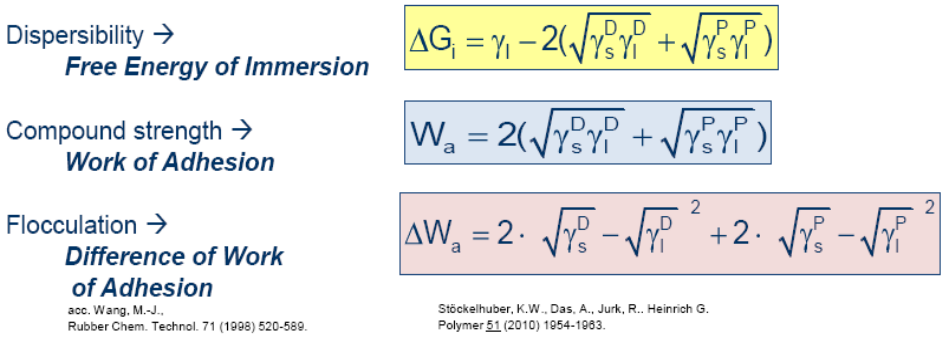

Fig. 2.13- Calculation of free energy, work of adhesion and filler flocculation

These interfacial interactions primarily depend on surface energies and polarities of filler and polymer. From the surface energetic values, the thermodynamic predictors for dispersibility, filler-polymer adhesion and filler flocculation can be derived by the equations shown in Fig. 2.13. The dispersibility of fillers in polymers matrix depends on free energy of immersion

of fillers as well as rubbers. Free energy of immersion (ΔG_i) for rubber / filler combination can be calculated by the following equation;

$$\Delta G_i = \gamma_l - 2\left(\sqrt{\gamma_s^D \gamma_l^D} + \sqrt{\gamma_s^P \gamma_l^P}\right)$$

With knowledge of the dispersive and polar components of surface energy of both

of filler (γ_s^D, γ_s^P), and

of rubber (γ_l^D, γ_l^P)

predictions of dispersibility are possible

Calculation of surface energy by fitting equations of a set of contact angle measurements of test liquids with different surface tension and polarity are shown in Fig. 2.14;

$$\cos\theta_l = -1 + \frac{2\sqrt{\gamma_s^d \gamma_l^d}}{\gamma_l} + \frac{2\sqrt{\gamma_s^p \gamma_l^p}}{\gamma_l}$$

measured data — data from literature — fit: surface energy of solid (dispersive and polar part)

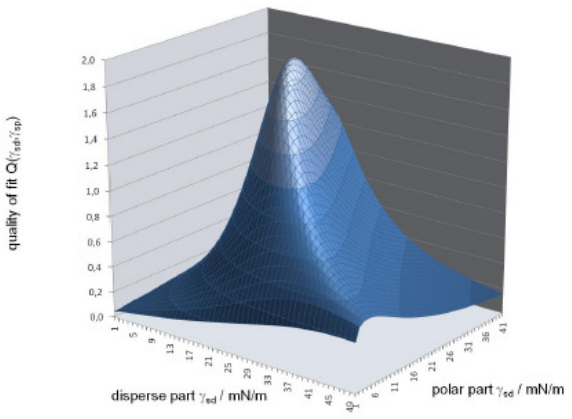

Fowkes F.M., J Phys Chem 67 (1963) 2538:

$$Q(\gamma_s^d, \gamma_s^p) = \frac{1}{\sum_{i=1}^{n} (\cos\theta_i(\gamma_s^d, \gamma_s^p)_{calculated} - \cos\theta_{i,measured})^2}$$

J.H. Clint, A.C. Wicks, Int. J. Adhesion & Adhesives 21 (2001) 267.

Fig. 2.14- Calculation of surface energy

Surface energy of different fillers and polymers are presented in Fig. 2.15 and 2.16 respectively.

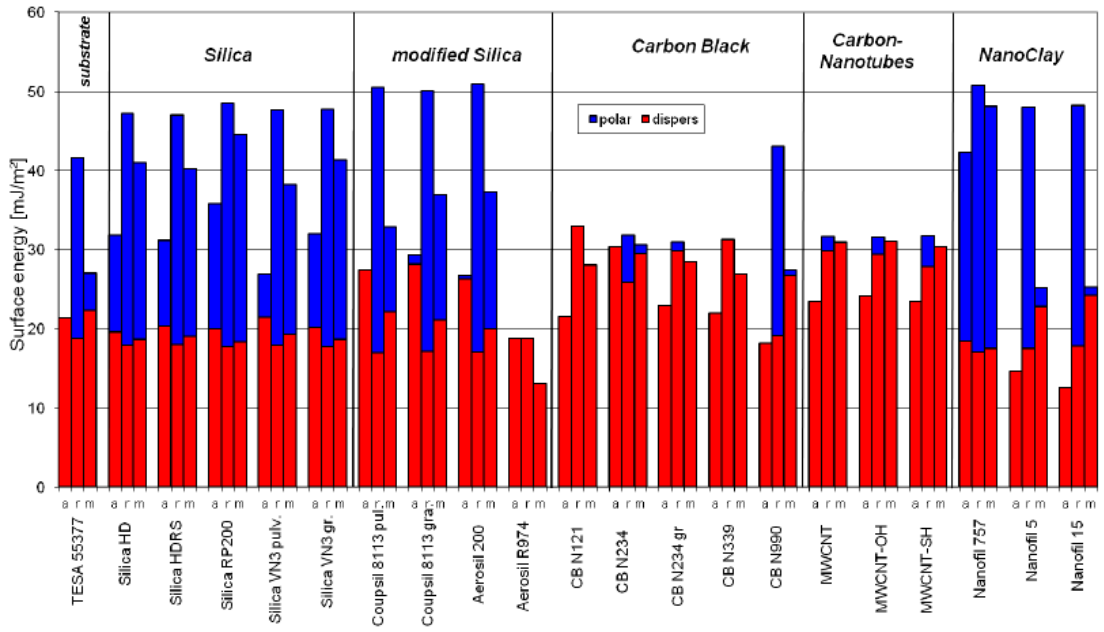

Fig. 2.15- Surface energy of fillers

[Stockhelhuber, K.W.,Das, A., Jurk, R., Heinrich, G. Polymer 51 (2010)]

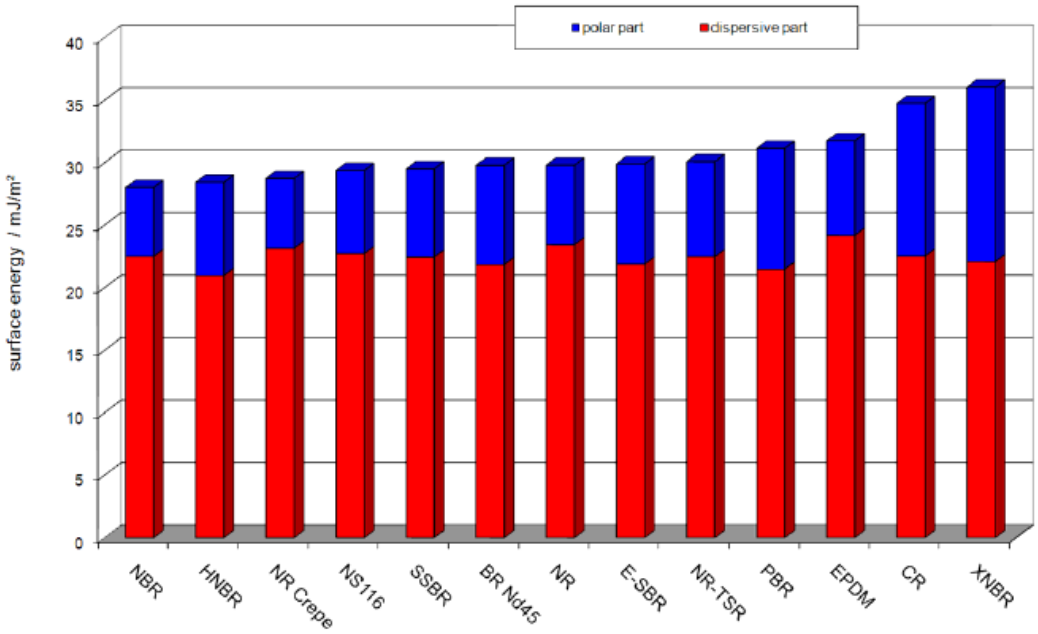

Fig. 2.16- Surface energy of rubbers

[Stockhelhuber, K.W.,Das, A., Jurk, R., Heinrich, G. Polymer 51 (2010)]

Free energy of immersion (ΔG_i) of different fillers polymers are shown in Fig. 2.17.

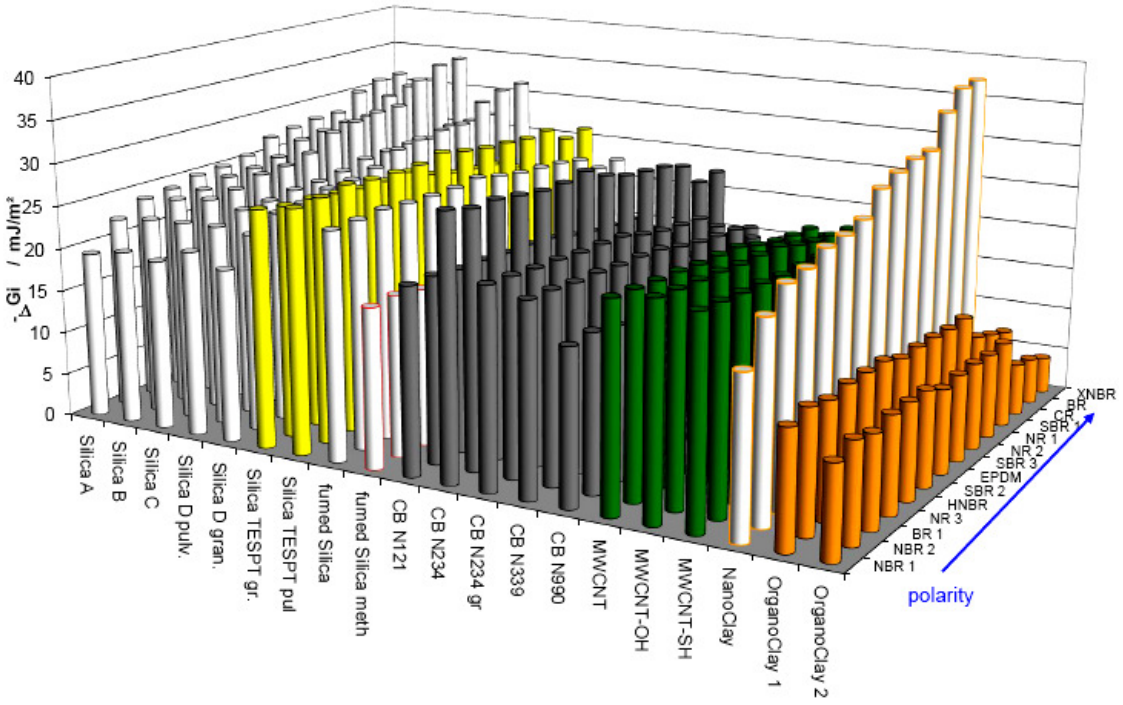

Fig. 2.17- Free energy of immersion of rubbers and fillers

[Stockhelhuber, K.W.,Das, A., Jurk, R., Heinrich, G. Polymer 51 (2010)]

The work of adhesion as calculated by Fowkes (1962) based on thermodynamic approach is shown in Fig. 2.18.

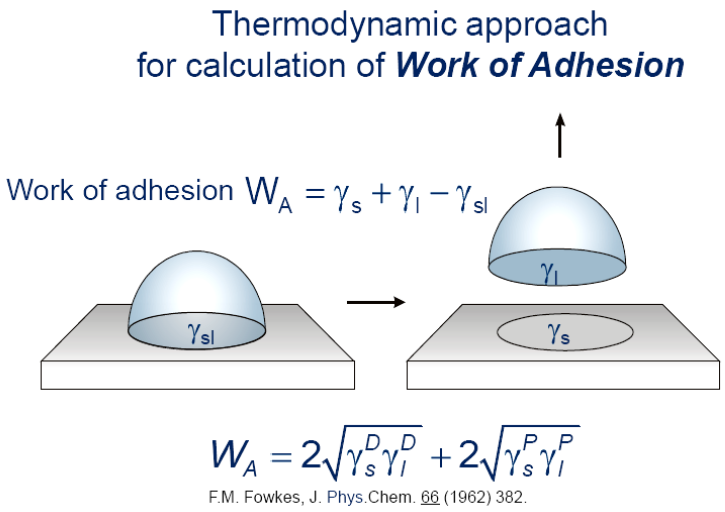

Fig. 2.18- Calculation of work of adhesion

Thermodynamics of filler flocculation is shown in Fig.2.19.

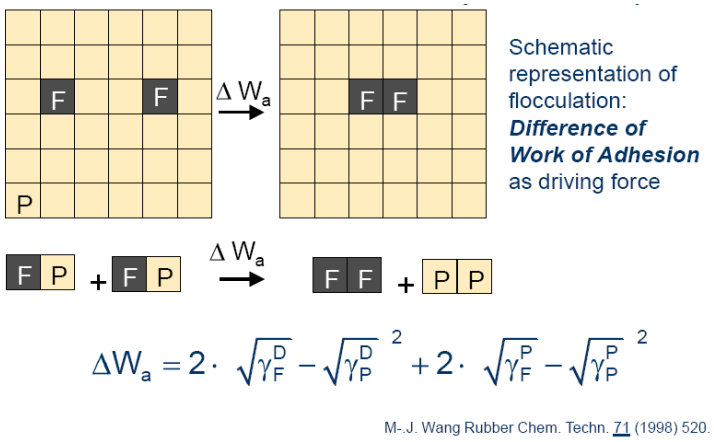

Fig. 2.19- Calculation of filler flocculation

2.5.3 Carbon black filler

Carbon black is the most important filler obtained till date for reinforcing rubber. Application of carbon black results in an increase in strength properties, wear resistance and fatigue resistance. In addition, due to its colour it is an excellent absorber of light. It therefore absorbs most of the ultraviolet components of sunlight, which can otherwise initiate oxidative degradation of the rubber. Carbon black is produced by thermal cracking of petroleum oil called carbon black feed stock. Carbon black is classified based on particle size and structure. Carbon black particle have diameter in nm range but they remain as aggregates state primary structure. Carbon black structure; SEM picture of carbon black; carbon black structures in filled rubbers on different length scales and nano structure surface carbon black are shown in Fig. 2.20 to 2.23 respectively.

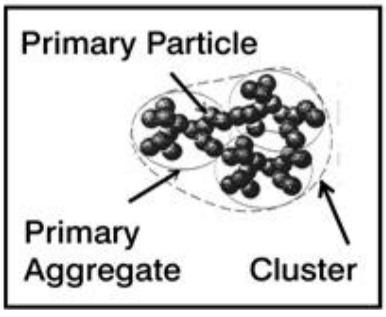

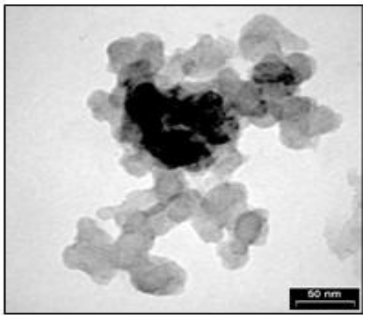

Fig. 2.20- Carbon black structure

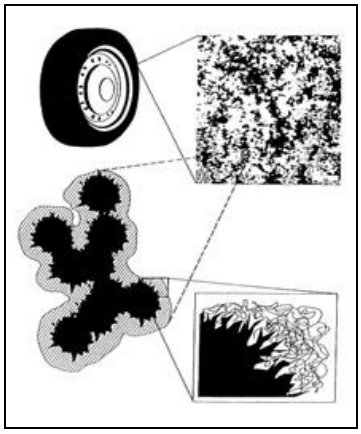

Fig.2.21- SEM image of carbon black

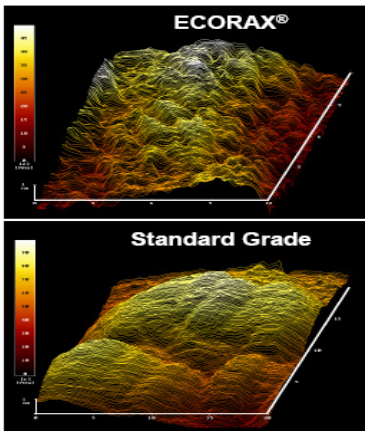

Fig. 2.22- Structures in filled rubbers on different length

Fig.2.23- ECOREX, Nano structures CB and standard CB
(Evonic Industries)

Carbon black was introduced as a reinforcing agent in rubber in year 1904 and since then it is being used as main reinforcing filler for rubber and tire compounds. Reinforcing fillers such as carbon black and silica are added to rubber compounds to improve their mechanical and dynamical properties required for the different diversified applications.

The reinforcement is governed by hydrodynamic effects and physical/chemical interactions of the filler surface with rubber matrix (Payne 1965; Donnet 1993). The reinforcing effect depends on several parameters such as filler particle size and their structure, surface energy, morphology and volume fraction of filler. However, filler-filler interaction also plays major role in rubber hysteresis behavior (Fro¨hlich, 2005). It is well established that lower filler-filler interaction leads to lower hysteresis loss of the compounds (Wang,1998).

2.5.4 Silica fillers

Silica occurs commonly in nature as sandstone, silica sand or quartzite. It is the starting material for the production of silicate glasses and ceramics. Silica is one of the most abundant oxide materials in the earth's crust. It can exist in an amorphous form (vitreous silica) or in a variety of crystalline forms. Often it will occur as a non-crystalline oxidation product on the surface of

silicon or silicon compounds. Silica is inorganic filler and widely used as reinforcing filler in rubber compounds.

The reinforcing effect of silica is related to its morphology. The morphology study of silica shows that it consists of three characteristic structures, namely primary particles, aggregates and agglomerates. A primary particle has cross-sectional dimensions of 5 – 100 nm. Aggregates of multiple primary particles are formed by chemical and physical-chemical interactions which has dimensions about 100 – 500 nm. The aggregate can be quantified by the size of the primary particles as expressed in their specific surface area, the number of primary particles and their geometrical arrangement in the aggregate. The term "structure" encompasses all these three parameters to give a general measure of the aggregate. The aggregates are then condensed into agglomerates by Van der Waals forces. Typical dimensions of agglomerates are in the order of magnitude of 1 – 40 μm. Silica agglomerates are disintegrated during rubber mixing, more or less to the size of aggregates or even primary particles. Thus precipitated silica has 0.02 micron in average particle size and an average surface area of 150-175 square meters per gram.

Silica aggregates are comparable to those of carbon blacks, but have a larger structure. This structure accounts for the greater reinforcing power relative to carbon black. Because of its high specific component of surface energy, silica has a strong tendency to agglomerate, and is difficult to disperse in rubber and rapidly re-agglomerates after mixing. Most often silica is used along with silane coupling agents when more than 5% silica is present in the rubber compound. Development of silane, bis (triethoxysilylpropyl)-tetrasulfan (TESPT), and based coupling agents changed the chemistry of silica reinforcement. The hydroxyl groups present in the silica surface react with silane coupling agent and form chemical bonds between silica and silane and this takes place during silica mixing process, thereafter, it forms bond with rubber during vulcanization. Silane acts as a chemical bridge between inorganic silica filler and organic rubber (Fig. 2.24). Silica filler particles form strong filler network because of hydrogen bonding of surface hydroxyl groups, thus giving rise to high filler-filler interaction. Higher filler-filler interaction results in higher hysteresis loss in the rubber.

Silane reacts with surface hydroxyl group of silica and results in substantial reduction in the filler-filler interaction. Silica filler along with silane when mixed in the rubber matrix under specific conditions offers high reinforcement with lower hysteresis loss. It is well established that lower filler-filler interaction leads to lower hysteresis loss of the compounds (Huber, 1999; Schon, 2003).

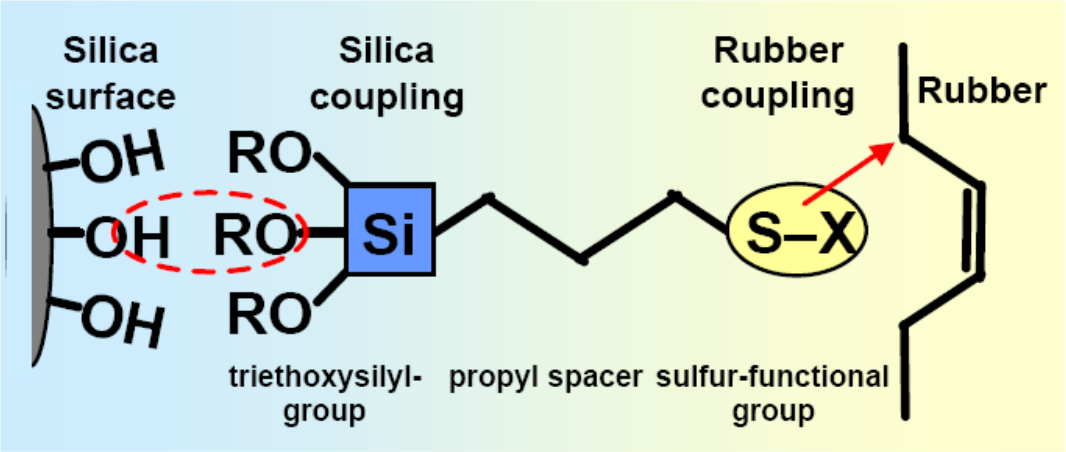

Fig.2.24- Silica-silane reaction

The use of silica (SiO_2) as reinforcing filler, in place of conventional carbon black (CB), has become popular in the last two decades (Ansarifar, 2003) after the introduction of silane coupling agent. Tire industries were successful to develop low rolling resistance passenger tread compound without sacrificing traction by using precipitated silica and silane and solution SBR. Such tires can reduce fuel consumption by approximately 6% and reduce emission of pollutants.

Due to the increasing demand for fuel economy and environmental concern, replacement of carbon black by silica and clay is gaining potential although silica is very successful in passenger tire for lower of rolling resistance but it is not so successful in the truck bus radial tire segment owing to its relatively poor bonding with natural rubber (Wang, 2000; Schon, 2003).

2.5.5 Nanoclay (Na-montmorilonite: Na-MMT)

Clays are naturally occurring minerals with variability in their constitution depending on their groups and sources. The essential nanoclay raw material is montmorillonite (MMT); a 2-to-1 layered smectite clay mineral with a layered structure. Individual layer thicknesses are just one nanometer, but surface dimensions are generally 300 to more than 600 nanometers, resulting in an unusually high aspect ratio. The clays used for the preparation of nanoclays belong to smectite group clays which are also known as 2 : 1 phyllosilicates, the most common of which

are montmorillonite {Si4[Al1×67Mg0×33]O10(OH)2×*n*H2O×X0×33 = Na, K or Ca} where octahedral site is isomorphically substituted as shown in Fig. 2.25.

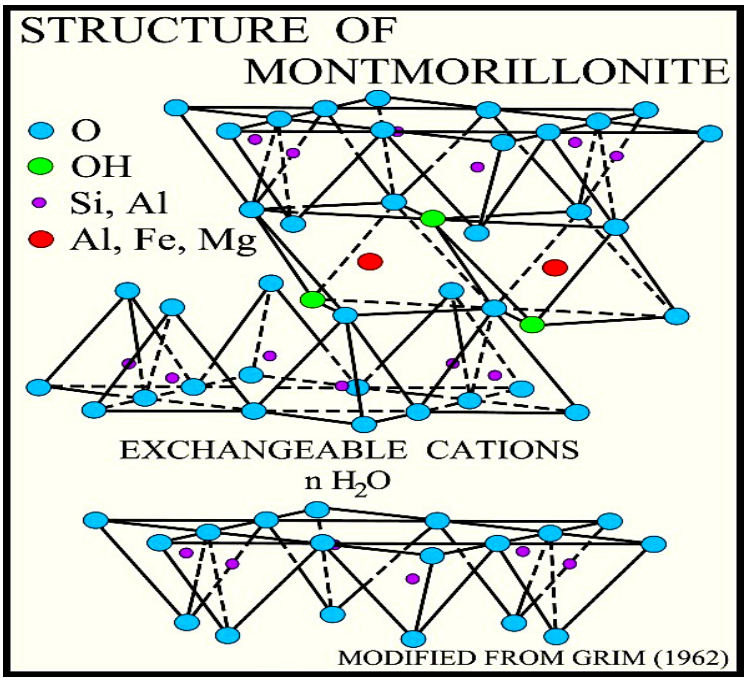

Fig. 2.25- Structure of montmorillonite (MMT) nanoclay

Microscopy image of smectite bentonite clays rock and montmorillonite are shown in the Fig. 2.26 and 2.27)

Fig. 2.26- SEM image of bentonite clay

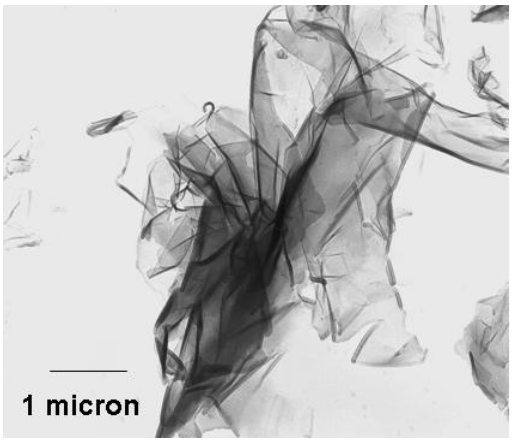

Fig. 2.27- TEM image of MMT

2.5.6 Organoclay (organic layer silicate)

Nanoclay (Na-MMT) has layer silicate structure and organically modified Nanoclay is known as organoclay. This is natural montmorillonite modified with a quaternary ammonium salt and its trade name is Cloisite® 15A produced by Southern Clay Products, USA. Cloisite® 15A is off white power material.

Kim *el al* (2006) investigated the X-ray diffraction patterns of the Na-MMT and the organoclay (Cloisite® 15A, Southern Clay Products, USA). The Na-MMT shows a diffraction pattern peak at $2\theta=7.2^{o}$, which corresponds to the average basal spacing (*d*-spacing) of 12.3 Å. In the organoclay, two peaks are shown. The first peak, which is the major peak, moved to lower angles, i.e., $2\theta=2.8^{o}$. The basal spacing increased from 12.3 to 31.5 Å. This spacing indicates that long alkyl (dimethyl dihydrogenatetallow) ammonium ions were inserted into the gallery of Na-MMT, as a result, an intercalated structure formed as shown in Fig. 2.28. The inserted long alkyl chains caused the hydrophilic nature of the clay to decrease, and this effect improved the dispersion of silicates in the rubber matrix. The second peak is shown at $2\theta=7.2^{o}$, which is same as the peak of the Na-MMT. This result indicates that some amounts of Na-MMT were not modified with alkyl ammonium ions.

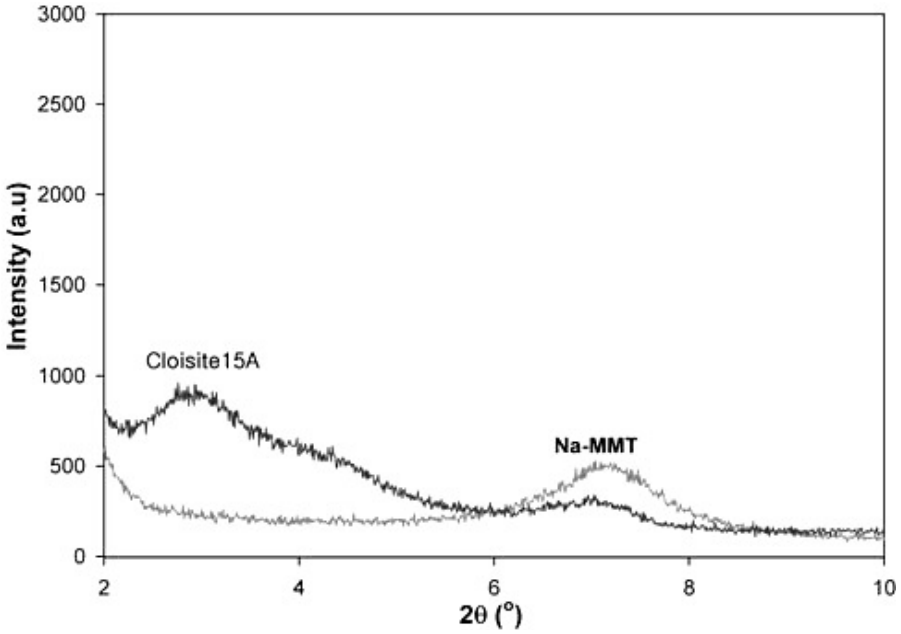

Fig. 2.28- XRD patterns of organoclay (Cloisite 15A®) and Na-MMT

2.6 NANOCOMPOSITES

2.6.1 Nano materials

Chemical structure or images of commonly investigated nano particles are shown below (Fig.2.29);

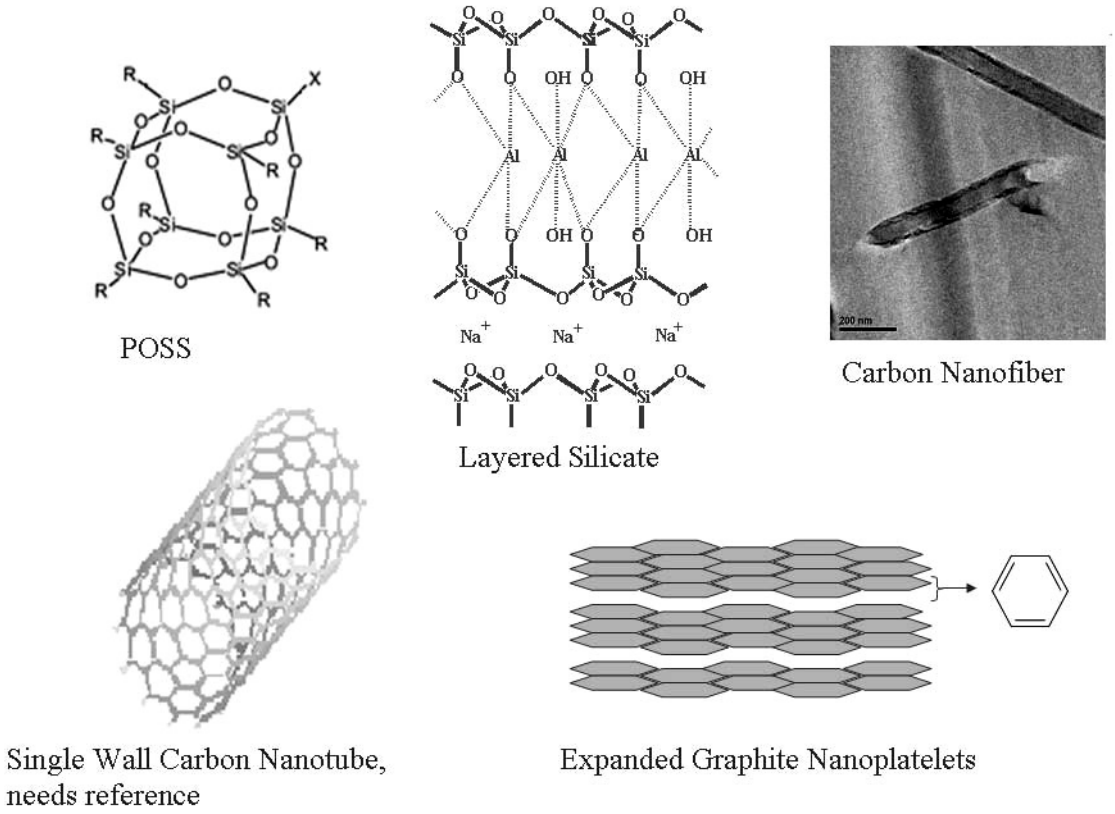

Fig. 2.29- Chemical structure of different nano particles

2.6.2 Polymer and rubber nanocomposites

The term "polymer nanocomposite" broadly describes any number of multi component systems, where the primary component is the polymer and the filler material has at least one dimension below 100nm. Rubbers are generally organophilic and naturally occurring montmorillonite is hydrophilic, hence unmodified nanoclay disperses in rubbers with great difficulty. Through clay

surface modification, montmorillonite can be made organophilic and, therefore, compatible with conventional organic polymers.

Polymer/clay nanocomposites are being extensively investigated because these nanocomposites have enormous potential for commercial utilization in diverse areas such as coating, flame-retarding, barrier, electronic materials and composite. Polymer nanocomposites were developed in late 1980's in both commercial research and academic laboratories. Toyota was the first company that synthesized clay-polyamide nanocomposite and used the same as structural components in their automobiles (Usuki,1993). Intercalated and exfoliated structure of rubber nanocomposite is shown in Fig. 2.30.

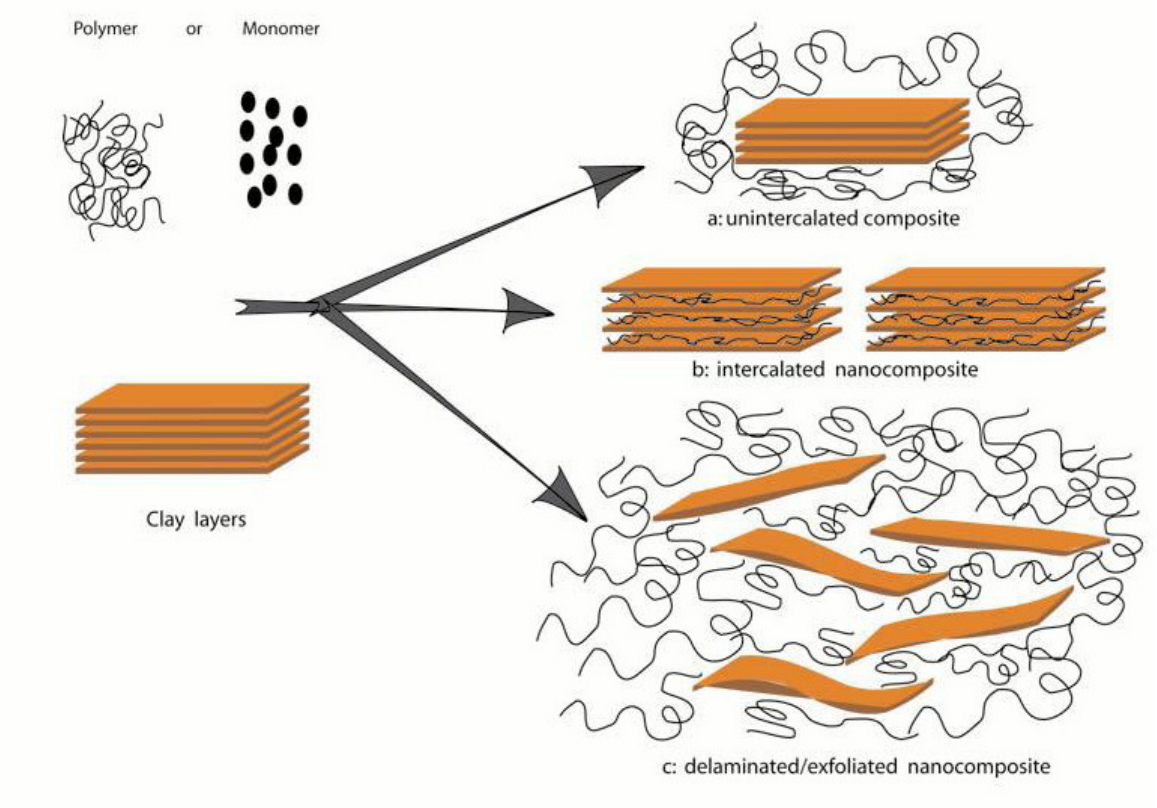

Fig. 2.30- Intercalated and exfoliated structure of rubber nanocomposite
[Meneghetti Paulo Cesar (2005)]

A good number of research papers are available on polymer/clay nanocomposites (Usuki,1993). Literature survey shows that a fair amount of interesting work has been published with organic layered silicate and different thermoplastics polymers like Nylon (Kojima,1993), polystyrene (Qutubuddin,2001) and polyethylene oxide (Vaia,1997). A number of interesting investigations

has been reported in the field of rubber nanocomposite using organic layer silicate (OLS) and different rubbers like EVA (Alexandre, 2000), ENR (Bandyopadhyay, 2000; Mark, 2001; Ray 2003) and Thermo Plastic Elastomer (TPE) (Ray 2001).

Varghese and Karger-Kocsis (2003) mixed NR latex with organoclay forming NR nanocomposites of high stiffness and low damping characteristics. Most of the NR nanocomposites however are derived from high molecular weight Natural rubber. NR-clay (10 phr) nanocomposites have also demonstrated comparable mechanical properties to NR filled with 40 phr carbon black (Arroyo, 2003). The clay improved the strength without reducing elasticity of the material. Gatner *et al*. (2001) prepared rubber nanocomposite based on BR and NR with OLS (Organic layered silicate) swollen in toluene and obtained very good tensile strength and elongation.

Organically modified montmorillonite (organoclay) is usually employed to prepare nanocomposites possessing much higher mechanical properties and gas barrier properties (Kojima, 1993). Preparation, structure, and properties of rubber/organoclay nanocomposites have been investigated for a number of rubber matrices, e.g., natural rubber, NR (Ganter, 2001; Joly, 2002; Varghese, 2003; Varghese, 2004), butadiene rubber ,BR (Ganter, 2001).

Some rubber/clay nanocomposites reported in the literature have mechanical properties similar to or better than rubber filled with carbon black. Arroyo *et al.* (2003) prepared natural rubber nanocomposites with 10 phr organoclay with similar modulus, tensile strength and hardness as natural rubber with 40 phr carbon black. Magaraphan *et al*. (2003) also prepared natural rubber nanocomposites with 7 phr of MMT functionalized with octadecylamine which presented higher tensile strength and elongation than NR with 20 phr carbon black.

Emulsion styrene butadiene rubber nanocomposite based on organic layered silicate has been investigated by a number of investigators (Zhang 2000, Wang 2000, Sadhu, 2003).

If properly dispersed, about 5-6 phr nano filler loaded rubber composites would provide properties equivalent to that of 40-50 phr carbon black or silica filled composites. However, the major challenge is to disperse the nano filler in polymer matrix. Over the years different techniques were applied to prepare the nanoclay composite with layered silicate structure in the

nano scale dispersion. The different mixing technique commonly used are melt intercalation (LeBaron, 1999; Usuki, 2002), reactive mixing (Liu, 2006), latex coagulation (Zhang, 2000) and solution method (Giannelis,1998). Mousa and Karger-Kocsis (2001) also prepared nanocomposites of SBR and organoclay mixed in two-roll mill. These nanocomposites showed very good tensile strength but supporting evidence like X-ray diffraction or TEM were not provided.

Giannelis and co-workers (1996) have found a way to alter non-reinforcing clay to very effective-reinforcing clay. Studies have been reported on clay reinforcement of emulsion SBR (Wang, 2000; Zhang, 2000; Fu, 2001; Ganter, 2001; Sadhu, 2003), however, the mechanical properties obtained render them unsuitable for practical applications.

Schon *et al.* (2003) prepared rubber compounds based on butadiene rubber (BR) and styrene butadiene rubber (SBR) containing organophilic layered silicates; they reported excellent dispersion of organoclay nano fillers in the rubber matrix by matrix–filler reactive bonding using bis(triethoxysilylpropyl)-tetrasulfan (TESPT).

Das *et al.* (Heinrich, 2008) developed a novel method to prepare nano composite comprising SSBR and organic layer silicate and obtained very good strength. Earlier workers have reported the properties of CB filled rubber vulcanizates. It has been amply demonstrated that the structure, particle size, and functional groups on the surface influence the critical performance properties.

Jia *et al.* (2005) reported a very high reinforcement and stiffening effect of nanoclay in nanoclay-carbon black filled rubber composites having 10, 20, 30 phr of total filler loading. Combined effect of nanoclay and nanoclay-carbon black on properties of natural rubber (NR) nanocomposites was evaluated, it was found that nanocomposites based on NR and nanoclay-carbon black retained advantages from both the fillers.

Meneghetti (2005) studied the effects of carbon black on SBR and on SBR/clay nanocomposites. While carbon black alone (40 phr) offered great improvement in the mechanical properties of the rubber, the synergism of organoclay and carbon black brought similar property enhancements but at half the total filler loading (10 phr each filler).

2.7 FINITE ELEMENT TIRE SIMULATION AND ROLLING RESISTANCE PREDICTION OF TIRE

Lou *et al*. (1978) studied the relationship of tire rolling resistance to the viscoelastic properties of the tread rubber. They have found the rolling resistance force was nearly a linear function of the tread material loss ratio (fractional hysteresis) measured at either constant strain or constant stress. They have calculated loss ratio as the ratio of energy loss (hysteresis) to total energy input obtained from constant crosshead speed loading cycles on an Instron UTM. Good correlation was also observed between rolling resistance force and a viscoelastic index (loss tangent) obtained from sinusoidal strain cycles on a Rheovibron instrument.

Although several factors, including tire-road friction and aerodynamic drag are known to contribute to tire rolling loss, it is generally agreed that hysteresis losses are dominant. Approximately 90% of tire rolling loss is attributed to viscoelastic behaviour of the rubber and cord component for a typical passenger car tire (Willett, 1973; Willett, 1974), of which hysteresis loss of tread rubber alone accounts for ~40% of total tire rolling resistance.

Glaeser (2005) of Federal Highway Research Institute, Germany reports that

1. At a constant speed of 100 km/h a passenger car needs ~50% of its fuel to overcome rolling resistance and the rest of the fuel is used to overcome air drag.

2. At a constant speed of 80 km/h a truck needs ~40% of his fuel to overcome rolling resistance

3. In all driving conditions an average of 25% of the fuel consumption of a passenger car is due to rolling resistance (75% air drag and acceleration)

4. Energy efficient tires having 20% less rolling resistance in comparison to conventional tires reduces the fuel consumption of a car by ~5%

Although the above mentioned figures are very impressive but much more needs to be attained. The challenge for further reduction of rolling resistance of tire from the present level are (a)

development of low hysteresis tread compound, (b) low weight optimized tire design and (c) prediction of the tire rolling resistance in the design stage. The recent development of rubber nanocomposites offers the opportunity to reduce hysteresis loss further and this could be used to develop low rolling resistance tire.

Measurement of tire rolling resistance using either a pulley wheel or flat track tire testing machine is time consuming as well as expensive because it requires a test tire to be prepared, hence to speed up the development process and to reduce testing costs, prediction of tire rolling resistance using simulation techniques has received considerable importance (Kobayashi, 1987; Warholic, 1987; Luchini, 1994; Park, 1997).

The method for the evaluation of energy dissipation in a tire using finite element analysis to prediction rolling resistance has been studied by many investigators. Kobayashi *et al.* (1987) evaluated the energy dissipation using the product of elastic strain energy obtained from structural simulation and the loss tangent of materials. Using finite element simulation Nakajima (1966) and Abe (1996) showed that tire structure and compound properties could be optimized to reduce rolling resistance.

Shida *et al.* have used a static finite element method for tire rolling resistance simulation (Shida 1999). The method implements a static deflection analysis first and the stress and strain thus obtained, together with the loss factors of the materials determined separately, are used to estimate the energy dissipation of a rolling tire. The loss factors of the rubber materials are experimentally obtained and the effective loss tangents of the fiber-reinforced rubber are determined by the homogenization theory of dynamic viscoelasticity. The rolling resistance simulation of a passenger car radial tire using this approach accurately captures the trends of an actual tire.

Ebbott *et al*. (1999) used a finite element-based method to predict tire rolling resistance and temperature distributions. The particular attention was given to the material properties and constitutive modeling as these have a significant effect on the predictions. A coupled thermo-mechanical method is described where both the stiffness and the loss properties are updated as a function of strain, temperature, and frequency. The simulation results for rolling resistance and steady state temperature distribution were compared with experiments for passenger and radial medium truck tires.

Pillai and Fielding-Russell (1992) proposed a simple predictive equation for tire rolling resistance that involves the concept of whole tire hysteresis ratio. Rubber is a highly non-linear viscoelastic material however; this method uses linear viscoelastic properties defined by Prony series.

Most of the above methods used non linear static simulation but uses linear viscoelastic approach for energy dissipation calculation to predict rolling resistance. However, rubbers are highly non-linear viscoelastic material and hence require non linear viscoelastic simulation. The viscoelastic simulation implemented in ABAQUS uses linear viscoelastic properties defined by Prony series (Abaqus, Example Problem manual, Version 6.7, Vol II and III). A software program is required to capture non linear viscoelastic characteristics of rubber from non linear viscoelastic material properties to evaluate energy dissipation for rolling resistance prediction.

2.8 SCOPE OF THE WORK

Although considerable amount of work has been done on SBR-clay and BR-clay nanocomposites but there is almost a total lack of literature on SBR/BR-clay nanocomposite. In the tire industry, SBR/BR blend is of considerable importance as it is widely used in passenger car tire tread compound. Hence, investigation of nanocomposite based on SBR/BR blends and organoclay would not only be interesting but also have wide applications.

Clay dispersion in SBR rubber is very difficult and when dispersed it still does not show much improvement in modulus, tensile strength, elongation at break, tear strength and tear and breaking energy. Uses of compatibilizer in SBR rubber has shown better clay dispersion and correspondingly improvement in mechanical properties compared to nanocomposite not using compatibilizer. Thus it is necessary to study the effect of compatibilizer having different polarity on clay dispersion, mechanical properties and nanocomposite morphology.

Different mixing techniques have been used by different researchers to prepare nanocomposite but comparison of the different mixing techniques with respect to clay dispersion and subsequent properties of nanocomposites is not reported in the literature this aspect also needs to be addressed.

Literature is available on clay dosages in different rubbers such as NR, SBR, BR, NBR, etc. but optimum dosages for SBR/BR was not found. To achieve the appropriate clay dispersion and nanocomposite properties, study on dosages of clay as well as compatibilizer is required and the optimum loading of clay and compatibilizer needs to be identified.

Hence the investigation on the effect of carrier polymer, mixing techniques, dosages of compatibilizer and organoclay in SBR/BR blends has immense importance for the development of nanocomposite for tread compounds that would result in desirable properties with low hysteresis losses.

Literature survey shows that some papers are available where nanocomposites were projected for tire tread application but properties reported are far from actual requirement. They have only focused on tensile strength and elongation at break of nanocomposite but for tire tread application the most important properties are hardness, low strain modulus, tear strength and abrasion resistance, wet grip and rolling resistance.

In the existing literature there is no report on rubber clay nanocomposite that can meet the properties required for tread application. Some literature was obtained where carbon black was introduced in SBR/clay nanocomposite and found synergistic effect but not aimed for any specific application.

In this investigatation, dual filler system comprising of organic layer silicate (organoclay) and conventional filler like carbon black or silica is introduced to prepare the nanocomposites based on SBR/BR blend. The three different SBR rubbers ESBR, SSBR and F-SSBR are incorporated in this study for comparison purposes. The objective of this investigation was to improve the

performance properties e.g. hardness, low strain modulus, tear strength, viscoelastic properties and abrasion resistance of the nanocomposites and, simultaneously, to minimize the hysteresis loss (rolling resistance).

Although, there exists a fair amount of literature on NR and BR and clay nanocomposite, but there is no literature on NR/BR blend and clay nanocomposite. For many practical applications NR/BR blends are used and especially in the automotive tire, NR/BR blends are used in truck bus radial tread and sidewall compounds. Therefore it is quite interesting and appropriate to investigate nanocomposite based on NR/BR blend and clay and the effect of carrier polymer, mixing technique, filler dosages etc.

Literature survey revealed that most of the works on NR nanocomposite were with nanoclay. Some investigators reported use of carbon black with clay to prepare nanocomposite. These nanocomposites were projected for tread application but the properties reported were far from the specified critical performance properties for tread applications.

In this investigation a dual filler system comprising of organoclay and conventional filler like carbon black or silica, was investigated to prepare the nanocomposite based on NR/BR blend. The aim of this investigation was to achieve performance properties e.g. hardness, low strain modulus, tear strength and abrasion resistance of nanocomposite that are comparable to commercial tread compound whereas to minimize the hysteresis loss (rolling resistance).

Development of low hysteresis PCR and TBR tread compounds based on nanocomposites and prediction of rolling resistance in tire would not only be highly interesting but also very much useful to improve fuel efficiency and thereby reduce the CO_2 emission. In this investigation, passenger car radial (PCR) and truck bus radial (TBR) tread compounds based on different nanocomposites were studied for rolling resistance and compared with respective standard tread compounds using simulation technique.

A steady state rolling resistance simulation was done and the strain energy and principal strains were extracted from the result file using an internal developed program (Rolling resistance code). Energy dissipation was evaluated using the product of elastic strain energy and the loss tangent of materials through post processing using Rolling resistance code (RR code). The post processing approach was adopted. The non-linear viscoelastic behavior was incorporated by providing strain and temperature dependent dynamic viscoelastic properties of rubber.

The work address the primary objective of development of nanocomposites that can match the prevalent tire tread compounds in term of physical properties while returning much lower rolling resistance without sacrificing other requirements viz. Wet traction, Dry traction, Wear, etc.

It also addresses the secondary objective of prediction of rolling resistance during the design stage through finite element simulation.

CHAPTER 3

MATERIALS AND METHODS

This Chapter describes materials, experimental methods and analytical techniques used in this investigation.

3.0 RAW MATERIALS

3.1.1 Raw material description

The rubbers, fillers and other compounding materials used in this investigation are presented in this section which includes brief material descriptions, grade, supplier and technical specification data of raw materials. Detailed information is presented in subsequent sections.

Table 3.1-Raw material summary

MATERIALS	GRADE	SUPPLIER	TECHNICAL DETAILS
Natural Rubber, (NR)	SMR 20	Hock Hin, Malaysia	Mooney viscosity (MV): 87
Emulsion styrene butadiene rubber (E-SBR)	SBR1502	Kumho Petrochemical, South Korea.	23.5% styrene; MV: 50
Solution styrene butadiene rubber (S-SBR)	Buna VSL 5025-0 HM	Lanxess A.G, Germany	25% styrene; 50% Vinyl, MV: 70
Functionalized SSBR (FS-SBR)	Nipol NS 116R	Zeon Corporation, Japan	MV: 45; 21% Styrene, 50% Vinyl; Sn coupled, chain end modified,
Polybutadiene rubber, BR	Cisamer 1220	Reliance Industries Ltd (IPCL), India	MV: 44; Cis content: 96%
Carboxylated nitrile rubber (XNBR)	Chemigum. XNBR146 and 750	Eliokem India Pvt. Ltd.	Carboxylation 1 and 7%;
Organoclay	Cloisite®15A	Southern clay products, Inc, USA	Montmorillonite (MMT) modified with a quaternary ammonium salt. Basal spacing of this organoclay is reported to be 3.15 nm.
Highly Dispersable Silica; Amorphous Precipitated Silica (10 SiO2, 1 H2O)	Ultrasil®7000GR	Evonic Degussa A.G, Germany	N_2 Surface Area (BET)-170 m^2/g; DBP (structure): 198

Table 3.1-Raw material summary (contd.)

MATERIALS	GRADE	SUPPLIER	TECHNICAL DETAILS
Silane coupling agent, Bis(triethoxysilylpropyl)-tetrasulfan	Si 69 (TESPT)	Evonic Degussa A.G, Germany	100% liquid silane, Sulfur content 22.5%
Silane coupling agent	X-50S	Evonic Degussa A.G, Germany	%50 TESPT and 50% Carbon black.
Carbon Black	ISAF, N220	PCBL, India	N_2 Surface Area (BET):121 m^2/g DBP No.:114
N-(1,3-dimethyl-butyl)-N'-phenyl-P-Phenylenediamine	6PPD	NOCIL, India	Molecular wt.: 268; M.P : 48-51^oC
N-Tertiarybutyl-2-benzothiazole-sulfenamide	TBBS	NOCIL, India	Molecular wt.: 238 ; M.P : 104^oC
Diphenyl guanidine	DPG	Hindustan Chemicals, India	Molecular wt.: 211; M.P : 142^oC
Zinc Oxide	ZnO	Upper, India	Density: 5.6 g/cc ZnO content: 99%
Stearic acid	Fatty acid (C18)	Palm Oleo, Malaysia	Solidification point 50-60 ^oC
Soluble Sulfur	Rhombic Sulfur (S_8)	Solar, India	Total Sulfur 99%

3.1.2 Natural Rubber (NR)

Natural rubber is one of nature's unique materials. Crude rubber is primarily hydrocarbon in nature. In 1826 English chemist Michael Faraday (1791–1867) analyzed natural rubber and found it to have the empirical formula C5H8, along with 2 to 4 percent protein and 1 to 4 percent acetone-soluble materials (resins, fatty acids, and sterols). Samuel Shrowder Pickles (1878–1962) proposed in 1910 that rubber is a linear polymer of isoprene. Natural rubber is produced commercially from the latex of *Hevea Brasiliensis*.

The natural rubber consists of Cis-1,4-Polyisoprene molecules and the molecular weights of rubber molecules range from 50,000 to 3,000,000. The latex has approximately the following composition (%): Water 55-70, Rubber 30-40, Resins 1.5-2, Protein1.5-3, Ash, 0.5-1, Sugar 1-2. The It is far more common to filter the harvested latex, dilute it with water and then to cause it to coagulate using substances such as acetic acid or formic acid or by means of electrophoresis.

The chemical structure of NR is shown in Fig. 3.1. The natural rubber trees and tapping and latex collection are shown in Fig. 3.2.

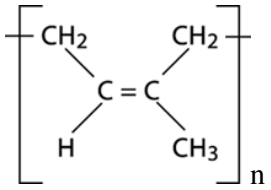

Fig. 3.1- Chemical structure of NR

Fig. 3.2- *Heavea Brasiliensis* tree and tapping

Standard international grades of NR;

- Sheets Rubber - Ribbed Smoked Sheet (RSS)
- Block rubber, Technically Specified Rubber (TSR)
- Latex Concentration
- Crepes rubber - Estate Brown Crepe (EBC)

In this investigation, SMR 20 (Standard Malaysian Rubber 20) was used. It was received from M/s Hock Hin (HR), Malaysia and its specification is shown in Table 3.2.

Table 3.2-Technical specifications of SMR 20

Parameters	***Values***
Dirt (max) %wt	0.20
Nitrogen (max) % wt	0.60
Mooney viscosity (ML, 1+4, 100°C), MU	80±7

3.1.3 Emulsion styrene butadiene rubber (ESBR)

Styrene butadiene rubber (SBR) is a synthetic rubber copolymer consisting of styrene and butadiene. It was originally developed prior to World War II in Germany. It has good abrasion resistance and good aging stability when protected by additives, and is widely used in car tire where it may be blended with natural rubber and polybutadiene rubber. SBR can be produced by two basically different processes; (a) from solution or (b) as emulsion. SBR–1502 used in this investigation is a cold polymerized by emulsion method. It is a high molecular weight styrene butadiene rubber combining good extrusion behavior and superior compound properties. It has relatively wide molecular weight distribution and the butadiene component has an average about 9% Cis-1,4, 54.5% trans and 13% 1,2 vinyl structure.

The chemical structure of SBR 1502 is shown in Fig.3.3.

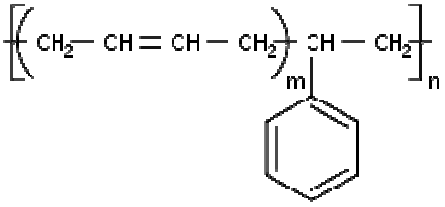

Fig. 3.3- Chemical structure of SBR

The rubber samples were received from M/s. Kumho Petrochemical, South Korea. The technical specification of SBR1502 is presented in Table 3.3.

Table 3.3-Technical specification of SBR 1502

Parameters	***Values***
Mooney viscosity (ML 1+4 AT 100^{o}C	50 +/- 6
Antioxidant (wt %)	1.00 - 1.40
Specific gravity	0,92
Bound styrene (wt %)	22.5 - 24.5
Free organic acids (wt %)	5.00 - 6.50

3.1.4 Solution styrene butadiene rubber (SSBR)

Solution polymerized styrene-butadiene rubber (S-SBR) is an elastomer synthesized from styrene and butadiene via anionic random copolymerization process. S-SBR is mainly used in automobile tire with characteristics of energy saving and high wet skid resistance. The solution SSBR BUNA VSL 5025-0 HM was received from Lanxess, Germany and the detail technical specifications and microstructure are specified in Table 3.4 and 3.5.

Table 3.4-Technical specification of SSBR BUNA VSL 5025-0

Parameters	***Values***
Mooney viscosity (ML 1+4 AT 100^{o}C	70 +/- 4
Bound styrene (wt %)	25 - 27
Polydispersity Index, Mw/Mn	2.64
Specific gravity	0.92

Table 3.5-Microstructure and macrostructure of S-SBR

S-SBR	Styrene,%	1.2 butadiene,%	1.4 butadiene, %	Tg, °C
BUNA VSL 5025-0	25	50	25	-13.2

3.1.5 Functionalized solution SBR (FSSBR)

Functionalized S-SBR is synthesized via anionic living polymerization process from styrene and butadiene in low carbon aliphatic hydrocarbon and/or naphthenic hydrocarbon in the presence of organic lithium compound as initiator. Functionalized S-SBR is mainly used in automobile tire with characteristics of energy saving and high wet skid resistance.

Nipol NS 116R of Zeon Corporation, Japan is a functionalized solution styrene butadiene rubber (FSSBR) with Sn coupled and chain ends modified COOH-groups was used in this investigation. The Sn coupling and chain end modification enhanced adhesion between the polymer chain and the silica. The details technical specification are provided in Table-3.6

Table 3.6-Technical specification of functionalized SSBR

Parameters	*Values*
Mooney viscosity (ML 1+4 AT 100^{o}C	45.0
Vinyl Content (wt%)	50.0
Bound styrene (wt %)	21.0

3.1.6 Polybutadiene rubber (BR)

Polybutadiene (BR) is the second largest volume synthetic rubber produced, next to styrene-butadiene rubber (SBR). Consumption was about 1,953,000 metric tons worldwide in 1999. The major use of BR is in tires with over 70% of the polymer produced going into treads and sidewalls. Cured BR imparts excellent abrasion resistance (good tread wear), and low rolling resistance (good fuel economy) due to its low glass transition temperature (T_g <–90^{o}C).

Butadiene rubbers are produced by the solution polymerization process of monomer 1,3-butadiene with the aid of organometallic catalysts such as neodymium, cobalt, lithium or titanium based which influences the microstructure and macrostructure of the polymers and therefore its properties.

The macrostructure of Co-BR is distinguished by a moderately broad molecular weight distribution and medium degree of branching. The micro and macrostructure of Co BR is shown in Table 3.7 and Fig. 3.4. The Co-BR (Cisamer 1220) used in this study was received from Reliance Industries Limited, India and its technical specification are provided in Table 3.8.

Table 3.7-Polybutadiene rubber – micro and macrostructures

Catalyst	cis 1,4	trans 1,4	vinyl 1,2	Tg (DSC)
Co	96	2	2	-107

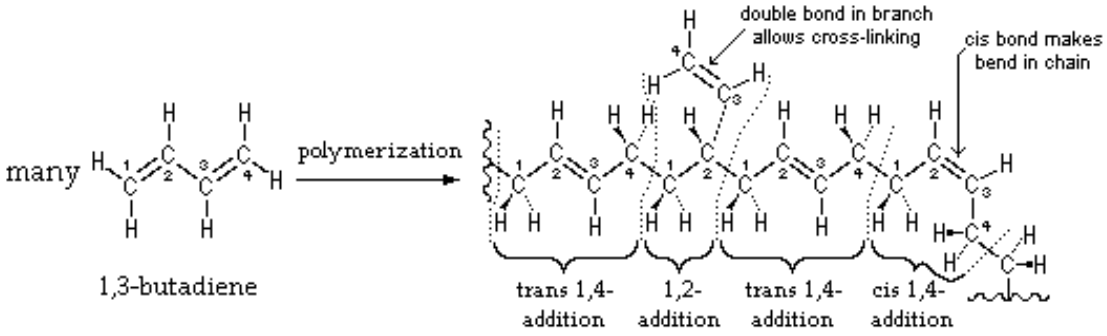

Fig. 3.4-Micro and macrostructure of BR

Table 3.8-Technical specification of BR

Parameters	***Values***
1,4-Cis content, %	96.0
Specific gravity	0.91
Mooney viscosity (ML 1+4 at 100^{o}C)	44.0

3.1.7 Nitrile rubber (NBR) and carboxylated NBR (XNBR)

Nitrile butadiene rubber (NBR) is a family of unsaturated copolymers of 2-propenenitrile and various butadiene monomers (1,2-butadiene and 1,3-butadiene). Although its physical and chemical properties vary depending on the polymer's composition of nitrile, this form of synthetic rubber is generally resistant to oil, fuel, and other chemicals (the more nitrile within the polymer, the higher the resistance to oils but the lower the flexibility of the material). The chemical structure of Nitrile rubber is shown in Fig.3.5.

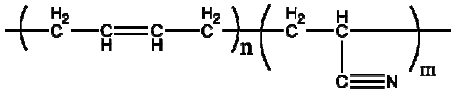

Fig. 3.5- Chemical structure of NBR

Chemigum® NX146 and NX 750 is a cold polymerized, medium ACN terpolymer based on acrylonitrile, butadiene and carboxylic acid, and emulsified with synthetic soap(s). The technical specifications are shown in Table 3.9.

Table 3.9-Technical specification of NBR/XNBR

	XNBR-0 (NBR)	XNBR-1	XNBR-7
Bound Acrylonitrile, %	32.0	33	32.5
Carboxylation, %	0	1.0	7.0
MV, ML (1+4) at 100°C	51.0	47.0	52.0
Specific gravity	0.99	0.98	0.98

3.1.8 Organoclay (Cloisite®15A)

Nanoclay (Na-MMT) has layer silicate structure and organically modified nanoclay is known as organoclay. This is natural montmorillonite modified with a quaternary ammonium salt and its trade name is Cloisite® 15A produced by Southern Clay Products, USA. Cloisite® 15A is off white power material. The chemical structure of quaternary ammonium salt used to modify nanoclay is shown in Fig. 3.6. The typical properties of Cloisite® 15A is given in Table 3.10.

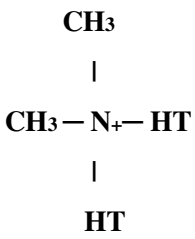

Fig. 3.6- Chemical structure of organoclay

The organic modifier 2M2HT is dimethyl, dihydrogenatedtallow, quaternary ammonium; where HT is Hydrogenated Tallow (~65% C18; ~30% C16; ~5% C14) and anion is chloride.

Table 3.10-treatment/properties of clay

	Organic Modifier (1)	Modifier Concentration	% Moisture	% Weight Loss on Ignition
Cloisite® 15A	2M2HT	125 meq/100g clay	< 2%	43%

Table 3.11-Typical dry particle sizes: (microns, by volume)

10% less than:	50% less than:	90% less than:
2µm	6µm	13µm

3.1.9 Carbon black (ISAF-N220)

Carbon black is a material produced by the incomplete combustion of heavy petroleum products such as FCC tar, coal tar, ethylene cracking, and a small amount from vegetable oil. Carbon black is a form of amorphous carbon that has high surface-area-to-volume ratio. Carbon black is used as a pigment and reinforcement in rubber and plastic products. The most common use (70%) of carbon black is as a pigment and reinforcing phase in automobile tires. Carbon black also helps conduct heat away from the tread and belt area of the tire, reducing thermal damage and increasing tire life.

Carbon black is a reinforcing filler and imparts reinforcing strength properties to rubber in a similar way an iron rod embedded in a cement matrix provides strength to the concrete. The carbon black produced through the furnace process has a small granular form and is easily incorporated and dispersed in a rubber matrix. The carbon black ISAF (N220) used in the investigation was received from M/s. Phillips Carbon Black Ltd., India and properties are presented in Table 3.12.

Table 3.12-Grades and properties of Carbon Black

Parameters	Values
Name /ASTM No.	ISAF (N220)
Iodine Adsorption (mg/g)	121.0
CTAB Surface Area (m^2/g)	111.0
BET, N_2SA (m^2/g)	119.0
DBP Absorption	114.0
Compressed DBP (ml/100g)	100.0
Tint (%ITRB)	115.0

3.1.10 Highly dispersible silica (HDS)

Silica or silicon dioxide (SiO2) in its pure form is colorless to white. Highly dispersible Silica's (HDS) are precipitated synthetic amorphous silica obtained from a process essentially using sand, which is the most abundant mineral present in the earth's crust. Precipitated silica is used as reinforcement filler in the rubber industry.

ULTRASIL® 7000 GR from Evonic Industries is highly reinforcing silica which was especially developed for application in low rolling resistant passenger car tire tread compounds, so called "Green Tire". HD silica in combination with bifunctional silanes imparts to tread compounds high abrasion resistance combined with excellent rolling resistance and wet traction. The technical specification of Ultasil® 7000GR is shown in Table 3.13

Table 3.13-Physico-chemical properties of ULTRASIL 7000GR

Parameters	**Units**	**Values**
Density	g/cm^3	2.1
Specific surface area (N_2)	m^2 / g	170
DBP Absorption	Nos.	198
Heating loss	%	5.2

3.1.11 Silane coupling agent

Si 69® is a bifunctional, sulfur-containing organosilane used in the rubber industry in combination with white fillers that carry silanol groups and this is a treade name of Evonic Industries. Si 69® reacts with fillers containing silanol groups during mixing and with the polymer during the vulcanization process with formation of covalent chemical bonds. This imparts better tensile strength, higher modus, reduced compression set, increased abrasion resistance and optimized dynamic properties. It is widely used in low rolling resistance tires tread production with silica filler and solution SBR. The chemical structure is presented in Fig. 3.7 and physico-chemical properties are given in Table 3.14.

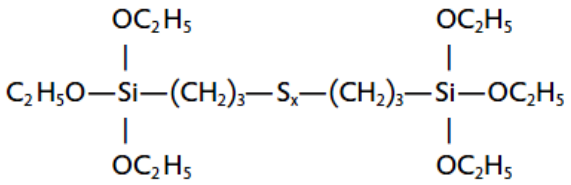

Bis(triethoxysilylpropyl) polysulfide, $\bar{x}$ = 3.70

Fig. 3.7- Chemical structure of Si 69®

Table 3.14-Physico-chemical properties of Si 69®

Parameters	**unit**	**values**
Density	g/cm^3	1.10
Average molecular weight	g / mol	532
Sulfur content	%	22.5
Average Sulfur chain length, HPLC		3.70

3.1.12 Antidegradant

The most widely used antidegradant in the rubber industry is 6PPD that has a generic name N-(1, 3-dimethylbutyl)-N'-phenyl-p-phenylenediamine. It's chemical structure is given below:

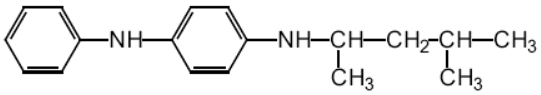

Fig 3.8- Chemical structure of 6PPD

6PPD acts as strong anti-ozonant as well as antioxidant. Technical specification of 6PPD is shown in Table 3.15.

Table 3.15- Properties of 6PPD

Parameters	**Values**
Molecular Weight	268
Melting Point (Final), °C	48-51
Specific Gravity @ 60°C	0.986-1.00

Pilflex® 13 is trade name of 6PPP of NOCIL India Ltd. 6PPD offers excellent resistance to rubber vulcanizates against degradative factors such as ozone (static and dynamic), flex cracking and fatigue, oxidative heat aging, metal-ion catalyzed oxidative aging, UV light and weathering. Pilflex® 13 is the most suitable PPD antidegradant for NR, NR-BR, SBR, SBR-BR and NBR based compounds.

3.1.13 Sulfenamide accelerator (TBBS)

TBBS (N-tert-butyl-2-benzothiazolesulfenamide) is a ultra fast delayed action sulfenamide accelerator for NR, SBR, BR, NBR and other sulfur cured diene rubbers. TBBS exhibits very good storage stability as compared to other sulfeamide accelerators. TBBS pellets disperse easily in rubber. The normal dosage of TBBS is in the range of 0.5-1.5. For TBBS normal dosages of zinc oxide and stearic acid are necessary for cure activation.

TBBS alone or in combination with secondary accelerators is widely used in NR, SBR, NR-SBR/BR blend, SBR/BR blend, NBR and other synthetic rubber based compounds for the manufacture of auto tires, NR-auto tubes, tire retreading materials and Molded and Extruded rubber products. Technical specification of TBBS is shown in Table 3.16 and chemical structure in Fig. 3.9.

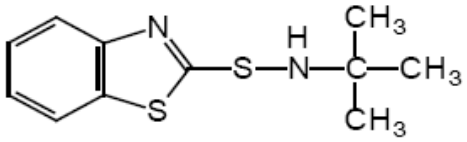

Fig. 3.9- Chemical structure of TBBS

Table 3.16-Properties of TBBS

Parameters	Values
Molecular Weight	238
Assay (Titration), % (min)	96.0
Melting Point (Initial), °C (min)	104
Specific Gravity @ 25°C	1.280

3.1.14 Diphenyl guanidine (DPG)

Guanidine, is called carbamidine. Diphenylguanidine is one of common accelerators for the vulcanization of rubber in combination with thiazoles and sulfenamides. Though it does not show better activity than thiuram and dithiocarbamates, it has better stability. It is used as a complexing agent for the detection of metals and organic bases.

DPG can be used for NR, IR, SBR, NBR and CR. Very useful basic accelerator that can be used in combination with acidic accelerators, it is very seldom used alone. It can be used as secondary accelerator with thiazoles and sulphenamides in NR and SBR compounds, giving good physical properties.

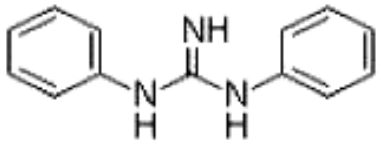

Fig. 3.10- Chemical structure of 1, 3-Diphenylguanidine (DPG)

Table 3.17-Properties of DPG

Parameters	Values
Product Name	1, 3-Diphenylguanidine
Molecular Formula	C13H13N3
Molecular Weight	211.26
Initial melting point ^{o}C	142

3.1.15 Rhombic sulfur

Sulfur is the chemical element with atomic number 16, represented by the symbol **S**. It is an abundant, multivalent non-metal. At normal conditions, sulfur atoms form cyclic octatomic molecules with chemical formula S_8. Elemental sulfur is a bright yellow crystalline solid. Chemically, sulfur can react as either an oxidant or reducing agent. Amorphous or "plastic" sulfur is produced by rapid cooling of molten sulfur—for example, by pouring it into cold water.

X-ray crystallography studies show that the amorphous form may have a helical structure with eight atoms per turn.

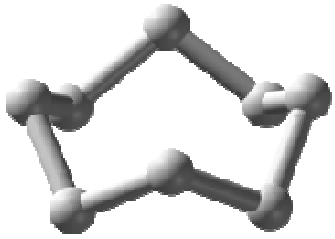

Fig. 3.11- Chemical structure of rhombic Sulfur (S_8)

Table 3.18-Technical specifications of rhombic sulfur

Parameters	Values
Name, symbol, number	Sulfur, S, 16
Density at 25.0°C	2.07 g·cm^{-3}
Total sulfur content	99%
Melting point	115.2 °C

3.1.16 Zinc oxide

Zinc Oxide is used as activator in rubber compounds. Zinc Oxide is manufactured using a physical vapour synthesis process. In this process, zinc metal is vaporized. This vapour is rapidly cooled in the presence of oxygen, causing nucleation and condensation of nano crystalline zinc oxide particles. The particles are non-porous and their surfaces are free of residual chemical contaminants. The TEM images of Zinc oxide particle size and morphology are shown in Fig. 3.12 and 3.13 respectively.

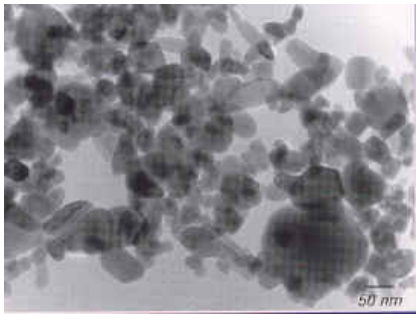

Fig. 3.12- Particle size distribution

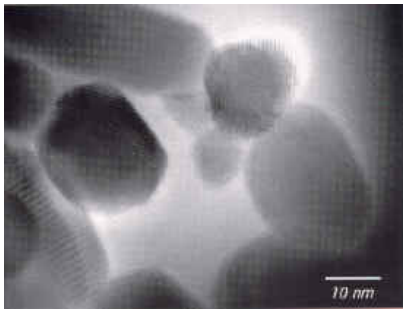

Fig. 3.13- Particle morphology

During the process, the particles form weak agglomerates up to tens of microns in size. These agglomerates can be reduced with suitable dispersion techniques, providing a typical particle size distribution ranging from a few nano meters to a few hundred nano meters. The technical specification of rubber grade Zinc oxide is presented in Table 3.19.

Table 3.19-Technical specifications of zinc oxide

Parameters	Value
ZnO content	99.0 %
Density	5.6 g/cm^3 at 25°C
Nitrogen surface area (BET)	4.0 m^2/g

3.1.17 Stearic acid

Stearic acid is a saturated fatty acid with 18 carbon chain and has the IUPAC name octadecanoic acid. It is a waxy solid, and its chemical formula is $C_{18}H_{36}O_2$, or $CH_3(CH_2)_{16}COOH$. The chemical structure is shown in Fig. 3.14.

Table 3.20-Technical specifications of stearic acid

Parameters	Values
Chemical composition	Mixture of predominantly saturated fatty acids
Solidification point	50.0 - 60
Fatty acid fractions, C16-C20)	90.0 % min
Acid number	195.0 mg KOH/g

Fig. 3.14- Chemical structure of stearic acid

3.2 MIXING AND PREPARATION OF NANOCOMPOSITES

3.2.1 Mixing equipments

The mixing equipment used in the investigations to prepare nanocomposite and rubber compounds are described below.

(a) Brabender Plasticorder

Brabender Plasticorder PL 2000E was used to mix rubber-clay master batch. It has 70 cc chambers for mixing and was heated with oil. It has variable rotor speed and temperature. A load is applied on the ram to apply pressure during mixing.

(b) Laboratory Banbury

This has capacity of 3.2 liters. It has four wing rotors with variable speed from 0 to 150 rpm. It has temperature control unit (TCU) temperature range 40 to 80^{o}C. It has timer and temperature controller to record mixing time and temperature and release batches as per set points. The Banbury had PLC control and had software that provided important information on mixing like batch temperature, mixing time, power and total input energy.

(C) Two roll Mill

This the oldest rubber mixing equipment and even today is widely used in the laboratory as well small scale industry. It has two rolls rotating in the opposite direction with different speed so that in-between rolls, a shear force is generated which helps to masticate rubber and subsequently incorporates ingredients into rubber to make compound.

The friction ratio varies from 1.1 to 1.3 and the back roll moves faster than front roll. The rolls have inside core through which cold water or steam can pass for cooling or heating. Both the rolls have same dimension, 6'' diameter and 13'' length. The rubber band is formed in the front roll where the mixing takes place.

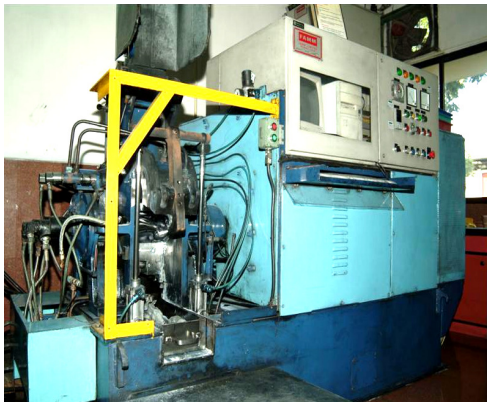

Fig. 3.15- Laboratory Banbury

Fig. 3.16- Two rolls mill.

3.2.2 Preparation of organoclay-XNBR master batch

Three different mixing techniques were employed to prepare Organoclay and XNBR (carboxylated nitrile rubber) master batches;

1. **Two-roll mixing:** In this technique, a uniform band of XNBR was made and filler was incorporated. The mixing was carried out for 10 minutes.
2. **Solution mixing:** XNBR was dissolved in an equi-volume solution of MEK and Toluene and kept for 24 hours. Organoclay was mixed in ethanol and gradually poured into the rubber solution with constant stirring for 4 hours. The solvent was removed by air drying and finally by drying in a vacuum oven at 60^{o}C for 8 hours.
3. **Internal mixer:** In this process the master batch was prepared in an internal mixer (Brabender Plasticorder PL2000E, Brabender A.G, Germany) at 160^{0}C with rotor speed of 50 rpm for mixing time of 10 minutes.

3.2.3 Preparation of SBR/BR and NR/BR-organoclay nanocomposites

Rubber nanocomposites were prepared in a two-step method;

Step I: Preparation of clay-XNBR master batch.

Step II: Mixing of the master batch prepared in step-I with SBR/BR or NR/BR blends in a two-roll mixing mill and then all other ingredients such as zinc oxide, stearic acid, 6PPD, Sulfur, TBBS and DPG were added and mixed thoroughly.

3.2.4 Preparation on SBR/BR and NR/BR-dual fillers nanocomposites

The dual filler rubber nanocomposites were prepared in three steps;

Step A: Preparation of clay-XNBR (7%) master batch in internal mixer.

Step B: Preparation of SBR/BR and NR/BR master batches with carbon black or silica-silane in a laboratory Banbury mixer at 40 rpm for 6 minutes and dumped at 150^{o}C.

Step C: Master batches prepared in Step A and B were mixed in a two roll mixing mill and, subsequently, all additives such as zinc oxide, stearic acid, antioxidant (6PPD), Sulfur and accelerators (TBBS and DPG) were added and mixed thoroughly.

3.3 EXPERIMENTAL DESIGN

3.3.1 SBR/BR-organoclay nanocomposites

The entire experimental investigation was conducted in four different stages as shown in schematic diagram (Fig. 3.17).

Stage-I: Effect of carboxyl group % in carrier polymer

The effect of carboxyl group % in carrier polymer (XNBR) on clay dispersion and properties of nanocomposite based on FS-SBR/BR and organoclay were investigated. The dosages of carrier polymer and organoclay were 10 and 6 phr respectively and the carboxyl group in XNBR was varied from 0 to 7%. In this case the master batch used was prepared by internal mixing process.

Stage-II: Influence of different mixing techniques

The influence of different mixing techniques like 2-roll mixing, solution mixing and internal mixing method used for the preparation of nanocomposite was investigated. The dosages of carrier polymer (7% Carboxylated nitrile rubber; XNBR-7) and organoclay were 10 and 6 phr respectively in FSSBR/BR and organoclay nanocomposite.

Stage-III: **Types of SBR rubber**

The mechanical and viscoelastic properties of different type of SBR (ESBR, SSBR and FSSBR)/BR based nanocomposites were evaluated. XRD and TEM characterization of some

selected nanocomposites were also done. The dosages of carrier polymer (XNBR-7) and organoclay were kept 10 and 6 phr respectively.

Stage-IV: Dosage optimization of Clay and XNBR

The dosage optimization of carrier polymer (XNBR-7) and organoclay in ESBR-clay nanocomposite was carried out. Clay dosages varied from 3.8 to 9.8 phr where as XNBR dosages were from 6.3 to 13.8 phr.

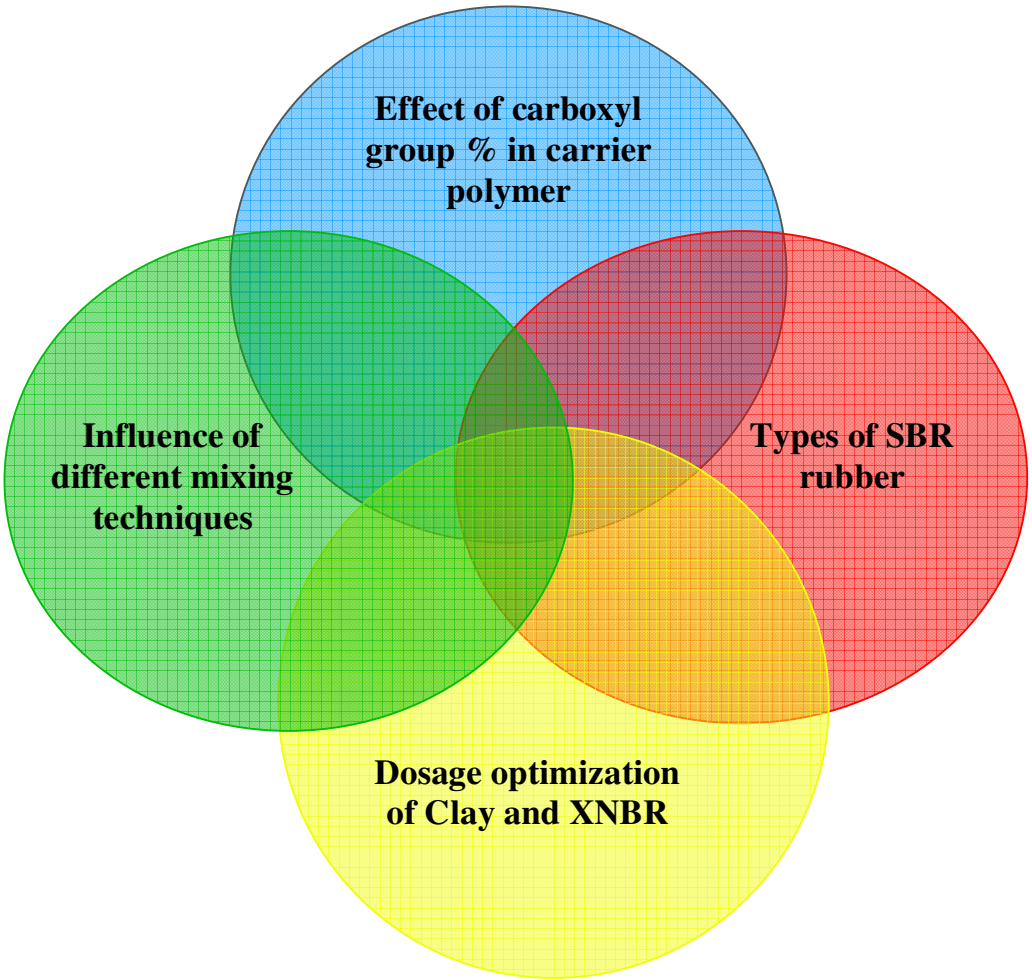

Fig. 3.17- Schematic diagram of experimental design of SBR/BR and clay nanocomposite

3.3.2 NR/BR - organoclay nanocomposites

The entire investigation was conducted in three parts as shown in schematic diagram (Fig. 3.18).

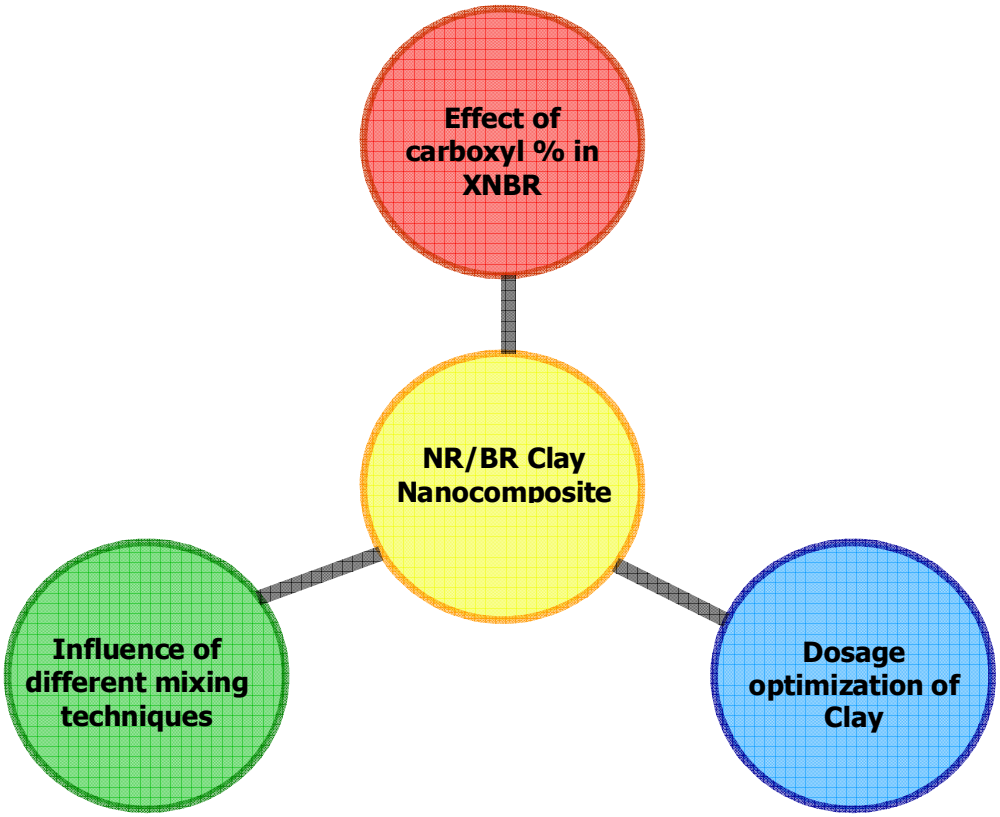

Fig. 3.18- Schematic diagram of experimental design of "NR/BR and clay" nanocomposite

Part I: Effect of carboxyl % in XNBR

The effect of carboxyl group % of carrier polymer on clay dispersion and properties nanocomposite based on NR/BR and organoclay were investigated. The dosages of carrier polymer and organoclay were 10 and 7 phr respectively and the carboxyl group in XNBR was varied from 1 to 7%. In this case the master batch used was prepared by internal mixing process.

Part-II: Influence of different mixing techniques

The influence of different mixing techniques like 2-roll mixing, solution mixing and internal mixing method used for the preparation of nanocomposite was investigated. The dosages of carrier polymer (7% Carboxylated nitrile rubber; XNBR-7) and organoclay were 10 and 7 phr respectively in NR/BR nanocomposite.

Part-III: Dosage optimization of Clay

The dosage optimization of organoclay in NR-clay nanocomposite was done. Clay dosages vary from 4.0 to 10 phr whereas XNBR was kept constant at 10 phr.

3.4 COMPOUND FORMULATIONS

3.4.1 SBR/BR- organoclay nanocomposites formulations

All the formulations were based on SBR/BR rubber blends and the detailed compound recipes used in this investigation are presented in Table 3.21 to 3.24.

Table 3.21-SBR/BR nanocomposite formulation-variation carboxyl group in XNBR

Compound ref.	C-0	C-1	C-4	C-7
Carboxyl group (%) in XNBR	0	1	4	7
Formulations *, phr	FSSBR 70.0, BR 30.0, XNBR 10.0, Clay 6.0, ZnO 3.0, stearic acid 2.0, 6PPD 1.0, Sulpfur 1.6, TBBS 1.7, DPG 1.8.			

Table 3.22-SBR/BR nanocomposite formulation - different mixing method

Compound ref.	M-1	M-2	M-3
Mixing Technique	2-roll Mill	Solution	Internal mixer
Formulations , phr	FSSBR 70.0, BR 30.0, XNBR (7%) 10.0, MMT 6.0, ZnO 3.0, Stearic Acid 2.0, 6PPD 1.0, Sulfur 1.6, TBBS 1.7, DPG 1.8.		

Table 3.23-SBR/BR gum vulcanizates and nanocomposite formulations

Formulations*	FSSBR: BR (70:30)		SSBR: BR (70:30)		ESBR: BR (70:30)	
	Gum (G1)	filled (R1)	Gum (G2)	filled (R2)	Gum (G3)	filled (R3)
XNBR (7%)	0	10.0	0	10.0	0	10.0
Clay	0	6.0	0	6.0	0	6.0

* Other common ingredients are ZnO 3.0, Stearic Acid 2.0, 6PPD 1.0, Sulfur 1.6, TBBS 1.7, DPG 1.8.

Table 3.24-SBR/BR nanocomposite formulation-clay and XNBR dosages optimization

Compound code	D0	D1	D2	D3	D4	D5	D6
Organoclay ,Phr*	0.0	3.8	6.0	8.3	4.4	7.1	9.8
XNBR (7%),phr	0.0	6.3	10.0	13.8	5.6	8.9	12.2

* Common ingredients: ESBR 70, BR 30, ZnO 3, Stearic Acid 2, 6PPD 1, Sulfur 1.6, TBBS 1.70, DPG 1.8.

3.4.2 Compound formulations of SBR/BR-dual fillers nanocomposites

The compound formulations of different nanocomposites and Control compounds (standard passenger car radial tread recipes) are shown in Tables 3.25 and 3.26.

Table 3.25-SBR/BR compound formulations- "dual filler" nanocomposites (phr) [a]

	ESBR	SSBR	FSSBR	PBR	XNBR	MMT	CB	Silica	TDESP
EG	70.0			30.0					
SG		70.0		30.0					
EOC-6	70.0			30.0	10.0	6.0			
SOC-6		70.0		30.0	10.0	6.0			
EC-5	70.0			30.0	10.0	4.0	5.0		
EC-15	70.0			30.0	10.0	4.0	15.0		
EC-25	70.0			30.0	10.0	4.0	25.0		
SC-25		70.0		30.0	10.0	4.0	25.0		
FC-25			70.0	30.0	10.0	4.0	25.0		
ES-5	70.0			30.0	10.0	4.0		5.0	2.0
ES-15	70.0			30.0	10.0	4.0		15.0	2.0
ES-25	70.0			30.0	10.0	4.0		25.0	2.0
SS-25		70.0		30.0	10.0	4.0		25.0	2.0
FS-25			70.0	30.0	10.0	4.0		25.0	2.0

[a] other common ingredients: ZnO 3.0, Stearic Acid 2.0, 6PPD 1.0, Sulfur 1.6, TBBS 1.70, DPG 1.8

Table 3.26-Control compound formulations (phr)

	ESBR	SSBR	BR	Carbon Black N220	Silica 7000GR	TDESP Si-69
Control-1	70.0	-	30.0	70.0	-	-
Control-2	-	70.0	30.0	-	70.0	7.0

3.4.3 NR/BR-organoclay nanocomposites formulations

The detailed compound formulations (phr) are presented in Table 3.27.

Table 3.27-NR/BR clay nanocomposites formulations* (phr)

			NR	BR	XNBR	Clay
Effect of carboxyl %	NBG	Gum	70.0	30.0	0.0	0.0
	NB1	1% carboxyl	70.0	30.0	10.0	7.0
	NB4	4% carboxyl	70.0	30.0	10.0	7.0
	NB7	7% carboxyl	70.0	30.0	10.0	7.0
Effect of mixing methods	OM	2 rolls mill	70.0	30.0	10.0	7.0
	SM	Solution	70.0	30.0	10.0	7.0
	IM	Internal Mixer	70.0	30.0	10.0	7.0
Clay dosages variation	F0	Gum	70.0	30.0	0.0	0.0
	F4		70.0	30.0	10.0	4.0
	F7		70.0	30.0	10.0	7.0
	F10		70.0	30.0	10.0	10.0

* Common ingredients: Zinc Oxide 5.0, Stearic acid 2.5, 6PPD 1.0, Sulfur 1.5, TBBS 1.3, and DPG 0.5.

3.4.3 Compound formulations of NR/BR-dual fillers nanocomposites

The compound formulations of NR/BR dual filler nanocomposites are presented in Table 3.28 and the formulation (phr) of Control compounds are as follows;

A. Control 3: NR 70.0, BR 30.0, Carbon Black (N220) 50 and Sulfur/accelerator = 1.5
B. Control 4: NR 70.0, BR 30.0, HD silica 45.0, X 50-S 10.0 and Sulfur/accelerator = 1.0

Table 3.28-Compound formations: NR/BR "dual filler" nanocomposites

Formulations*	NM-7	NC-10	NC-15	NC-20	NS-10	NS-15	*NS-20*
NR	70.0	70.0	70.0	70.0	70.0	70.0	*70.0*
BR	30.0	30.0	30.0	30.0	30.0	30.0	*30*
XNBR	10.0	10.0	10.0	10.0	10.0	10.0	*10.0*
Clay	7.0	5.0	5.0	5.0	5.0	5.0	*5.0*
Carbon Black		10.0	15.0	20.0			
Silica					10.0	15.0	*20.0*
Silane, X 50S					*2.0*	*3.0*	*4.0*

*Common ingredients: Zinc Oxide 5.0, Stearic acid 2.5, 6PPD 1.0, Sulfur 1.5, TBBS 1.3, DPG 0.5

3.5 MATERIAL TESTING AND CHARACTERIZATION

3.5.1 Rheological properties

The cure characteristic of the rubber nanocomposites was studied using a moving die rheometer (MDR 2000E, Alpha Technology, USA). This rheometer is capable of measuring rubber compound cure under isothermal test conditions at constant strain and frequency. Temperature range is ambient to 200°C. The oscillation frequency is 1.667 Hz and strain 0.5, 1.0 or 3.0 degrees (2.8%, 7%, 14% or 42%).

Fig. 3.19- MDR 2000E

Rheometric studies were carried out with 0.5° torque for 30 minutes at 160°C for all SBR/BR compounds and 150°C for all NR/BR compounds including nanocomposites.

3.5.2 Sample preparation

Rubber samples were prepared in compression mould under pressure at temperature and time mentioned in Table 3.29.

Table 3.29-Rubber sample vulcanization conditions

Compound	Samples	Temperature	Time
SBR/BR	Rubber sheet of 2±0.1 mm thickness(6''X6'')	160°C	Tc90 + 3 minutes
	Abrasion and Heat build Up	160°C	Tc90 + 10 minutes
NR/BR	Rubber sheet of 2±0.1 mm thickness(6''X6'')	150°C	Tc90 + 3 minutes
	Abrasion and Heat build Up	150°C	Tc90 + 10 minutes

The sample was cured in hydraulic presses of 100 tons having and 50 tons (M/s.Santosh, India) as shown in the Fig. 3.20. Different samples specimens were cut from tensile rubber sheet using pneumatic hollow die punch of M/s.Ceast, Italy (Fig. 3.21).

Fig. 3.20- Hydraulic curing press

Fig. 3.21- Hollow die punch

3.5.3 Rubber specimens for mechanical and dynamic test

The rubber samples used for mechanical and dynamic mechanical testing are presented in Fig.3.22.

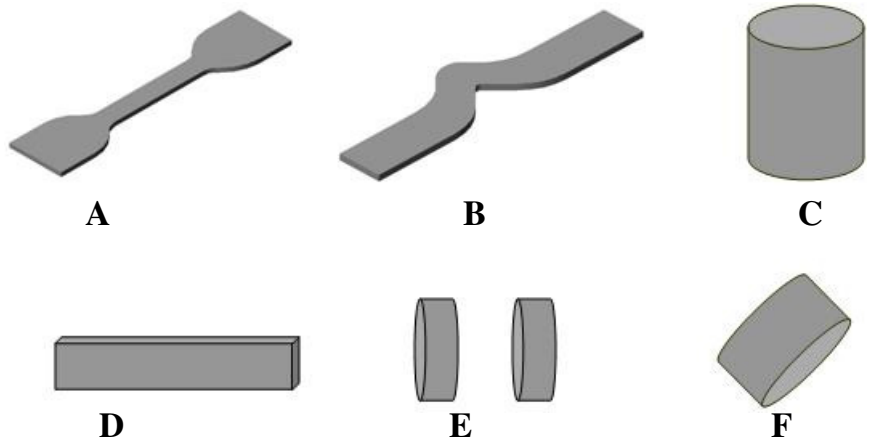

Fig. 3.22 - Rubber specimens (A) Tensile dumbbell (B) Angle tear specimen (C) HBU specimen (D) DMA Tension- compression (E) DMA Shear (F) DIN abrasion specimen

3.5.5 Stress-Strain properties

Stress-Strain properties (modulus, tensile strength, elongation at break and breaking energy) were measured using a universal tensile testing machine (Zwick Z010, Zwick, Germany) using 2.5 kN load cell. Test was done with a cross head speed of 200 mm/min as per ISO 527. The extensometer gauge length was 25 mm, sample width was 6 mm and thickness was 2.0±0.2 mm.

3.5.6. Tear properties

Tear strength and tear energy were measured by using Zwick UTM as per ASTM D-624 using angle tear specimen. The test speed was 200 mm/min and load cell used was 2.5 kN and temperature was 25^{o}C.

3.5.7 Hardness test

The rubber hardness was measured using a circular sample of 30 mm diameter and 6 mm thickness. Measurement was carried out using Automatic Hardness Tester (Ceast, Italy) with fixed load as per ASTM D2230.The rubber hardness was expressed in Shore-A.

Fig. 3.23- Zwick UTM

Fig. 3.24- Hardness tester

3.5.8 DIN abrasion test

Abrasion loss was determined using Zwick Abrader Zwick 6012 (Zwick, Germany) as per DIN 53516. The circular rubber sample fitted the holder in the abrader against rotation drum while sample is moving from one end to other end. The path length was 40 meter. The load on the sample was 10 N.

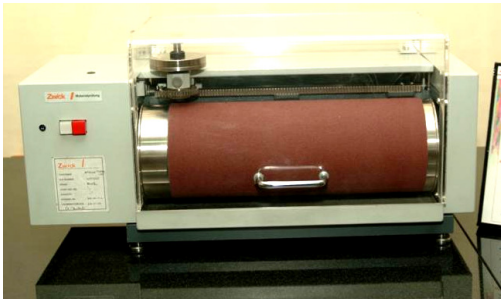

Fig. 3.25- Zwick DIN abrader

The volume loss of rubber sample is calculated using the following formula;

$$\text{Volume loss } (mm^3) = \frac{\text{Weight loss of sample X 200}}{\text{Density of sample X Weight loss of standard sample}}$$

3.5.9 Heat build up test

Heat development was measured using BF Goodrich Flexometer Model II from BF Goodrich, USA as per ASTM D623. The sample was cylindrical having height 25 mm and diameter 17 mm. The sample is vibrating with frequency of 10 Hz and strain 17.5% with 55 lbs load on the sample. The test time was 25 minutes and preheat time was 60 minutes. The initial base

temperature PCR and TBR are 50°C and 100°C respectively. The increase in temperature measured after 25 minutes was the heat build up in the sample.

Fig. 3.26- BF Goodrich Flexometer

Fig. 3.27- Viscoanalyse VA 400

3.5.10 Dynamic mechanical test

The viscoelastic properties of rubber compounds were determined by dynamic-mechanical analysis using Viscoanalyzer VA4000 (Metravib RDS, France). The temperature sweep was done in tension compression mode from –30 °C to 80 °C with a heating rate of 2°C/min at 10 Hz and 0.25 % single strain amplitude (SSA) for SBR/BR blend. For NR/BR blends temperature sweep was done in tension compression mode from –110 °C to 80 °C with a heating rate of 2 °C/min at 3 Hz and 0.1 % single strain amplitude (SSA)

3.5.11 Filler characterization

Fig. 3.28- Particle size analyzer

The particle size distribution of all the fillers carbon black, silica and nanoclay were measured by Particle Size Analyzer- Master Sizer 2000 (Malvern Instruments , UK). The test conditions were Stirrer rpm: 750; Pump rpm: 1250; Sonication: 50% for 10 min and obscuration around 5%.

BET Nitrogen surface area of carbon black and silica were measured by Nitrogen Surface Area Analyzer- Nova 1200 (Quantachrome, USA). The drying condition for silica was 1 hour at 160^{o}C and for carbon black 30 minutes at 300^{o}C and partial pressure was maintained at 0.05 to 0.3 and Nitrogen flow rate was at 15 psi. Structure of carbon black and silica was measured by Brabender

Carbon black structure is determined by DBP absorption method using DBP (Dibutylphthalate) Absorpto meter (Brabender A.G, Germany). Test conditions are sample weight is 20 gm, drying at 125^{o}C for 1 hour and rotor speed is 125 rpm.

3.5.12 X-ray diffraction (XRD)

The nanocomposites were also characterized by X-ray diffraction and transmission electron microscopy (TEM). The basal spacing of the organoclay was evaluated by means of wide-angle X-ray diffraction in a Phillips X-pert Pro diffractometer (PANalytical, Eindhoven, NL) at narrow angular range of 2^0–10^0 using Cu K_α-radiation (k = 0.154 nm).

In these studies acceleration voltages of 40 kV and beam current of 30 mA were used. The scanning rate was maintained at 1.5^0/min. The d-spacing of the particles were calculated using the Bragg's law.

3.5.13 Transmission electron microscopy (TEM)

The microstructure of nanocomposite was imaged using Transmission Electron Microscopy. Ultra-thin sections of nanocomposite were cut by microtome at about -100°C (below glass transition temperature, Tg of rubber), and the images were taken by JEM 2010 with an acceleration voltage of 200 kV.

3.6 MATERIAL PARAMETER IDENTIFICATION FOR TIRE SIMULATION

A tire is a composite material and consists of different materials such as rubber compounds, textile fabrics, steel cords and bead wire; however for different tire components different rubber compounds are used. For structural simulation stress-strain properties of all these materials in uniaxial tension and compression mode are required and were measured in the laboratory using Zwick UTM.

The rubber samples were subjected to repeated cyclic stress-strain cycle before testing to remove the Mullins effect. Test speed was kept low 5 mm/ minute to capture equilibrium stress-strain data. Stress-strain properties of fabrics (polyester and nylon) and steel cords were also determined by Zwick UTM and test speed were 50 mm/min in tension mode.

Viscoelastic properties of rubber (tanδ) were measured using dynamic mechanical thermal analyzer (VA 4000) from Metravib, France by strain sweep which was carried out in a simple shear mode at two different temperatures 30^{o} and 60^{o}C at 10 Hz and double strain amplitude was varied from 0.02 % to 80% .

3.7 ROLLING RESISTANCE EXPERIMENT

The rolling resistance computed through finite element tire simulation was validated by indoor rolling resistance measurement using drum type pulley wheel machine attached with rolling resistance measurement kits.

3.8.1 Passenger car radial (PCR) tire

Rolling resistance test of 205/60R15 and 155/70R14 PCR tires with Control (standard) tread compounds were carried out on Pulley Wheel (drum type) machine attached with rolling resistance measurement kits as per SAE test standard. Two numbers of tires in each category were tested and average rolling resistance value was taken for validation. The test conditions are described in Table 3.26.

3.8.2 Truck bus radial (TBR) tires

Rolling resistance test of 10.00R20 , 295/80R22.5 and 315/80R22.5 TBR with Control carbon black tread compounds (standard tread) were carried out on Pulley Wheel (drum type) machine as per ISO 18164 test standard. Average results of two tires in each category were used for validation. The test conditions are described in Table 3.30.

Table 3.30- Rolling resistance (RR) test conditions

Parameters	**PCR**	***TBR***
Test Standard	SAE J 1269	*ISO 18164*
Wheel Speed	80 kmph	*80 kmph*
Room Temperature	25 ± 2 °C	*25 ± 2 °C*
Inflation Pressure (I.P)	35 psi	*Rated Inflation*
Load	80% rated load	*85% of Rated Load*
Conditioning	*30 min warm up at rated load and rated inflation*	*90 min warm up at rated load and rated inflation*

The standard tire rolling resistance measurement equipment is shown in the Fig. 3.29.

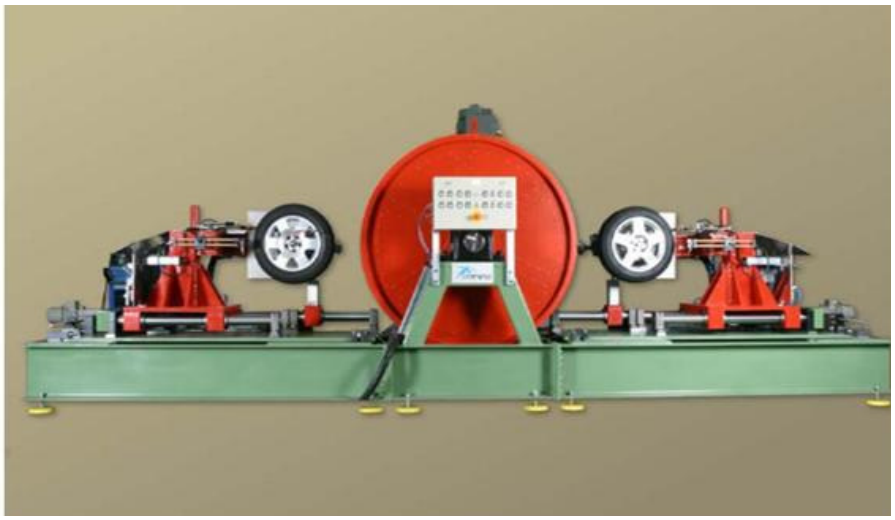

Fig. 3.29- Tire rolling resistance measurement equipment

CHAPTER 4

DEVELOPMENT AND CHARACTERIZATION OF NANOCOMPOSITES FOR PASSENGER CAR RADIAL (PCR) TIRE TREAD APPLICATION

Passenger car radial (PCR) tire tread compounds are almost always prepared from blends of SBR/BR. One objective of this study was to develop low hysteresis passenger car radial tread compound with SBR/BR – organoclay nanocomposite. To achieve these goals two different types of high performance SBR/BR based nanocomposites were developed and characterized. In this Chapter the effect of organoclay and dual fillers on mechanical and viscoelastic properties of these nanocomposites are elaborated and the results obtained are discussed in detail.

Fig. 4.1- PCR Tire

4.1 PREPARATION AND CHARACTERIZATION OF NANOCOMPOSITES BASED ON ORGANOCLAY AND BLENDS OF DIFFERENT TYPES OF SBR WITH BR

4.1.1 Introduction

Polymer/clay nanocomposites are being extensively investigated because these nanocomposites have enormous potential for commercial utilization in diversified areas such as coating, flame-retarding, barrier materials, electronic materials and composite. Rubbers are generally organophilic; unmodified nanoclay (Na-Montmorilonite) disperses in rubbers with great

difficulty. However, through clay surface modification, nanoclay can be made organophilic called organoclay and, therefore, compatible with conventional organic rubbers. Modified organoclay disperse readily in rubbers. Cloisite®15A organically modified nanoclay (Na-MMT) used in this investigation is referred as organoclay (OC) in the subsequent Chapters.

In this investigation, nanocomposites based on 70/30, SBR/BR and organoclay using XNBR as compatibilizer were prepared and characterized aiming for PCR tire tread applications. The performance of nanocomposites depends on several parameters such as nature of rubber, dosage of organoclay and most importantly exfoliation of the organoclay. Similarly organoclay dispersion also depends on a number of parameters such as;

a) Polarity of compatibilizer (Carboxyl group % in XNBR)
b) Mixing techniques
c) Types of SBR rubbers
d) Dosages of organoclay and XNBR

To achieve the best performance properties in the nanocomposite, the effects of all these parameters were studied independently and sequentially and finally the nanocomposite that gave the best performance was selected and used in the preparation of high performance tread compounds. The raw materials, compound formulations, synthesis of nanocomposite, testing and characterization methods are detailed in Chapter 3 in Materials and methods; however compounds codes and brief descriptions are presented in Table 4.1. The results and discussion incorporating the influence of each parameter on mechanical and dynamic mechanical properties of nanocomposites are elaborated in the subsequent sections.

4.1.2 Rheometric properties

The importance of rheometric properties is undisputed since it provides valuable information on compound processing and curing characteristics. The time required to cure any rubber compound at a particular temperature is known as optimum cure time (Tc90) and it is obtained from rheometric data. It also provides additional information like minimum torque (ML) representing the compound viscosity, maximum torque (MH) representing compound modulus and scorch time (Ts2) representing process safety. Table 4.2 presents rheometric properties of gum compounds and various other nanocomposite formulations. Gum compound has minimum viscosity as well as minimum modulus since it does not have any filler. Gum compound (G1)

shows highest scorch safety and slowest curing rate among all the compounds. With addition of organoclay, cure became faster and scorch time gets reduced substantially as observed in C-0.

Table 4.1-Compound codes and brief descriptions

	Code	Rubber (Phr)	XNBR (phr)	Organoclay (phr)	Mixing Method
% Carboxyl group in XNBR	C-0	FSSBR/BR (70/30)	XNBR-0 (10)	6.0	Internal mixer
	C-1		XNBR-1 (10)		
	C-4		XNBR-4 (10)		
	C-7		XNBR-7 (10)		
Mixing Methods	M-1	FSSBR/BR (70/30)	XNBR-7 (10)	6.0	2 roll Mill
	M-2				Solution
	M-3				Internal mixer
Type of SBR	G1	FSSBR/BR (70/30)	XNBR-7 (10)	0.0	Internal mixer
	R1			6.0	
	G2	SSBR/BR (70/30)	XNBR-7 (10)	0.0	Internal mixer
	R1			6.0	
	G3	ESBR/BR (70/30)	XNBR-7 (10)	0.0	Internal mixer
	R1			6.0	
Dosage variation of XNBR and organoclay	D0	ESBR/BR (70/30)	0.0	0.0	Internal mixer
	D1		XNBR-7 (6.3)	3.8	
	D2		XNBR-7 (10.0)	6.0	
	D3		XNBR-7 (13.8)	8.3	
	D4		XNBR-7 (5.6)	4.4	
	D5		XNBR-7 (8.9)	7.1	
	D6		XNBR-7 (12.2)	9.8	

In nanocomposite, with the increase of carboxyllation of compatibilizer, compound viscosity as well as compound modulus increases which are attributed to higher filler-rubber interaction at higher % of carboxyl groups. However; with the increase of % carboxyl group, the scorch times

were higher and cure became slower. Carboxyl groups being acidic in nature retards the curing reaction as a results cure rate becomes slower.

Table 4.2-Rheometric properties (MDR; 160^{o}C/ 20 min)

	G1	C-0	C-1	C-4	C-7
Min. Torque (ML) dN-m	0.23	0.43	0.47	0.48	0.53
Max. Torque (MH) dN-m	6.58	7.41	7.99	8.14	8.34
Δ Torque (MH – ML), dN-m	6.35	6.94	7.56	7.66	7.81
Scorch Time (Ts2) min	**2.68**	**1.57**	**1.63**	**1.72**	**1.83**
50% Cure Time (Tc50) min	3.09	1.85	2.02	2.08	2.17
Optimum Cure Time (Tc90) min	**6.21**	**3.36**	**4.40**	**4.60**	**5.78**

4.1.3 Mechanical Properties

4.1.3.1 Effect of carboxyl content of compatibilizer in nanocomposite.

Organoclay is a polar material and has layer silicate structure. SBR is non polar rubber and it has bulky styrene group in its side chain. To achieve good clay dispersion, there should be good interaction between organoclay and rubber. Further rubber molecules also penetrate easily into the gap among the silicate layers and expand the layer structure. SBR shows less interaction with organoclay due to its non polar nature and bulky styrene group which is evident from poor mechanical property of SBR nanocomposite (Bhowmick *et al*. 2003). However, use of polar rubber as compatibilizer (Das *et al.* 2008) has improved the mechanical properties of SBR nanocomposite remarkably due to fine dispersion of clay.

The polarity of the carrier polymer (compatibilizer) has an immense influence on the mechanical properties of the SBR/BR nanocomposites. Natural rubber (NR) undergoes strain induced crystallization and hence shows very high strength without any filler at higher strain, on the other hand SBR is a non-crystallize rubber, therefore 40-50 phr reinforcing filler such as carbon black is necessary to get comparable strength to NR. The role of filler in SBR is not only to improve modulus, hardness and tear strength but also to improve tensile strength.

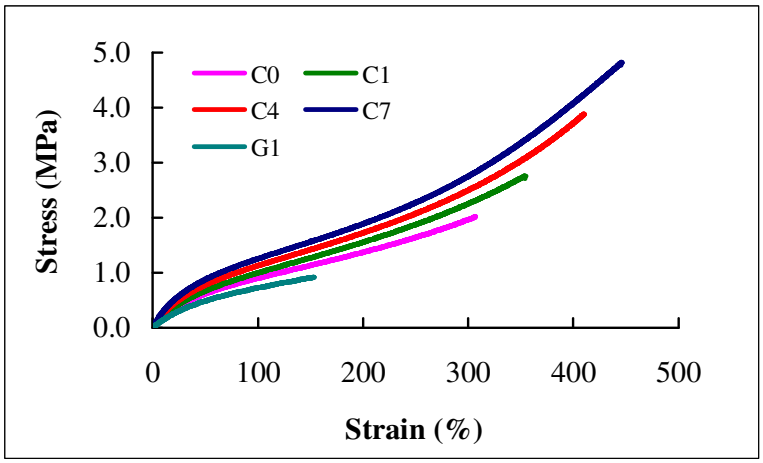

Fig. 4.2-Effect of carboxyllation on stress-strain properties

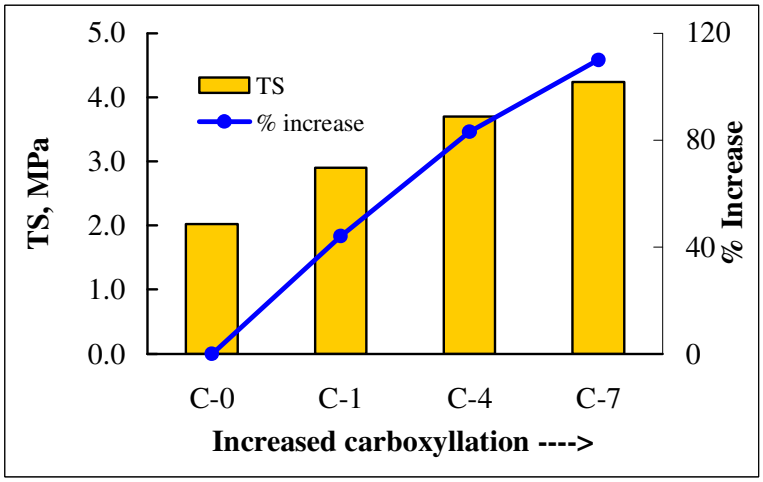

Fig. 4.3-Effect of % carboxyl group on T.S properties of nanocomposite

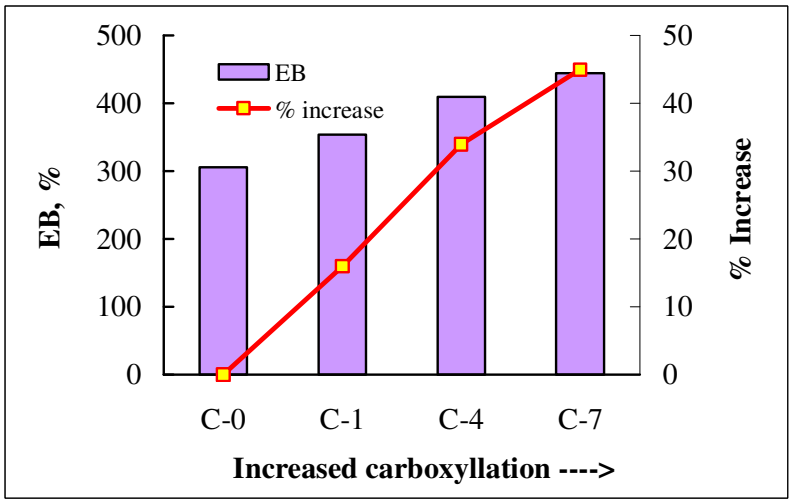

Fig. 4.4-Effect of % carboxyl group on E.B properties of nanocomposite

The stress-strain properties of the nanocomposites with varying percentage of carboxyl group are presented in Fig. 4.2. Substantial improvement in stress strain properties was observed in nanocomposite (C0) compared to gum compound (G1). As % carboxyl group in XNBR increases, the polarity of the polymer also increases. It was observed that all the mechanical properties like modulus, tensile strength, elongation at break and breaking energy increase with the increase of carboxyl group percentage in XNBR. This behavior is attributed to higher interfacial interaction between organoclay and XNBR which increases with the increasing polarity of XNBR due to higher carboxyl content. Higher interfacial interaction between the filler and the rubber leads to better intercalation and exfoliation of organoclay within the rubber matrix, which leads to enhanced mechanical and dynamic mechanical properties. In elastomeric nanocomposite, interfacial interactions between filler particles and rubber matrix affect;

a) Dispersibility of the nano-fillers in the rubber
b) Adhesion properties of fillers and rubber
c) Filler flocculation (re-agglomeration) within rubber matrix.

XNBR has the highest polarity among all the rubbers used and organoclay is highly polar filler in comparison with other fillers, hence combination of XNBR with organoclay show the highest free energy compared to any other rubber-filler combination; this in turn indicates that the dispersion of organoclay in XNBR rubber is likely to be very good.

Effect carboxyl percentage on tensile strength (TS), elongation at break (EB) and breaking energy (BE) are presented in Fig. 4.3, 4.4 and 4.5 respectively. It is observed from Fig. 4.2 that tensile stress increases from 2.0 MPa to 4.2 MPa when carboxyl content in XNBR increases from 0 to 7%. Improvement of TS, EB and BE are 110, 45 and 154 % respectively when carboxyl % changed from 0 to 7%.

4.1.3.2 Effect of mixing techniques

It is known that mixing technique has a great influence on the mechanical property of nanocomposites hence three different mixing techniques viz. 2 roll mill, solution method and internal mixer were used to prepare the nanocomposite. It was noticed that mixing of organoclay was extremely difficult in 2 roll mill, while solution method required a large quantity of solvent which had to be removed after mixing.

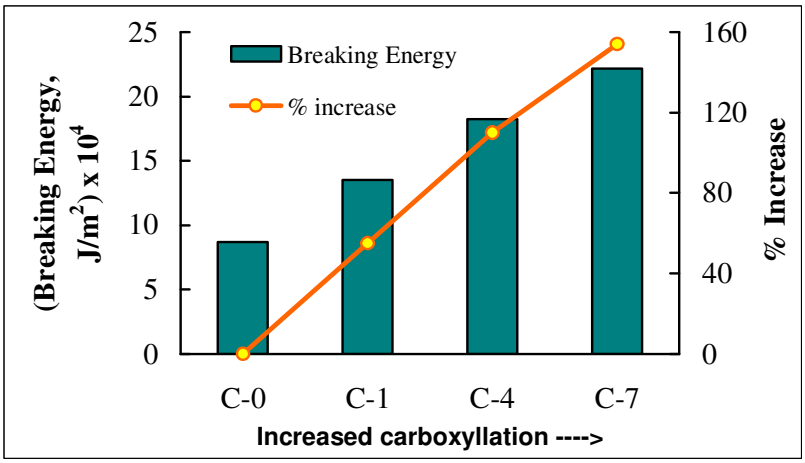

Fig. 4.5-Effect of % carboxyl group on breaking energy properties of nanocomposite

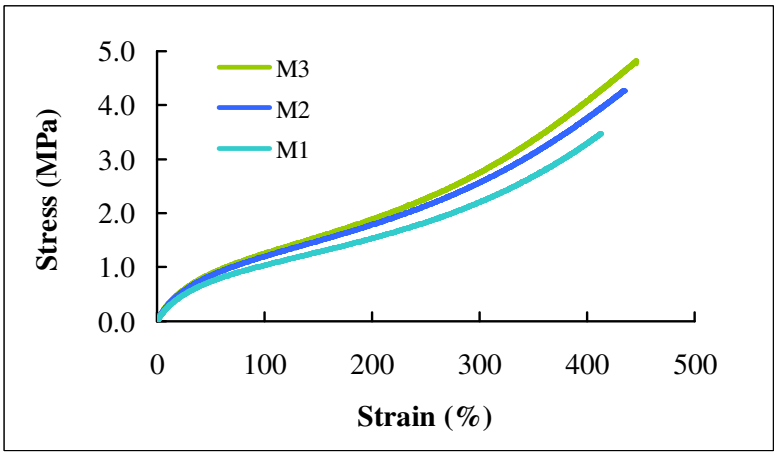

Fig. 4.6-Effect of different mixing techniques on stress-strain properties of nanocomposites

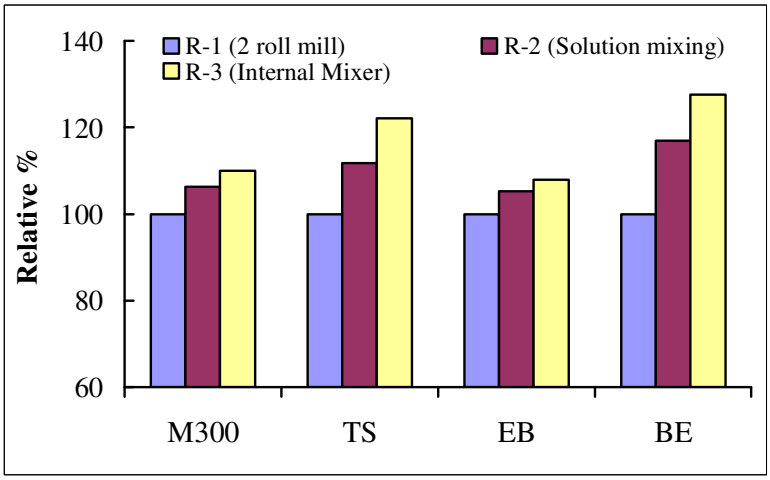

Fig. 4.7-Comparative properties of different mixing techniques taking 2 roll mill as 100

In comparison to these techniques the internal mixer provides very easy and convenient mixing. The stress-strain properties of nanocomposites are shown in Fig. 4.6. Internal mixer exhibited the best mechanical properties like modulus, tensile strength, elongation at break and breaking energy followed by solution mixing and 2 roll mill mixing, hence internal mixing was adopted here for further investigation. Comparative properties of different mixing techniques are shown in Fig. 4.7 considering the properties obtained using 2 roll mill as reference.

4.1.3.3 Compatibilizer (XNBR) and filler(organoclay) dosage optimization

The dosages of organoclay and compatibiliser have immense influence on mechanical properties. The combined effect of organoclay and XNBR dosages on mechanical properties was studied and is presented in Fig. 4.8 and Table 4.3. Nanocomposites with 10 phr XNBR and 6 phr organoclay exhibited the best properties such as tensile strength, elongation at break and breaking energy.

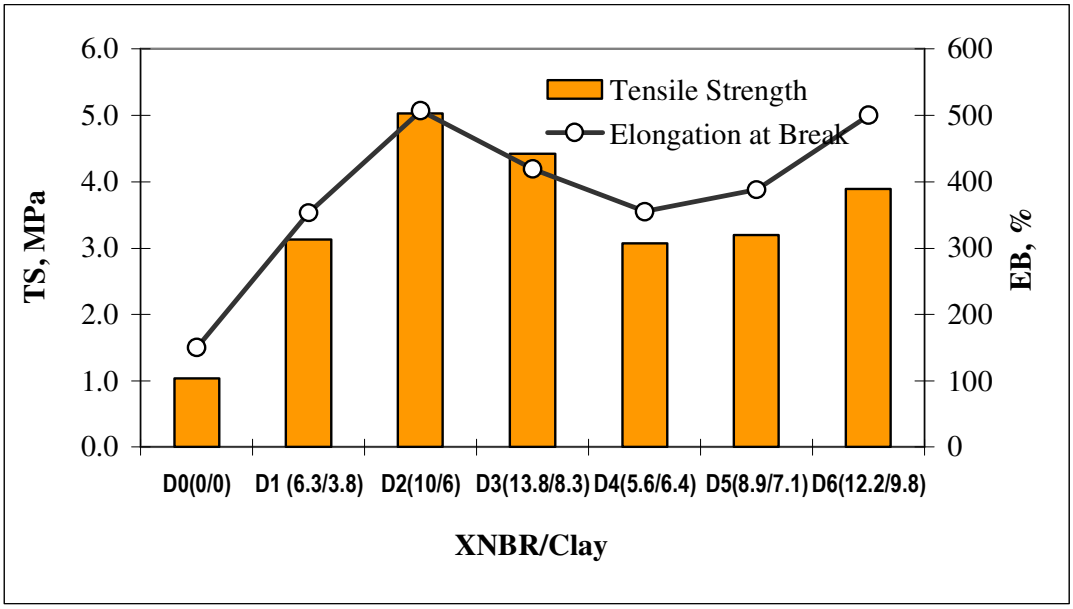

Fig. 4.8- Optimization of Clay and XNBR dosages in nanocomposite

4.1.3.4 Effect of type of SBR

The properties of nanocomposites with different type of SBR were also studied in this work. The mechanical properties of three styrene butadiene rubbers functionalized solution styrene butadiene rubber (FSSBR), solution styrene butadiene rubber (SSBR) and emulsion styrene butadiene rubber (ESBR) were very close, however ESBR showed better mechanical properties

than SSBR and FSSBR (Table 4.4). ESBR has higher polarity than SSBR and hence better interfacial interaction with organoclay is expected which resulted in better mechanical properties.

Table 4.3-organoclay and XNBR dosages optimization- formulations, rheometric and mechanical properties

Compound code	D0	D1	D2	D3	D4	D5	D6
MH-ML (dN-m)	7.6	7.3	7.0	6.8	7.5	7.2	7.0
Scorch time, Ts2 (min)	3.85	1.95	1.76	1.90	1.92	1.87	1.85
Optimum cure time, Tc90 (min)	6.43	4.93	5.68	5.45	4.67	5.18	5.80
300% Modulus, M300 (MPa)	-	2.62	2.68	2.63	2.54	2.44	2.41
Tensile Strength, T.S (MPa)	1.04	3.13	5.03	4.42	3.07	3.20	3.89
Elongation at Break, E.B (%)	150	353	507	419	355	388	500
Breaking Energy, BE (J/m^2) x 10^4	2.44	14.30	30.21	25.44	14.26	16.26	26.84

Table 4.4-Mechanical properties of gum compounds and SBR/BR-organoclay nanocomposites

Properties	FSSBR/BR		SSBR/BR		ESBR/BR	
	G1	R-1	G2	R-2	G3	R-3
	Gum	filled	Gum	filled	Gum	filled
Hardness, Shore A	49	54	50	55	51	56
100% Modulus, MPa	0.73	1.26	0.76	1.22	0.84	1.27
300% Modulus, MPa	-	2.77	-	2.65	-	2.75
Tensile Strength, MPa	0.93	4.76	1.10	4.90	1.10	5.36
Elongation at Break,%	154	445	169	470	155	507
Breaking Energy, J/m^2 x 10^4	2.27	22.13	2.76	24.2	2.63	32.20

4.1.4 Viscoelastic Properties

The viscoelastic properties of nanocomposites were measured by dynamic mechanical testing. The dynamic mechanical properties of nanocomposites of all three types of SBR gum compounds (G1, G2 and G3) and corresponding nanocomposites (R1, R2 and R3) were studied by temperature sweeps from –110°C to +70°C (Table 4.5 and Fig. 4.9 and 4.10). ESBR showed the highest storage modulus, loss modulus and Tan δ followed by SSBR and FSSBR as reported in Table 4.5.

Table 4.5-dynamic mechanical properties of gum compounds and SBR/BR-organoclay nanocomposites

Properties	FSSBR		SSBR		ESBR	
	G1	R-1	G2	R-2	G3	R-3
Tg (°C)	***-29.0***	***-30.5***	***-26.2***	***-28.5***	***-50.0***	***-53.5***
Tan δ at Tg	1.001	0.821	0.928	0.679	0.981	0.572
Storage Modulus, E' at 25°C, MPa	2.90	4.43	2.66	4.58	2.87	6.74
Loss Modulus, E'' at 25°C, MPa	0.209	0.412	0.226	0.531	0.196	0.995
Tan δ at 25°C	0.072	0.093	0.085	0.116	0.068	0.148

Both SSBR and FSSBR compounds and their nanocomposites have glass transition temperatures (Tg) in the range –26°C to –30°C. However, Tg of ESBR gum compound was at –50°C and its nanocomposite was at –53.5°C. Due to high vinyl content in SSBR and FSSBR, Tg gets shifted towards ambient temperature. All the nanocomposites exhibited lower Tan δ at Tg compared to the corresponding unfilled gum compounds as shown in Fig. 4.9 and 4.10. At glass transition temperature (Tg), nanocomposites show higher dynamic modulus in comparison with gum compounds and this pattern is attributed to the enhancement of stiffness in the matrix by organoclay. The Tan δ maximum decreased with the addition of organoclay, indicating good polymer-filler interaction which affected the relaxation mechanisms. However at higher temperature Tan δ values of nanocomposites were higher than corresponding gum vulcanizates and these are attributed to filler-filler interaction of organoclay which increases the loss modulus and hence returns higher Tan δ.

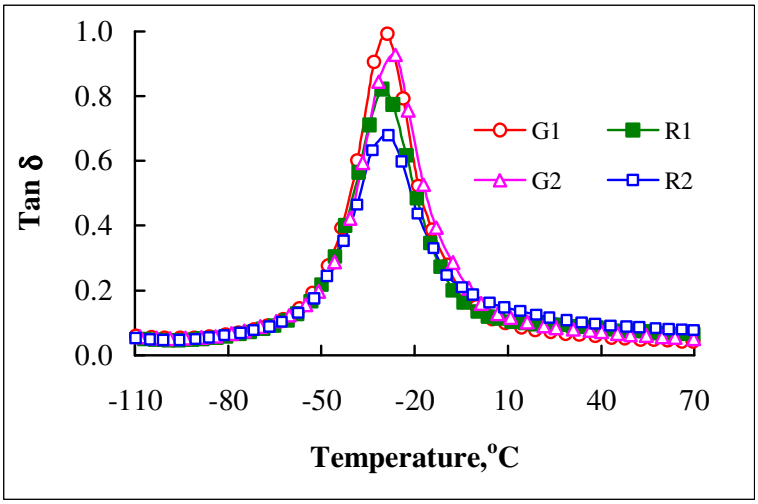

Fig. 4.9- Tan δ versus temperature of SSBR - Gum compounds and nanocomposites

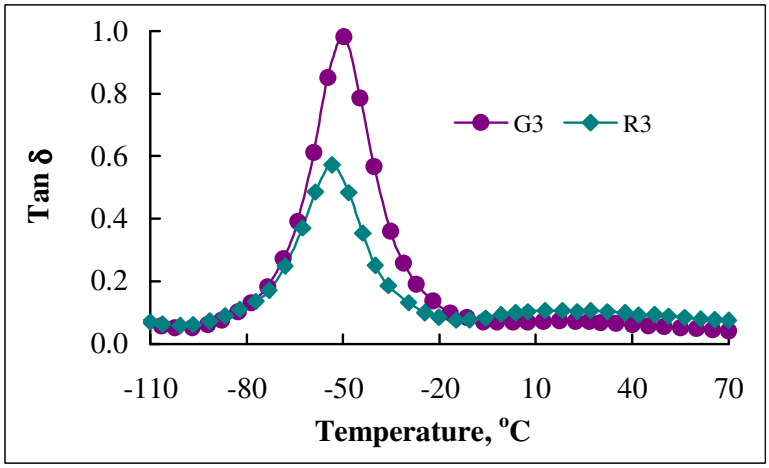

Fig. 4.10- Tan δ versus temperature of ESBR - Gum compounds and nanocomposites

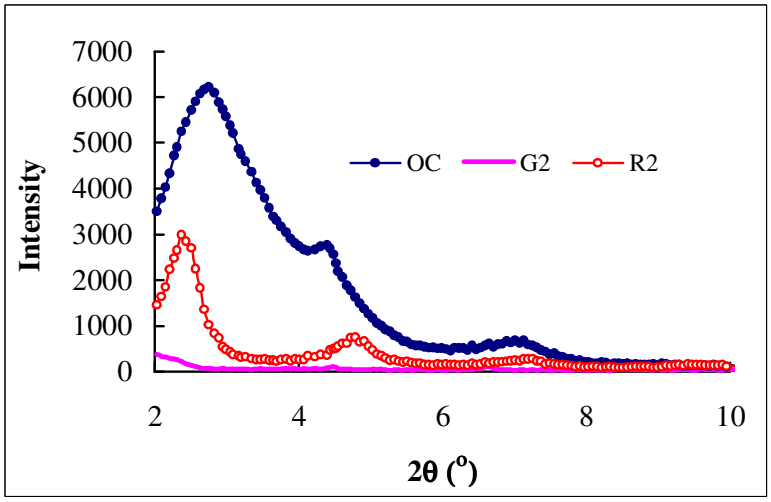

Fig. 4.11-XRD graph of Clay (OC), SSBR/BR gum (G2) and SSBR/BR nanocomposite (R2)

X-Ray Diffraction Study

High-resolution Wide-Angle XRD at lower angular range was used to identify intercalated and aggregated clay structures in rubber matrices. In such nanocomposites, the repetitive multilayer structure is well preserved, allowing the interlayer spacing to be determined. The intercalation of the polymer chains usually increases the interlayer spacing, in comparison with the spacing of the organoclay used, leading to a shift of the diffraction peak toward lower angle values. The diffraction angle or glancing angle (θ) and layer spacing values being related through the Bragg's relation, $n\lambda=2d \sin\theta$, where ''λ'' corresponds to the wave length of the X-ray radiation used in the diffraction experiment, ''d'' is the spacing between diffractional lattice planes and n is the order of diffraction (Alexandre, 2000).

The XRD patterns were obtained for organoclay (OC), gum rubber compound (G2) and nanocomposite (R2). XRD studies of organoclay showed the diffraction peaks at around 2.8^{o}, 4.4^{o}, 7.1^{o} and 9.5^{o}, corresponding to d-spacing 3.1, 2.0, 1.3 and 0.93 nm respectively. The nanocomposite (R2) had shown the diffraction peaks at around 2.39^{o}, 4.79^{o}, and 7.25^{o} corresponding to d-spacing 3.7, 1.8 and 1.2 nm respectively (Fig. 4.11). Diffraction peaks at lower degree and reduction of peaks at higher degree in the nanocomposite indicated that d-spacing between silicates layers had increased. The increase of d_{001}-spacing and reduction of peaks intensity revealed that silicate layers were expanded which resulted in the intercalated/exfoliated structure of nanocomposite.

4.1.6 Transmission Electron Microscopy

The filler dispersion in the nanocomposites was studied by transmission electron microscopy (TEM). TEM images of ultrathin sections of FSSBR/BR nanocomposites mixed by three different methods 2 roll mill mixing, solution methods and internal mixer containing 10 phr XNBR and 6 phr organoclay were studied in this investigation. Fig. 4.12 shows the TEM images of samples prepared by 2 roll mill mixing method (M1). The dark regions are the hard layered silicates while the light region is the soft rubber matrix. TEM reveals mostly intercalated and partially exfoliated structure of the organoclay and it is seen that the ordered structure of layer silicate is also partially retained in 2 roll mill mixing.

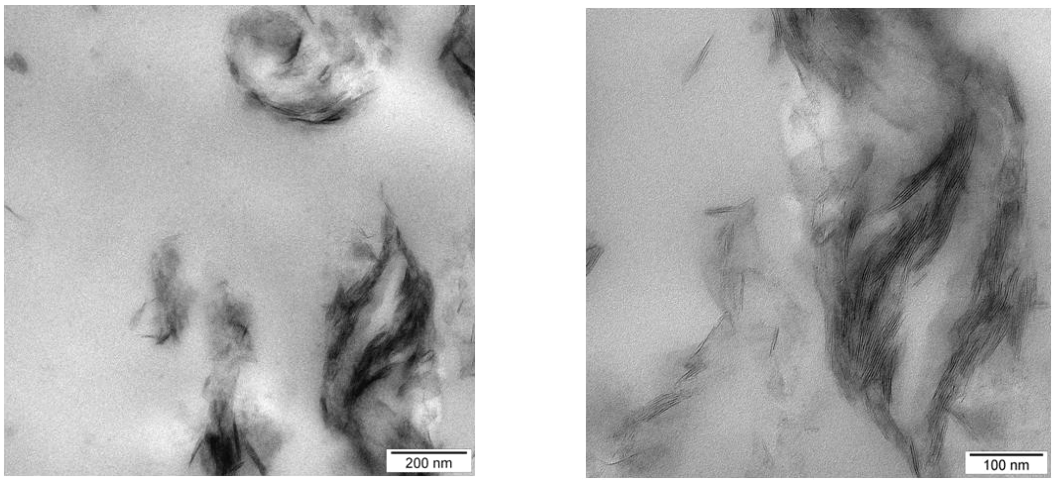

Fig. 4.12- TEM image of nanocomposite (M1) prepared in 2 roll mill.

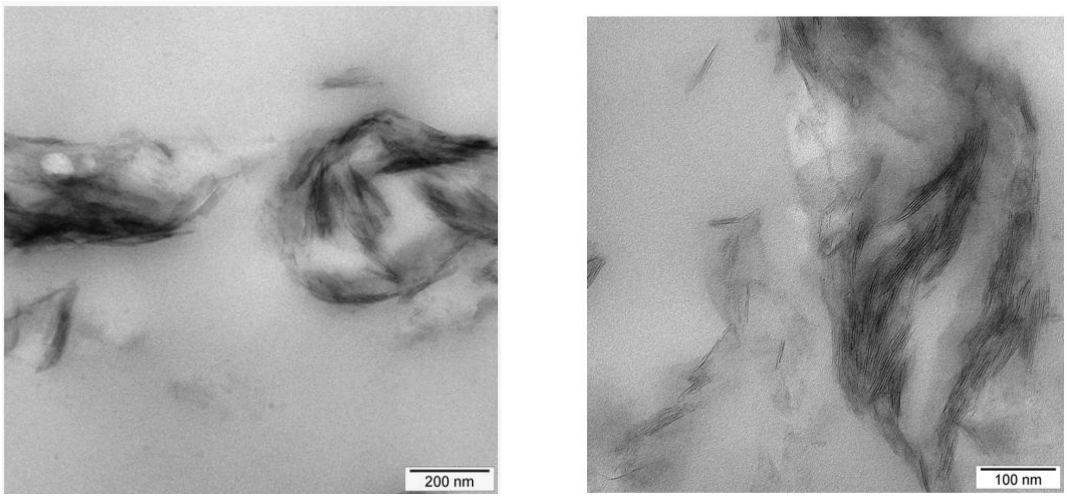

Fig. 4.13- TEM image of nanocomposite (M2) prepared by solution mixing method

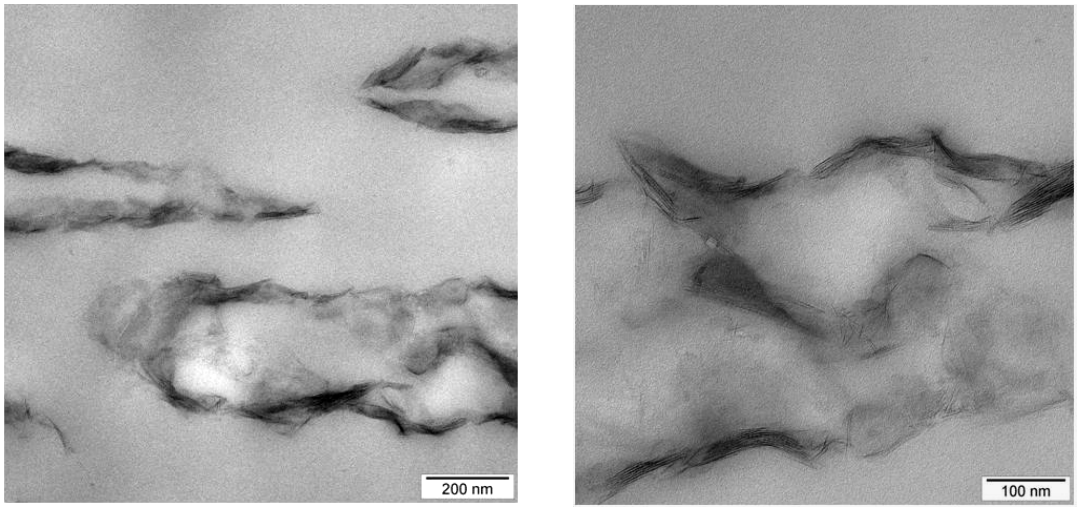

Fig. 4.14- TEM image of nanocomposite (M3) prepared by internal mixer

In solution mixing (M2) mixed intercalated and exfoliated structure was evident from TEM images (Fig. 4.13). In internal mixer, mostly exfoliated and partially intercalated morphology was noticed in TEM images (Fig. 4.14). In internal mixer silicate layer were expanded and randomly oriented. Internal mixer showed the best clay dispersion among all three mixing methods.

4.1.7 Conclusions

i. The mechanical and dynamic mechanical properties of the investigated rubber nanocomposites improved as the carboxyl content in XNBR increased.
ii. Among the three mixing techniques used in this investigation internal mixing resulted in the best properties. Moreover, this method is very convenient for industrial applications. The solution method provided better properties than 2 roll mill mixing but removal of solvent was difficult, time consuming and therefore not feasible for industrial applications where as, mixing of clay in 2 roll mill was quite difficult.
iii. For SBR/BR=70/30 blends, the optimum dosages of organoclay and XNBR were found to be 6 and 10 phr respectively.
iv. Among three types of SBR investigated, ESBR showed the best mechanical properties followed by SSBR and FSSBR.
v. All SBR nanocomposites showed slightly lower glass transition temperature and lower Tan δ values at Tg compared to their corresponding gum counter parts in dynamic mechanical testing.
vi. TEM images of SBR nanocomposites prepared by all three mixing technique exhibited mixed intercalated and exfoliated structure of layer silicate in the matrix; however internal mixer showed the best exfoliated morphology.
vii. XRD investigations also supported the intercalated and exfoliated morphology of nanocomposite which was evidenced by the increase of d-spacing of layer silicate and reduction of peaks intensity.
viii. Although organoclay nanocomposite showed excellent mechanical properties but hardness, modulus and other performance properties such as abrasion resistance, tear strength were not sufficient for tire tread application. Further research is required in this field to improve these properties.

4.2 DEVELOPMENT AND CHARACTERIZATION OF HIGH PERFORMANCE NANOCOMPOSITES BASED ON DUAL FILLER SYSTEM AND BLENDS OF DIFFERENT TYPES OF SBR WITH BR

4.2.1 Introduction

The main objective of this work was to develop nanocomposites which can be used for passenger car radial tire tread to reduce hysteresis loss i.e. rolling resistance of the tire. Besides mechanical properties, nanocomposites used as tread compounds also have to meet the performance requirement of tire treads such as wet and dry traction, handling, rolling resistance and tire wear.

SBR/BR-organoclay nanocomposite showed remarkable improvement of high strain modulus, tensile strength, elongation at break, tear strength and tear energy but could not meet the requirements of hardness, low strain modulus, wear properties and dynamic modulus of tire tread compounds. Tread hardness, low strain modulus and dynamic modulus are important for handling, cornering, braking and tire noise; wear resistance is important for tire durability and hysteresis property is important for wet traction and rolling resistance. Higher hysteresis loss at $0^{o}C$ or below provides higher wet traction and lower value at 60-$70^{o}C$ gives lower rolling resistance.

In order to overcome these deficiencies the concept of dual filler was adopted so as to attain the required compound properties without increasing the hysteresis losses too much. In this section, preparation and characterization of 70/30 SBR/BR dual filler high performance nanocomposites is discussed. The mechanical, viscoelastic and other critical properties of nanocomposites and its comparison with commercial tread compounds with carbon black (Control-1) and silica (Control-2) are elaborated.

The detailed compound formulations are described in Chapter 3, Materials and methods, however compounds codes and their brief descriptions are also given in Table 4.6 for ready reference.

Table 4.6-Compounds code and descriptions

	ESBR	SSBR	FSSBR	PBR	XNBR	MMT	CB	Silica	TDESP
EG	70.0			30.0					
EOC-6	70.0			30.0	10.0	6.0			
SG		70.0		30.0					
SOC-6		70.0		30.0	10.0	6.0			
EC-25	70.0			30.0	10.0	4.0	25.0		
SC-25		70.0		30.0	10.0	4.0	25.0		
FC-25			70.0	30.0	10.0	4.0	25.0		
ES-25	70.0			30.0	10.0	4.0		25.0	2.0
SS-25		70.0		30.0	10.0	4.0		25.0	2.0
FS-25			70.0	30.0	10.0	4.0		25.0	2.0

4.2.2 Filler Characterization

In this investigation, three different fillers like Carbon Black (N220), highly dispersible silica and organoclay are used. The filler particle size and the size distribution of all the fillers are shown in Fig. 4.15. Carbon black (N220) showed bimodal distribution; one in the range of 1 to 50 µm and another is in the range of 50 to 400 µm. Silica showed unimodal distribution in the range of 2 to 40 µm with maximum frequency at around 10 µm. Nanoclay showed broader distribution compared to silica and ranges from 0.4 to 40 µm with maxima at 10 µm.

Surface area of carbon black and silica fillers measured by BET method were 120.5 and 160.2 m^2/g respectively. The secondary structures of agglomerates measured by DBP adsorption number were 116.0 and 198 respectively. The organoclay has layer silica structure with one dimension in nanometer level. It was not possible to separate the layered silicate structure by ultra sonic vibration used during the measurement of particle size and particle size distribution; as a result the particle size of nanoclay measured by particle size analyzer is not in the nano scale. Ahmed (2009) measured the particle size distribution of nanoclay using image analysis software from the TEM image of Nanocomposite and reported particle size in the range 10 to 60 nm.

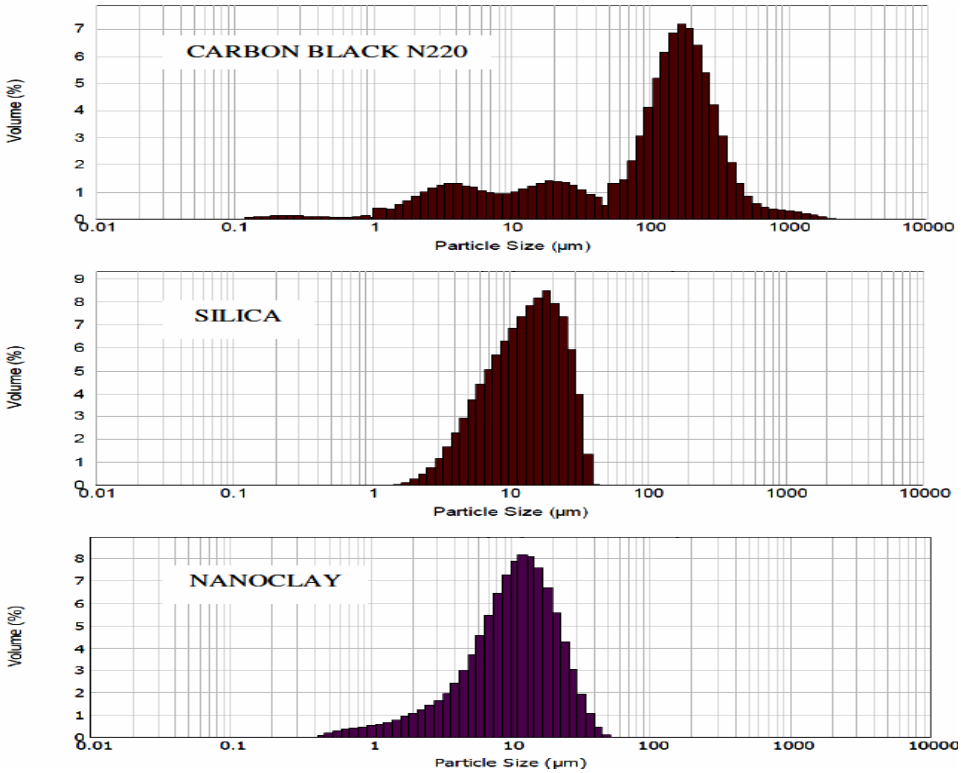

Fig. 4.15- Particle size distribution of carbon black, silica and nanoclay.

4.2.3 Rheometric Properties

The rheometric properties of dual filler nanocomposite were studied at 160°C for 30 minutes and are shown in Table 4.7.

Table 4.7-Rheometric properties of dual filler nanocomposites

	EOC-6	EC-5	EC-15	EC-25	ES-5	ES-15	ES-25	SC-25
ML, dN-m	0.53	0.78	0.94	1.16	0.81	1.00	1.25	1.16
MH, dN-m	8.34	8.35	9.9	11.4	8.30	9.89	11.54	11.4
MH-ML, dN-m	7.81	7.57	8.96	10.24	7.49	8.89	10.29	10.24
Ts2, min	**1.83**	**1.72**	**1.53**	**1.38**	**1.82**	**1.73**	**1.62**	**1.38**
Tc50, min	2.17	2.05	1.9	1.8	2.10	2.07	2.00	1.8
Tc90, min	**5.78**	**5.00**	**4.88**	**4.72**	**4.63**	**4.13**	**3.90**	**4.72**

Incorporation of carbon black in the nanocomposites makes the curing faster and reduces the scorch safety and the effect is more when carbon black dosages are increased. Addition of silica also shows the similar behaviour like carbon black. Replacement of 2 phr organoclay by 5 phr carbon black or silica reduces the reinforcement in comparison with 7 phr organoclay as evident from the lowering of rheometric modulus in EC-5 and ES-5. Combination of 25 phr carbon black or silica and 4 phr organoclay shows much improvement of rheometric modulus in nanocomposite EC-25 and ES-25 indicating high extent of reinforcement.

4.2.4 Mechanical properties

The nanocomposite EOC-6 and SOC-6 showed excellent improvement in mechanical properties when compared with their corresponding gum vulcanizates EG and SG respectively as shown in Figure 4.16 and 4.17. In this investigation, as reported in section 4.1 it was found that for 70/30 SBR/BR blend 6 phr is optimum loading of organoclay and offered the best properties. To incorporate second filler in the SBR/BR-organoclay nanocomposite, reduction of organoclay dosage is essential otherwise filler dosages will be more than optimum that leads to higher filler-filler interaction and increases the hysteresis loss and reduce mechanical properties. 5-6 phr organoclay gives reinforcement equivalent to 50-60 phr carbon black or silica in SBR/BR system, hence 2 phr organoclay was replaced by 15 – 20 phr carbon black or silica and investigated in this section

To develop the dual filler system, 15 and 25 phr of carbon black or silica were added along with 4 phr of organoclay in 70/30 ESBR/BR blends. It was observed that with an increased dosage of the second filler (carbon black or silica) mechanical properties of the nanocomposite improved. The properties of nanocomposite developed with 4 phr organoclay and 25 phr carbon black or silica are close to commercial carbon black and silica tread compounds as evidenced by Stress strain curves shown in Fig. 4.16 and 4.17. In a similar way, nanocomposites based on other SBR rubbers, such as SSBR and functional SSBR (FSSBR), with dual filler systems were developed.

The properties of nanocomposite treads are within typical performance parameters range of passenger car radial tire tread compounds that was noted for PCR tires published in Smithers ***Tire analysis*** report (2004, 2008) and also analyzing commercial tread compounds (Table 4.8).

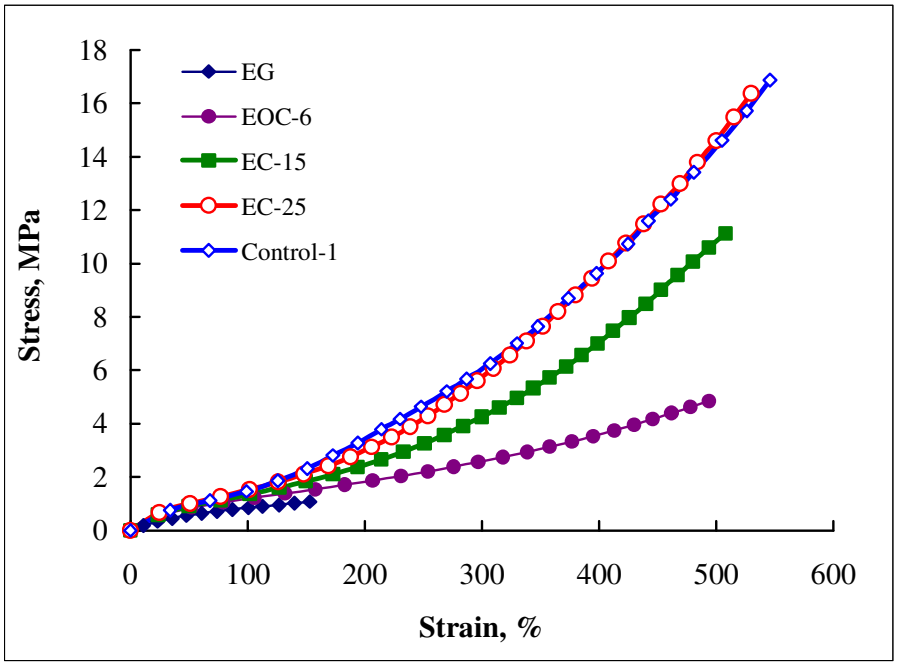

Fig. 4.16- Stress-strain properties of nanocomposites based on ESBR/BR blend and organoclay-carbon black dual filler

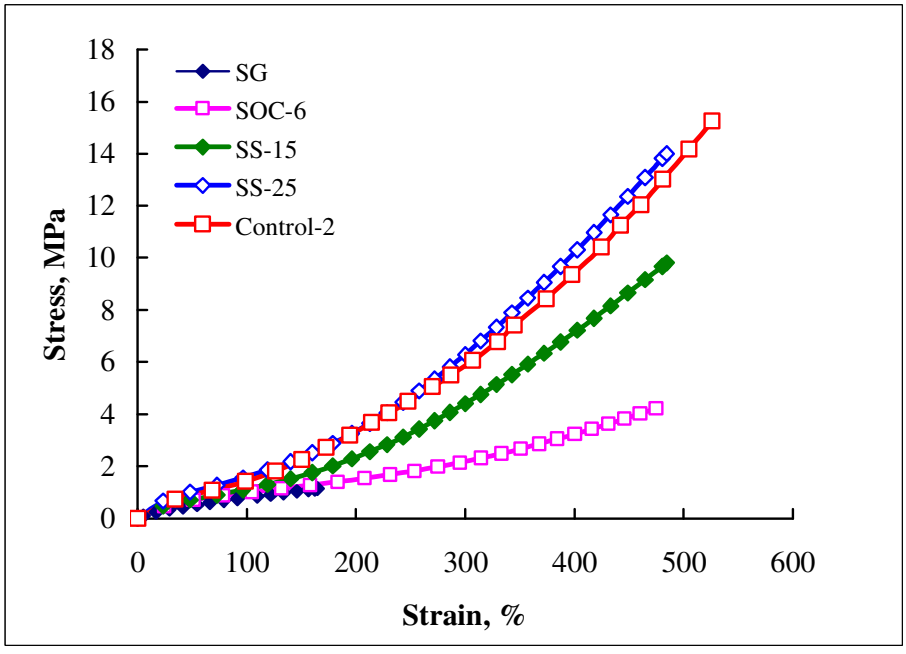

Fig. 4.17- Stress-strain properties of nanocomposites based on SSBR/BR blend with organoclay-silica dual filler

Table 4.8-Mechanical properties of dual filler nanocomposites

	Typical Performance value[b]	organoclay-carbon black			organoclay-silica		
		EC-25	SC-25	FC-25	ES-25	SS-25	FS-25
100% Modulus, MPa	1.6 – 2.5	1.62	1.77	1.80	1.51	1.61	1.60
300% Modulus, MPa	5.0 - 9.0	6.03	6.60	6.94	5.07	6.29	6.46
Tensile Strength, MPa	12.5 min	17.7	14.5	14.8	17.5	14.0	13.0
Elongation at Break,%	350 min	544	483	460	597	484	452
Hardness, Shore A	60-70	64	62	62	63	62	61
Tear Strength, N/mm	30 - 50	43.0	45.9	40.7	47.3	41.9	38.3
Abrasion Loss, mm^3	90 - 150	93	129	134	94	127	125
Heat Build Up, ΔT , ^oC	25- 40	25.6	25.6	23.9	25.6	22.8	20.6

[b] Typical performance parameters range of passenger car radial tire tread compounds.

4.2.5 Viscoelastic Properties

Viscoelastic properties of nanocomposites were determined by dynamic mechanical measurement and are presented in Fig. 4.18 to 4.20. Different dynamic properties such as storage modulus (E'), loss modulus (E''), Tan δ, Loss compliance (J'') have great influence on viscoelastic behaviors of the compounds and their performance during applications. Tan δ is the ratio of loss modulus to storage modulus of the compound and it represents the hysteresis loss of the compound. In a tire tread compound, Tan δ values at different temperatures correlate, as a rule of thumb, with different performance properties of tires, e.g. –25 ^oC represents ice or snow traction, 0^oC represents wet traction and 10-25 ^oC represents dry traction. The higher the Tan δ values at these temperatures, the higher will be the corresponding tire tractions.

Tan δ value at 60^oC represents tire rolling resistance, lower this value lower will be the rolling resistance. All nanocomposite based tread compounds show much lower Tan δ values at 60^oC when compared with the typical range of Tan δ values of commercial tread compounds as shown in Table 4.9.

Further, tread compounds based on SSBR/BR and FSSBR dual filler nanocomposite also meet the traction requirements of tire tread as observed from their Tan δ values at temperatures of -25°C, 0°C and 25°C (Table 4.9). The ESBR/BR nanocomposite shows lower rolling resistance but poor ice and wet traction as evidenced by lower Tan δ values at -25°C and 0°C. This can be attributed to the much lower glass transition temperature of ESBR (Tg:-55°C) compared to SSBR (Tg: - 26°C) and FSSBR (Tg: -28°C).

Lower Tan δ values of nanocomposites at 60°C are attributed to lower loading of fillers in these compounds in comparison with the commercial tread compounds. The SSBR/BR and FSSBR/BR dual filler nanocomposites offer much lower rolling resistance when used as tread compound in tires without sacrificing performance and traction properties. ***ESBR/BR dual filler nanocomposites offer lower rolling resistance comparable to other nanocomposites developed but because of poor ice and wet tractions, it not suitable for low rolling resistance high traction tread compound.***

Table 4.9-Viscoelastic properties (Tan δ) at different temperatures of dual filler nanocomposites

Compound as specified in Chapter 3	Tan δ			
	Temperature			
	- 25°C	0°C	25°C	60°C
	Ice/snow Traction	Wet Traction	Dry Traction	Rolling Resistance
Typical Value [c] *of conventional tread*	0.30 -0.6	0.20 – 0.4	0.15 – 0.25	0.15 – 0.20
FC-25	0.615	0.202	0.154	0.104
FS-25	0.740	0.223	0.128	0.095
SC-25	0.522	0.226	0.184	0.117
SS-25	0.683	0.271	0.145	0.104
EC-25	0.183	0.144	0.168	0.113
ES-25	0.198	0.135	0.142	0.106

[c] Typical performance parameters range of high performance passenger car radial tread compounds

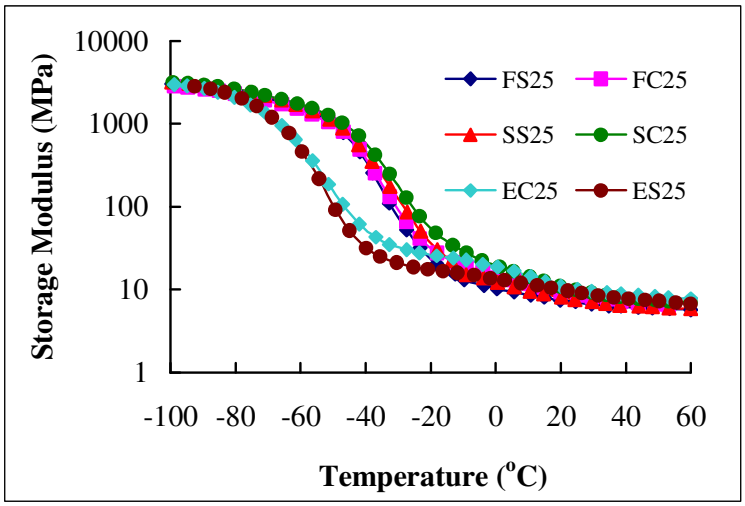

Fig. 4.18- Storage modulus versus temperature

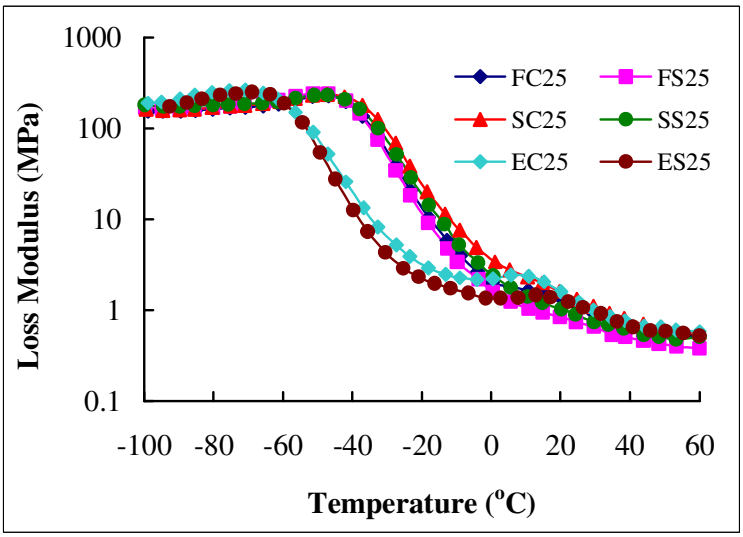

Fig. 4.19- SBR/BR dual filler nanocomposite: Loss modulus versus temperature

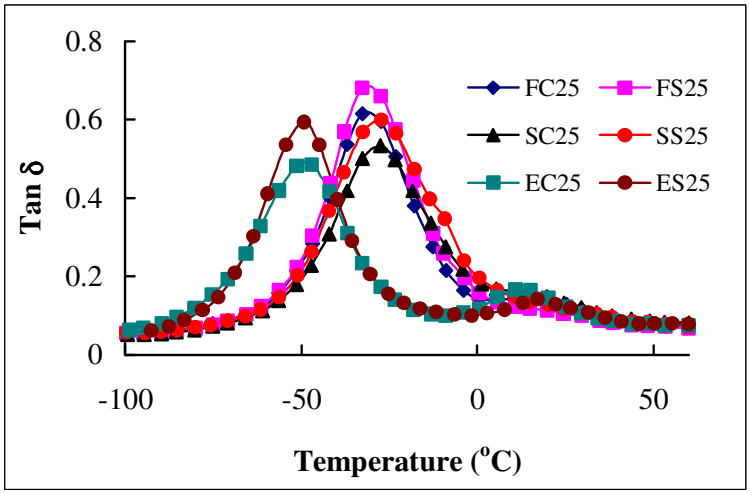

Fig 4.20- Tan δ versus temperature

The hysteresis loss in rubber originates predominantly due to filler-filler interaction in the rubber matrix. Filler-filler interaction is accounted by measuring the difference in shear modulus (ΔG) at very low strain (G_0 ~ 0.1%) and very high strain ($G\infty$ ~ 100%) i.e. $\Delta G = G_0 - G\infty$. At low strain strong filler aggregates gives very high modulus and modulus starts decreasing as the filler aggregates break down when strain level increases. This behavior was first investigated by Payne (1965) and is known as Payne's effect. Strong filler network originated from high filler-filler interaction results in big difference in modulus measured at low strain and high strain i.e. drop in modulus is very high indicating high Payne's effect. For the reduction of rolling resistance of tread compounds, magnitude of Payne's effect at 60°C has to be brought down as higher Payne's effect is associated with higher Tan $\delta_{max.}$

Dual filler nanocomposites shows much lower Payne's effect in comparison with commercial tread compounds (Control-1 and Control-2) as shown in the Table-4.10. ***Lower Payne's effect in nanocomposites are due to lower volume fraction (dosages) of filler and better filler-polymer interaction compared Control compounds as observed in and Fig. 4.21 and Fig.4.22.***

Table 4.10-Payne's effect of Control compounds and nanocomposites

	Control-1	Control-2	EC-25	SC-25	FC-25	ES-25	SS-25
Go	7.70	6.93	2.68	1.73	1.60	2.15	1.46
G∞	1.31	1.49	1.38	0.94	0.91	1.17	0.88
ΔG (G∞- Go)	***6.40***	***5.44***	***1.30***	***0.79***	***0.69***	***0.98***	***0.58***

It is observed from Fig. 4.23 and 4.24 that tan δ become maximum when filler aggregates break during strain sweep of dynamic mechanical test. Tan δ_{max} represents the hysteresis loss arising from break down of fillers network that highly influence the tire rolling resistance and it was found that higher the Tan δ_{max} higher is the tire rolling resistance. ***Organoclay-silica based nanocomposites (SS-25 and FS-25) have lower Tan δ values than the organoclay-carbon black based nanocomposite (SC-25 and FC-25) as observed during viscoelastic test (Fig. 4.23 and Fig. 4.24).*** In organoclay-silica nanocomposite, silane coupling agent was used to modify the silica filler surfaces which reduce the filler-filler interaction in strong silica filler network due to hydrogen bonding. Silane coupling agent makes chemical bond between inorganic silica filler and organic rubber hydrocarbon.

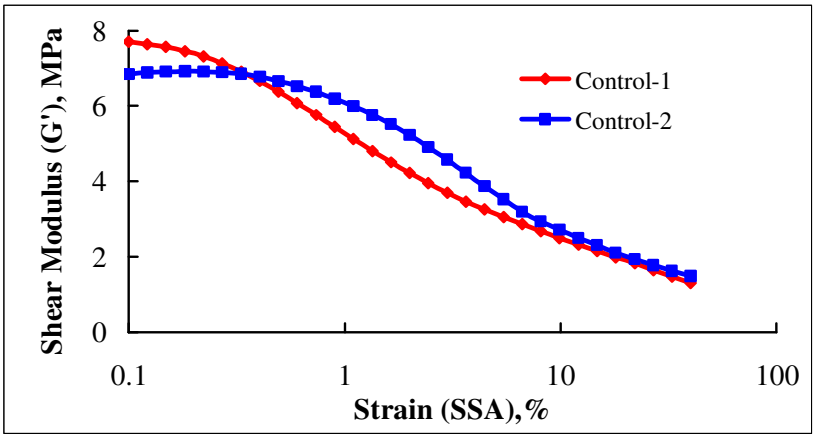

Fig. 4.21- Strain sweep at 10 Hz and 60°C: Shear modulus versus strain of Control compounds

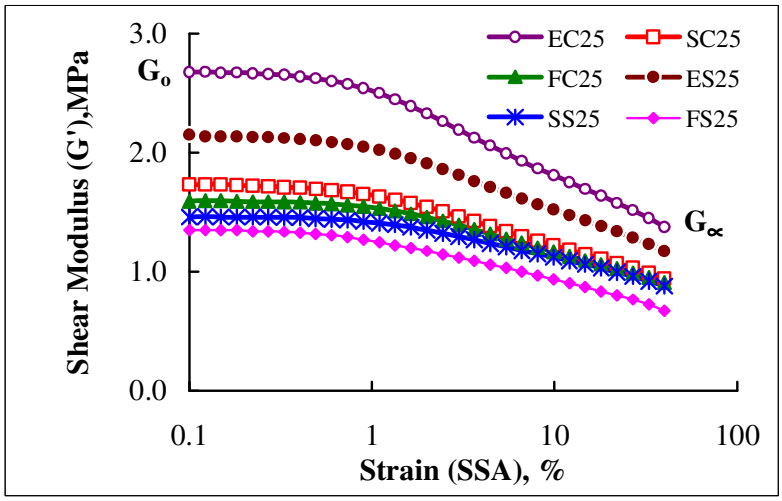

Fig. 4.22- Strain sweep at 10 Hz and 60°C: Shear modulus versus strain of nanocomposites

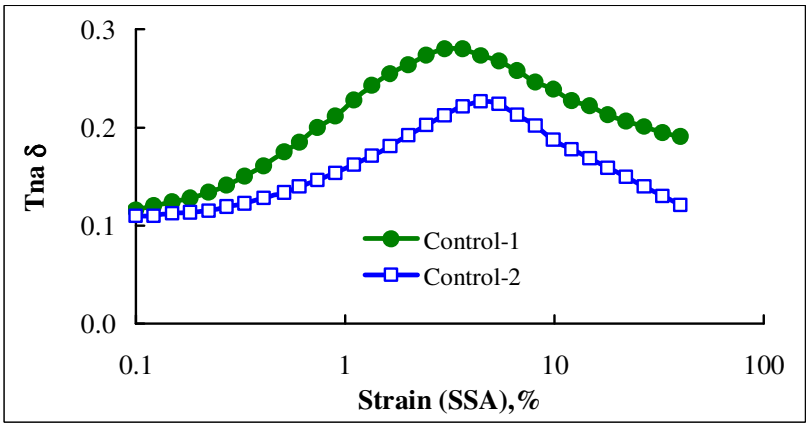

Fig. 4.23- Strain sweep at 10 Hz and 60°C: Tan δ versus strain of Control compounds

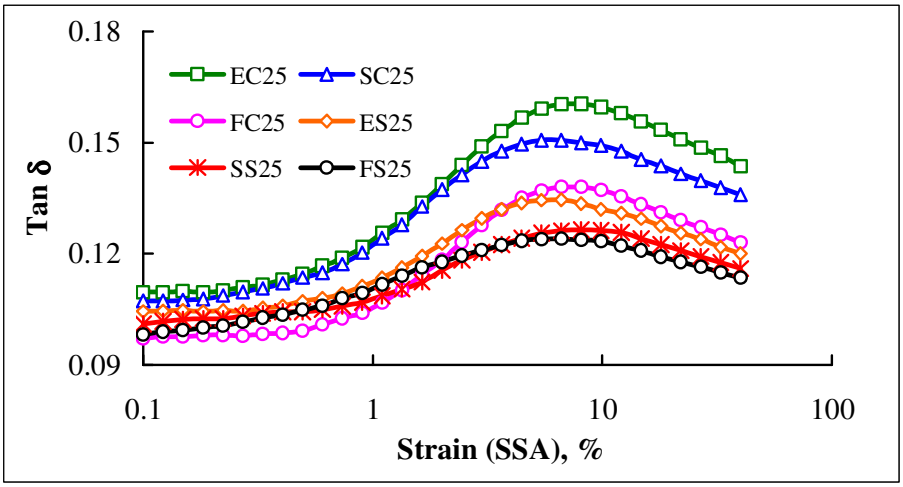

Fig. 4.24- Strain sweep at 10 Hz and 60°C: Tan δ versus strain of Control compounds

The silane coupling agent also reduces filler-filler interaction in organoclay and improves the filler-polymer interaction as observed by Ganter *et al.* (2001). The may be attributed to the reaction of hydroxyl group present in the organoclay with silane coupling agent.

4.2.6 X-Ray Diffraction Study

The X-ray diffraction patterns of organoclay, gum rubber vulcanizate and Organoclay nanocomposites, organoclay-carbon black and organoclay-silica dual filler system are shown in Fig.4.25.

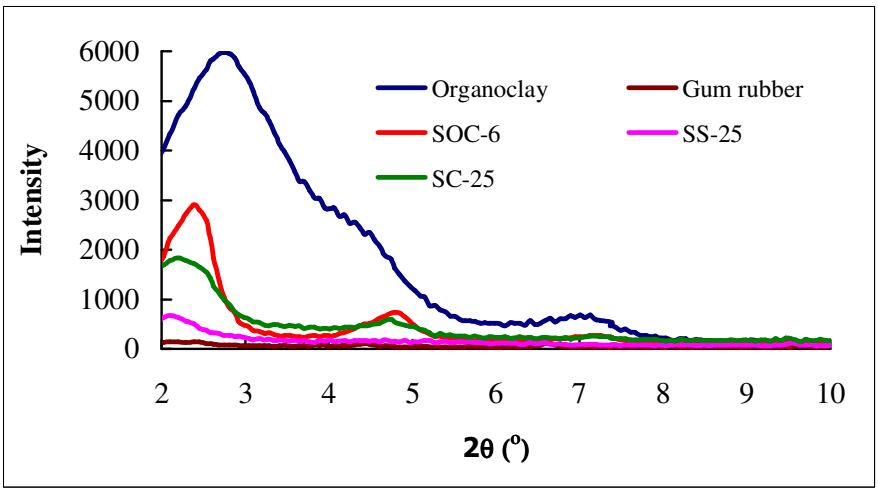

Fig. 4.25- XRD graph-Organoclay, Gum rubber and Nanocomposites

The organoclay showed X-ray diffraction peaks at 2θ angles of 2.8°, 4.4°, 7.1 ° and 9.5°, corresponding to d-spacing 3.1, 2.0, 1.3 and 0.93 nm respectively. For gum rubber vulcanizate no peak was identified since gum rubber is amorphous in nature.

The nanocomposite SOC-6 based on 6 phr organoclay and SSBR/BR blend showed diffraction peaks at 2θ angles of 2.39°, 4.79° and 7.25° corresponding to d-spacing of 3.69, 1.85 and 1.22 nm respectively. Diffraction peaks at lower degree and reduction of peaks at higher degree in the nanocomposite revealed that d-spacing between silicate layers were increased. The increase of d_{001}-spacing revealed that silicate layers were expanded which leads to the intercalated/ exfoliated structure of nanocomposite.

The nanocomposite SC-25 based on SSBR/BR and organoclay-carbon black dual filler had diffraction peaks at 2θ angles of 2.2°, 4.7 °, and 7.13° corresponding to d-spacing 4.02, 1.88 and 1.24 nm respectively. Incorporation of carbon black in the nanocomposite improved the dispersion as well as distribution of organoclay and resulted in better exfoliated structure and excellent mechanical properties of nanocomposite.

The nanocomposite SS-25 based on SSBR/BR and organoclay-silica dual filler showed the diffraction peak at 2θ angle of 2.1° corresponding to d-spacing 4.21 nm. No other peak was observed at higher angle. Like carbon black, incorporation of silica filler also improved the dispersion as well as distribution of organoclay and resulted in better exfoliated structure than carbon black which was evident from much higher d_{001}-spacing and absence of peaks at higher angle.

Organoclay has crystalline structure whereas rubber is amorphous in nature thus incorporation of organoclay in rubber imparts an element of crystallinity in the nanocomposites. The crystallinity in the nanocomposite decreases as intercalation and exfoliation of organoclay increases. Hence, with completely exfoliated structure of the organoclay in the nanocomposite, the matrix will be close to amorphous. Highly exfoliated structure of organoclay in dual filler system reduces the crystallinity compared to organoclay alone and this was observed in XRD..

4.2.7 Transmission Electron Microscopy

Transmission electron microscopy (TEM) was used to image the filler dispersion in the nanocomposites. These images were observed at different magnifications ranging from 0.5 microns to 100 nm.

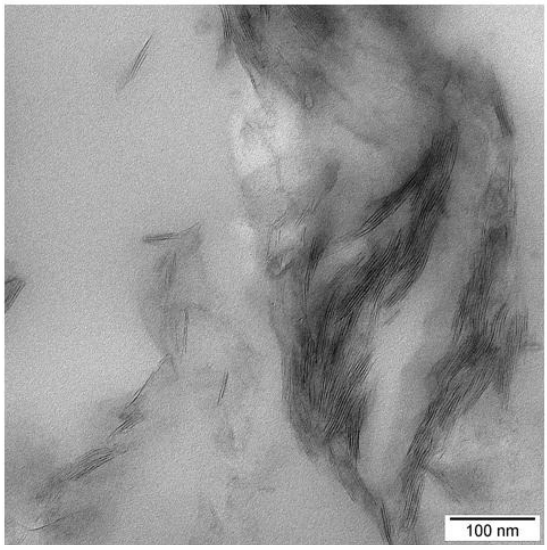

Fig 4.26- TEM image of SSBR/BR-organoclay nanocomposite (SOC-6)

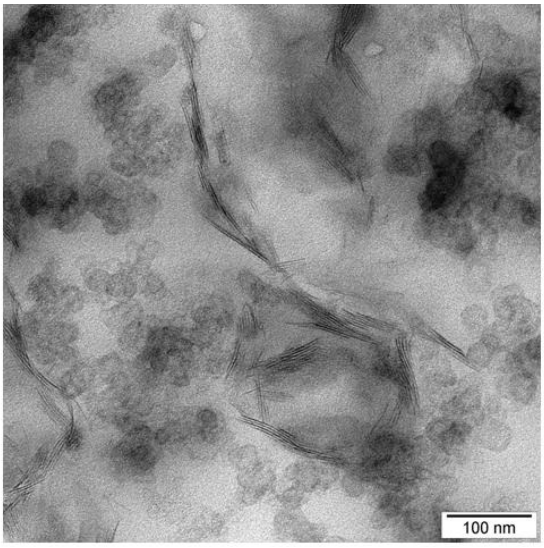

Fig. 4.27- TEM image of ESBR/BR and organoclay-carbon black dual filler system nanocomposite (EC-25)

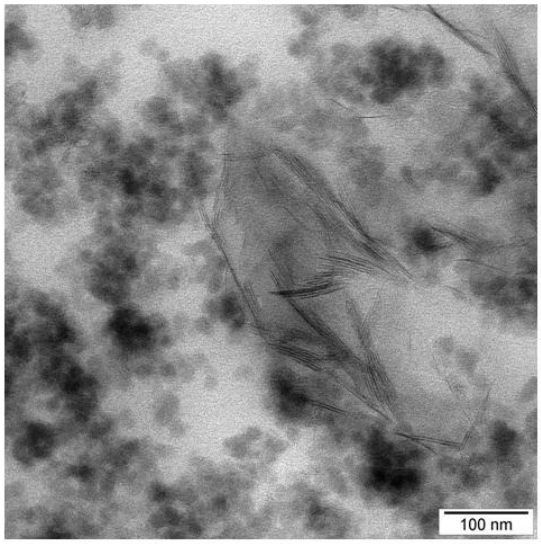

Fig. 4.28- TEM image of ESBR/BR and organoclay-silica dual filler nanocomposite (ES-25)

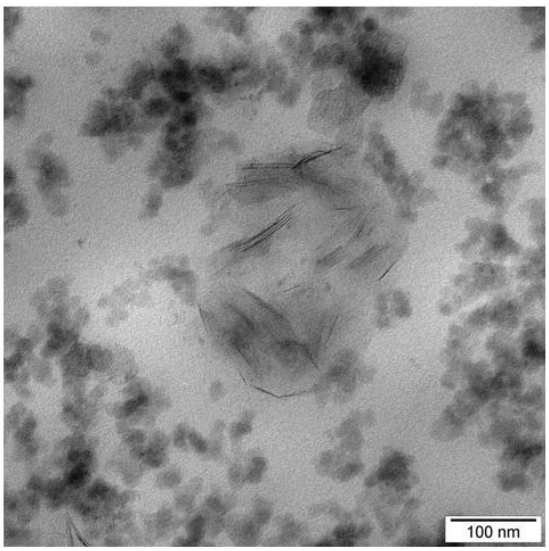

Fig. 4.29- TEM image of SSBR/BR and organoclay-silica dual filler nanocomposite (SS-25)

The exfoliated morphology of organoclay in the nanocomposite (SOC-6) was evident from images as shown in Fig. 4.26.

In organoclay-carbon black dual filler system the TEM images showed a large extent of exfoliation of the organoclay, which appeared to have a fiber like structure in the image whereas carbon black particles have a spherical shape and are deeper in color. The dispersion of both organoclay and carbon black is very fine in the nanocomposite (EC-25) as shown in Fig. 4.27. Similar patterns were also observed in organoclay-silica dual filler system nanocomposites (ES-25 and SS-25) which are shown in Fig. 4.28 and 4.29.

Much superior exfoliation of the organoclay was observed in both the dual filler systems (organoclay-carbon black and organoclay-silica) in comparison with organoclay alone. Higher shear force generated during mixing in presence of carbon black or silica filler in the matrix resulted in better exfoliation of organoclay, thereby providing superior reinforcement and excellent mechanical properties.

4.2.8 Conclusions

a) Nanocomposites based on SBR/BR blends with organoclay showed remarkable improvement in mechanical properties like hardness, modulus, tensile strength, elongation at break, breaking energy and tear strength compared to gum vulcanizate.

b) To meet the requirements of tire tread, special types of nanocomposites were developed with organoclay-carbon black and organoclay-silica dual filler systems based on SBR/BR blend.

c) The dual filler nanocomposites showed excellent mechanical properties and are well within the target performance range of passenger car radial tire tread compounds. The nanocomposites also fulfilled the requirement of abrasion properties; wet traction and dry traction which are very important for PCR tread application.

d) Since nanocomposites contain much lower dosage of filler, they show lower hysteresis loss which was reflected in lower Tan δ values at 60^{o}C.

e) Nanocomposite based passenger car tread compounds showed lower rolling resistance without sacrificing other performance parameters like mechanical properties, tear properties, wear properties, wet traction and dry traction.

f) The properties achieved by dual filler nanocomposites with reasonably small amount of the filler content are close to commercial tread compounds that are highly loaded with fillers.

g) This investigation revealed the potential of nanocomposites which in future could be used as high performance passenger car radial tread to reduce rolling resistance and improve fuel economy in automotive transport.

CHAPTER 5

PREPARATION AND CHARACTERIZATION OF NR/BR NANOCOMPOSITES FOR TRUCK BUS RADIAL (TBR) TIRE TREAD APPLICATION

Truck bus radial (TBR) tire tread compounds are usually formulated using NR/BR rubber blends. The main focus of this investigation was to develop tread compounds from NR/BR blends having low hysteresis losses. To obtain the target properties, two different types of NR/BR nanocomposites were developed. The characterization of nanocomposites; the effect of organoclay as well as dual fillers on mechanical and dynamic mechanical properties of the compounds are reported and their salient properties are discussed in this Chapter.

Fig. 5.1- 10.00R20 TBR Tire

5.1 PREPARATION AND CHARACTERIZATION OF NANOCOMPOSITES BASED ON NR/BR BLENDS AND ORGANOCLAY.

5.1.1 Introduction

Ever since Toyota group introduced organoclay polyamide nanocomposites (Usuki,1993; Okada,1993), several researchers have studied a variety of polymer nanocomposites using organoclay. Clays such as montmorillonite are composed of silicate layers. The dimensions of the silicates are, approximately, 1 nm thickness and 100-1,000 nm in the lateral dimensions. Dispersion of such clays into polymeric materials is very difficult because of their hydrophilic

nature, leading to formation of aggregates in the hydrophobic matrix. However, through clay surface modification, nanoclay can be made organophilic and, therefore, compatible with conventional organic rubbers. Such modified clays are called organoclay and they disperse readily in rubbers offers good mechanical properties.

In this investigation, a nanocomposites based on 70/30, natural rubber (NR)/ polybutadiene rubber (BR) blend and organoclay using XNBR as compatibilizer were prepared and characterized aiming for truck bus radial (TBR) tire tread applications. The performances of nanocomposites depend on several parameters such as nature of rubber, dosage of organoclay and most importantly exfoliation of the organoclay. Similarly organoclay dispersion also depends on parameters such as;

a) Polarity of compatibilizer (Carboxyl group % in XNBR)
b) Mixing techniques
d) Dosages of organoclay

To achieve the best performance properties in the nanocomposite the effects of all these parameters were studied independently and sequentially and finally the nanocomposite that gave the best performance was selected and used in the preparation of high performance nanocomposite. The raw materials, compound formulations, synthesis of nanocomposite, testing and characterization methods are detailed in Chapter 3 in Materials and methods; however compounds codes and brief descriptions are presented in Table 5.1. The results and discussion incorporating the influence of each parameter on mechanical and dynamic mechanical properties of nanocomposites are elaborated in the subsequent sections.

5.1.2 Rheometric Properties

Rheometric studies show that organoclay has strong influence on cure rate. Nanocomposites based on NR/BR and organoclay cure much faster and are scorchier when compared to gum compound (without organoclay). The carboxyl content in XNBR has also influence on cure time and as its % increases, cure time moderately increases, however scorch safety remains unaffected. Nanocomposites prepared by 2 roll mill, solution methods and internal mixer exhibit comparable cure characteristics. The rheometric properties of all nanocomposites are shown in Table 5.2.

Table 5.1-Compound codes and brief descriptions

	Code	XNBR (phr)	Organoclay (phr)	Mixing Methods
Effect of carboxyl % in XNBR	**NBG**	**0.0**	**0.0**	**Internal Mixer**
	NB1	**XNBR-1 (10.0)**	**7.0**	
	NB4	**XNBR-4 (10.0)**	**7.0**	
	NB7	**XNBR-7 (10.0)**	**7.0**	
Effect of mixing methods	**OM**	**10.0**	**7.0**	**2 roll mill**
	SM			**Solution**
	IM			**Internal Mixer**
Effect of organoclay dosages variation	**F0**	**0.0**	**0.0**	**Internal Mixer**
	F4	10.0	4.0	
	F7	10.0	7.0	
	F10	10.0	10.0	

Table 5.2-Rheometric properties at 150^{o}Cfor 30 minutes in MRD

		Min Torque, dN.m	Max Torque, dN.m	Ts2, Minute	Tc50, Minute	Tc90, Minute
Effect of carboxyl %	NBG	0.33	7.30	6.45	6.92	10.30
	NB1	0.53	8.19	2.10	2.52	4.53
	NB4	0.45	8.02	2.32	2.77	4.88
	NB7	0.37	7.43	2.82	3.28	5.68
Effect of mixing methods	OM	0.33	7.41	2.50	2.97	5.35
	SM	0.45	7.25	2.70	3.18	5.58
	IM	0.37	7.43	2.82	3.28	5.68
Clay dosages variation	F0	0.37	7.43	2.73	3.28	5.68
	F4	0.38	7.45	3.17	3.67	6.33
	F7	0.37	7.43	2.82	3.28	5.68
	F10	0.21	7.95	2.55	3.07	5.50

5.1.3 Mechanical Properties

It was observed that all the physical properties like modulus, tensile strength and elongation at break increases as carboxyl content in XNBR increases from NB1 to NB4 as shown in Fig. 5.2. Increase of 300% modulus in NB1, NB4 and NB7 compared to NBG (gum) are 50, 76 and 96% respectively. 7% carboxylated XNBR shows the highest tensile strength and energy at break; the increases are 68% and 126% respectively compared to gum vulcanizate (NBG). Similar trend is also observed in case of hardness, tear strength and tear energy as shown in Table 5.3. As carboxyl group percentage increases, the polarity of XNBR also increases; therefore the organoclay being polar in nature has greater interaction with the more polar rubber. Greater interaction between clay and XNBR result in better clay dispersion and due to this 7% XNBR shows enhancement of physical and tear properties. Hence, 7% XNBR was used for further investigation.

Table 5.3-Effect of carboxyl % in XNBR on physical properties

	Carboxyl %	Clay Phr	Hardness Shore A	M 300 MPa	T.S MPa	Energy at Break J/m² x 10^4	Tear Strength N/mm	Tear Energy J
NBG	0	0.0	50	2.00	14.66	52.3	26.7	7.3
NB1	1	7.0	56	3.00	17.45	81.9	34.2	8.5
NB4	4	7.0	57	3.52	21.13	89.8	36.0	9.6
NB7	7	7.0	58	3.87	24.65	123.7	39.1	11.0

An appropriate mixing technique is very important for clay dispersion. The properties of nanocomposites prepared by three different mixing techniques were compared. Nanocomposites prepared by all the three mixing methods (OM, SM and IM) showed remarkable improvement of hardness, tensile strength, elongation at break and tear strength compared to gum compound (NBG) however, mixing using internal mixer (IM) showed better results compared with solution method (SM) and open two-roll mill (OM) mixing as represented in Fig. 5.3 and Table 5.4. It was noticed that clay mixing was extremely difficult in 2-roll mill. Solution method required a large quantity of solvent which had to be removed after mixing. In comparison to these techniques the internal mixer provided very easy and convenient mixing method and was adopted here for further investigation.

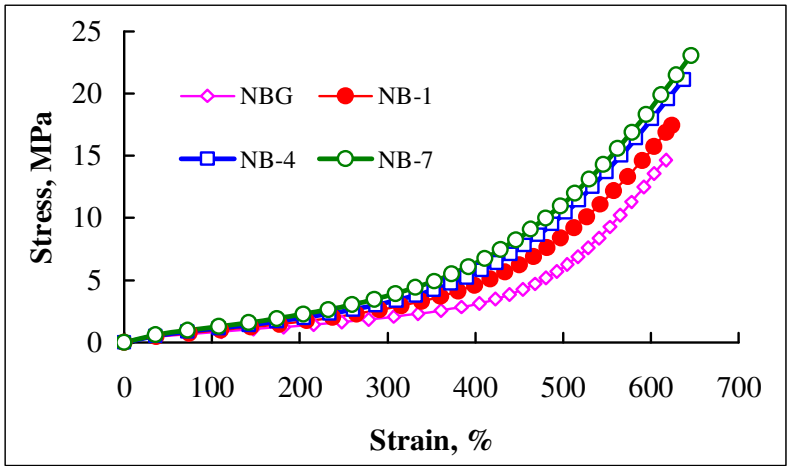

Fig. 5.2- Effect of carboxyl % in XNBR on stress strain properties of nanocomposites

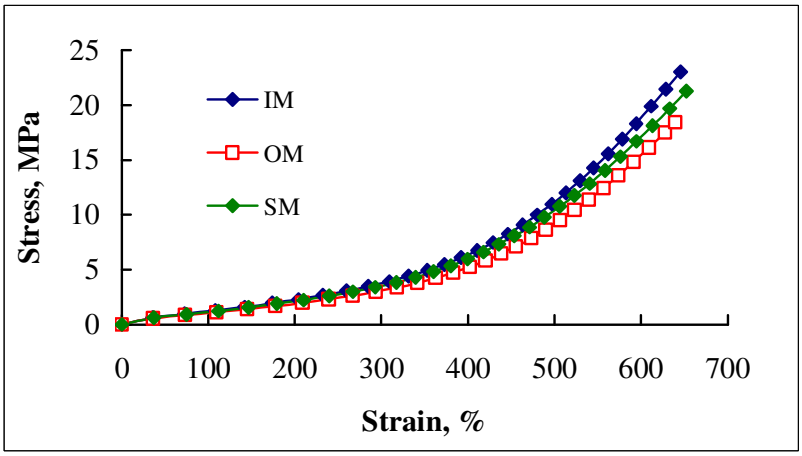

Fig. 5.3- Effect of mixing techniques on stress-strain properties on nanocomposites

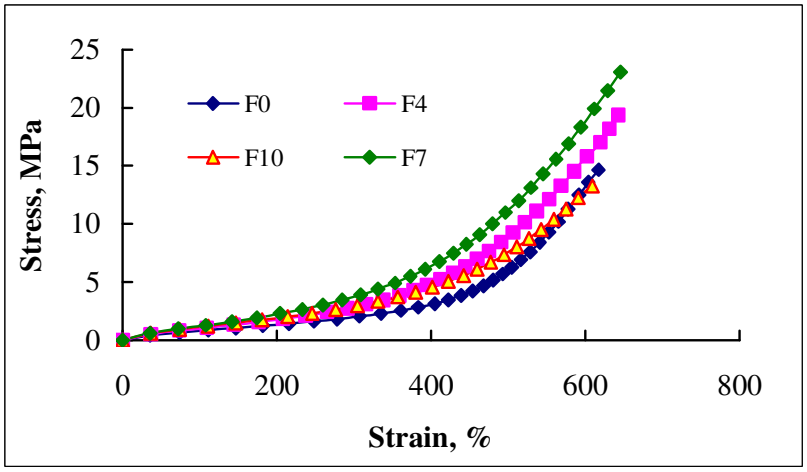

Fig. 5.4- Effect of organoclay dosages on stress strain properties of nanocomposites

Table 5.4-Effect of different mixing techniques on physical properties

		Hardness Shore A	M 300 MPa	T.S MPa	Energy at Break, J/m² x10^4	Tear Strength N/mm	Tear Energy, J
OM	2-roll mill	55	3.35	18.46	90.5	35.3	8.7
SM	Solution	56	3.67	21.31	103.2	37.1	10.6
IM	Internal mixer	58	3.87	24.65	123.7	39.1	11.0

The influence of clay dosages on properties was investigated and the improvement of modulus, tensile strength , elongation at break and tear strength were observed as clay loading increases and reached the maxima at 7 phr. Further increase of clay phr resulted in deterioration of all properties as shown in Fig. 5.4 and Table 5.5. Mixing of 10 phr clay was very difficult and loss of properties is attributed to poor dispersion.

Table 5.5-Effect of clay dosages on physical properties

	clay (phr)	Hardness Shore A	M 300 MPa	T.S MPa	Energy at Break, J/m² x 10^4	Tear Strength N/mm	Tear Energy , J
F0	0	50	2.20	14.91	91.9	27.0	7.6
F4	4	52	2.82	18.43	102.5	33.3	8.8
F7	7	58	3.87	24.65	123.7	39.1	11.0
F10	10	54	2.91	13.29	115.8	37.6	10.7

5.1.4 Dynamic Mechanical Properties

The viscoelastic properties of nanocomposite were measured by dynamic mechanical testing in the temperature range from -110°C to +60°C to capture the behavior of the rubber in the glassy as well as in the rubbery states. NR/BR gum compound shows two glass transition temperatures; one is at -95°C corresponding to BR and other is at -50°C corresponding to NR. NR and BR are physically miscible but thermodynamically not compatible and hence the two glass transition temperatures. There is no significant shift of glass transition temperatures observed in NR/BR-organoclay nanocomposite when compared with its gum compound. The dynamic mechanical properties of gum (NBG) and nanocomposites with 4 phr (F4) and 7 phr (F7) organoclay were studied and are presented in Fig. 5.5 to Fig. 5.7.

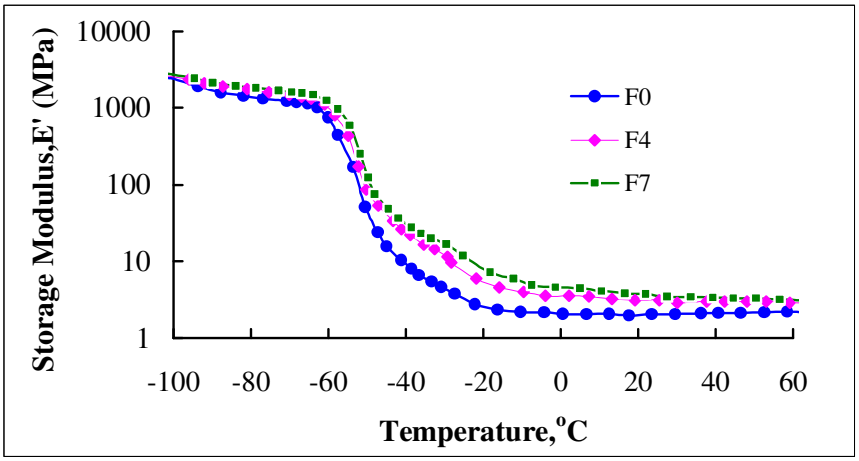

Fig. 5.5-Dynamic mechanical property: storage modulus versus temperature.

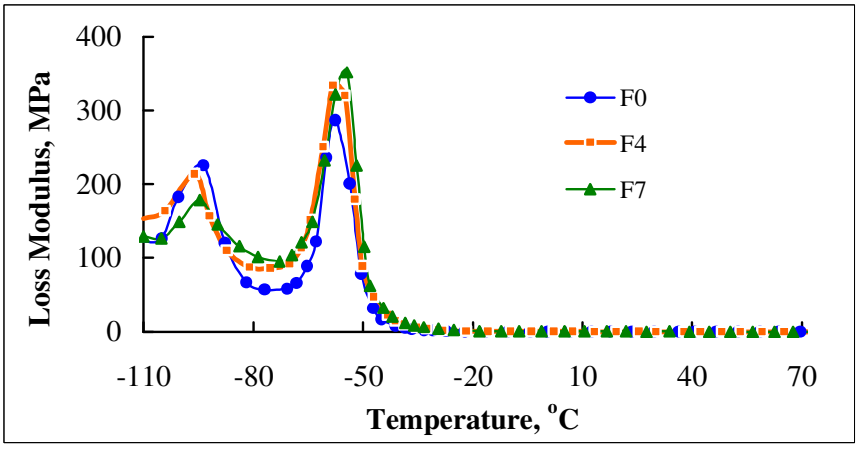

Fig. 5.6- Dynamic mechanical property: loss modulus versus temperature

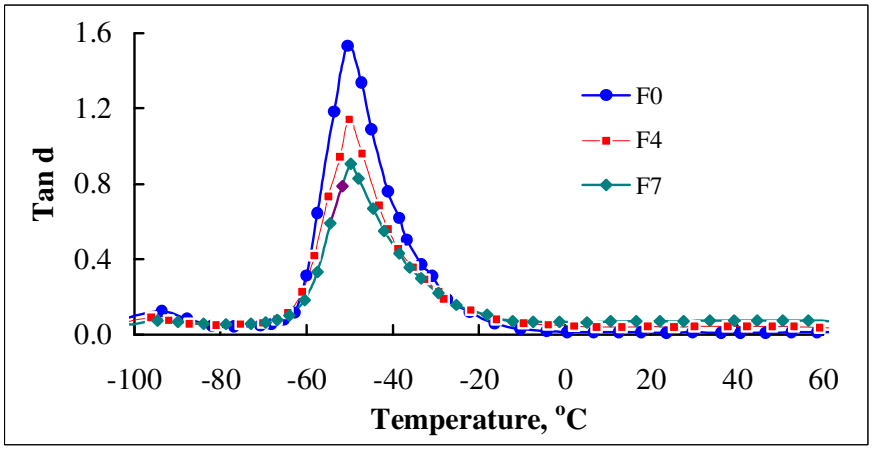

Fig. 5.7- Dynamic mechanical property: Tan δ versus temperature

Dynamic modulus of nanocomposite increases steadily with the increase of organoclay dosages at all temperature. Tan δ shows maximum value at glass transition temperature (Tg) which steadily reduces with increasing organoclay loading, indicating good polymer-filler interaction that the relaxation mechanisms. The increase of stiffness imparted by the organoclay in rubber matrix in the glassy states is due to the higher polymer-filler interaction thus reduces the damping characteristics of nanocomposite. Reduction of Tan δ is results of lowering of the damping characteristics.

5.1.5 X-Ray Diffraction (XRD)

High-resolution Wide-Angle XRD at lower angular range is used to identify intercalated and aggregated clay structures in rubber matrices. In such nanocomposites, the repetitive multilayer structure is well preserved, allowing the interlayer spacing to be determined. The intercalation of the polymer chains usually increases the interlayer spacing, in comparison with the spacing of the organoclay used leading to a shift of the diffraction peak toward lower angle values.

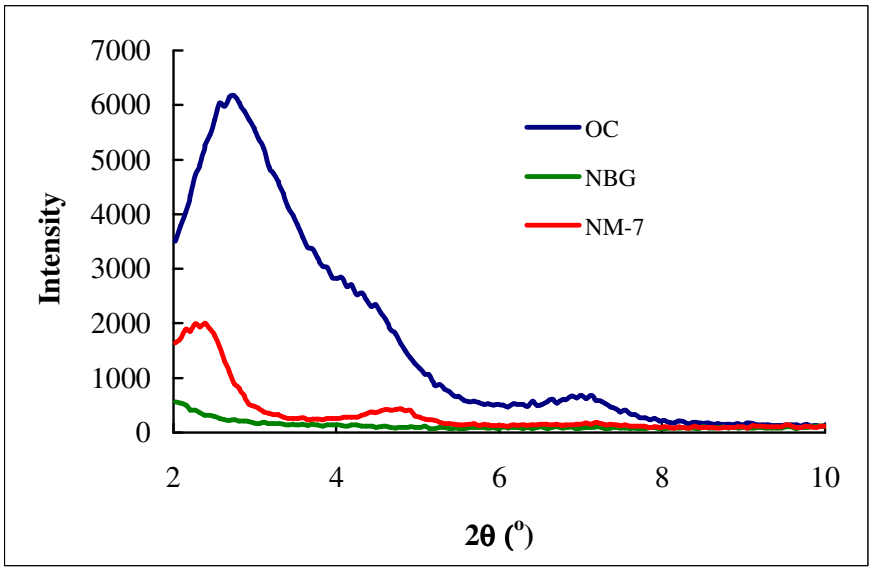

Fig. 5.8- X-ray diffraction patterns of the organoclay, Gum compound and nanocomposite with 7 phr organoclay

The XRD graphs of organoclay and NR/BR-clay (NB7) with 7 phr clay are shown in Fig. 5.8. The XRD studies also support the intercalated and exfoliated morphology of the nanocomposite.

XRD of organoclay showed the diffraction peaks at around 2.8°, 4.4° and 7.1° corresponding to d-spacing 3.15, 2.01 and 1.24 nm respectively. The nanocomposite (NB7) based on 7 phr clay shows the diffraction peaks at around 2.6° and 4.4° corresponding to d-spacing 3.4 nm (Intercalation) and 1.76 nm (layer collapse) nm respectively. Lower peak intensity in nanocomposite with 7 phr organoclay (NB7) at low d-spacing in comparison with organoclay indicates expansion of silicate layer in the nanocomposite (intercalation). The increase of d_{001}-spacing to 3.4 nm and shifting of d_{002} peak toward higher angle as well as decrease of peaks intensity indicate expansion of silicate layer. Absence of peaks at higher angle suggests exfoliated structure of nanocomposite.

The decrease in the intensity of intercalation peak (d =3.4 nm) is due to the decrease in the coherent layer scattering. The WXRD results can be explained on the basis of the intercalation of the polymer chains into the clay layers (Kim 2001), which lead to the disordering of the layered clay structure, thereby a decrease in the WXRD coherent scattering intensity being observed.

5.1.6 Transmission Electron Microscopy (TEM)

The filler dispersion was studied by TEM of ultrathin section of rubber prepared by ultra microtome at temperatures below glass transition temperature (Tg) of the rubber matrix. Fig. 5.9 shows TEM micrographs of NR/BR nanocomposite (scale bar: 0.5μm, 0.2 μm 50 nm). The dark lines in the TEM image are the intersections of the silicate layers. As shown in Fig. 5.9, organoclay are well dispersed in the rubber matrix and many parts of the organoclay in the NR/BR nanocomposites were separated from the original layers.

The NR and BR are hydrocarbons having non polar in nature whereas organoclay is polar material. The hydrocarbon nature of rubber favours more filler–filler interaction than rubber filler interaction. Introduction of XNBR, a polar rubber as compatibiliser gives higher Flory-Huggins interaction parameter that favours the penetration of rubber into the inter layers of organoclay (Kim, 2001). TEM micrographs reveal a disordered layered structure in NR/BR-clay nanocomposite. The morphology appears to be exfoliated with some intercalation of the silicate layers. The dark regions are the hard layered silicates while the light regions are soft rubber matrix.

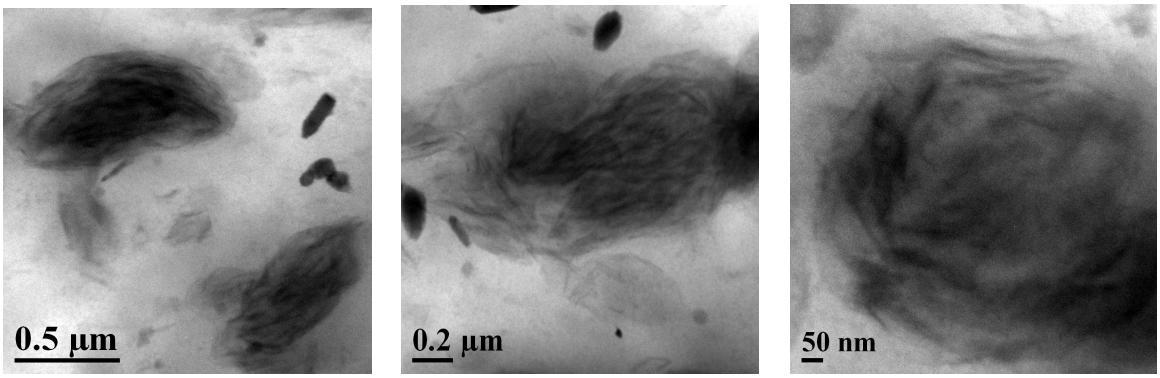

Fig. 5.9- TEM images of nanocomposite with 7 phr organoclay.

5.1.7 Conclusions

Investigations on nanocomposites of NR/BR (70/30) with organoclay (Closite®15A) using XNBR as a compatibiliser reveals the following:

I. All mechanical properties like modulus, tensile strength and elongation at break increases as the carboxyl content of XNBR increases from NB1(1% carboxyllation) to NB7 (7% carboxyllation). As carboxyl % in XNBR increases, the surface energy of the rubber increases which leads to higher interfacial interaction between filler and polymer (Das *et al*, 2008).

II. The mixing technique used also influences the organoclay dispersion and ultimately the mechanical properties. Internal mixer lead to the best clay dispersion and mechanical property enhancement followed by solution mixing and 2 roll mill. The mixing temperature (140^{o}C) and high shear force in internal mixer has influence on the filler-polymer interaction which may be the reason for better clay dispersion and properties of nanocomposite compared to solution and 2 roll mill mixing.

III. The NR/BR-organoclay nanocomposite with 7 phr organoclay was found optimum as it exhibited the best physical properties like hardness, modulus, tensile strength, elongation at break and dynamic mechanical properties. The XRD study of the same nanocomposite reveals the silicate layers were expanded. TEM image also shows the intercalated and exfoliated morphology of the nanocomposite.

IV. The strong interfacial interaction between highly polar XNBR and organoclay played an important role in clay dispersion with in the rubber matrix. Strong interaction between carboxyl group and polar organoclay formed a thermodynamically stable composite and help clay dispersion when mixed with rubber.

5.2 DEVELOPMENT AND CHARACTERIZATION OF HIGH PERFORMANCE NANOCOMPOSITES BASED ON NR/BR BLENDS AND DUAL FILLER SYSTEM

5.2.1 Introduction

The objective of this investigation was to develop nanocomposites for truck bus radial (TBR) tire tread with reduction in the rolling resistance of the tire. To attain this objective nanocomposites of NR/BR (70/30) with organoclay (Closite®15A) using XNBR as a compatibiliser were formulated and characterized. Although substantial improvement of mechanical properties such as 300% modulus, tensile strength and elongation at break were attained with 70/30 NR/BR blend and 7 phr organoclay but other performance requirements of tire treads such as traction, tire wear and durability were not met with organoclay alone.

In case of tire tread application hardness and low strain modulus such as 50% and 100% modulus are also very important since tire handling; cornering and steering response depend on these properties. Similarly abrasion resistance is very critical for tire wear and durability.

Table 5.6-Compound descriptions (NR/BR: 70/30)

Code	XNBR (7% carboxyllation)	Organoclay (Closite 15A)	Carbon Black (N220)	Silica (HDS)	Silane, X 50-S (50% Si 69 + 50% CB)
NM-7	10.0	7.0			
Control-3			***50.0***		
NC-10	10.0	5.0	10.0		
NC-15	10.0	5.0	15.0		
NC-20	10.0	5.0	20.0		
Control-4				***45.0***	***10.0***
NS-10	10.0	5.0		10.0	2.0
NS-15	10.0	5.0		15.0	3.0
NS-20	10.0	5.0		20.0	4.0

Organoclay alone could not provide all desired properties; hence the concept of ***dual filler system*** was explored so that required compound properties could be obtained without substantially increasing hysteresis losses. The details of the raw materials used, compound formulations, preparation of dual filler nanocomposite, testing and characterization methods are described in ***Chapter 3*** and briefly described in Table 5.6 for reference. In this section, the results obtained for dual filler nanocomposites are elaborated.

5.2.2 Filler Characterization and Dispersion

In this investigation, three different fillers namely carbon black (N220), highly dispersible silica and organoclay (modified Na-MMT) were used. The particle size distributions of all the fillers are presented in Chapter-4. The other characterization such as BET surface area and DBP absorption were also described in Chapter-4.

The dispersion of carbon black and silica fillers in organoclay-carbon black and organoclay-silica dual filler nanocomposites were studied by Dispergrader (Opigrade, Sweden). A freshly cut thin rubber sample was placed in the sample holder. Surface of the sample was scanned and the image of the test sample surface was instantly presented on the monitor, powerfully magnified, side by side with one of the reference picture. Sample image was automatically classified against reference images stored in the software. The dispersion is rated by 1 to 10 scale where 10 represents best filler dispersion. The dispersion of organoclay-carbon black and organoclay-silica were 7.5 and 6.6 respectively.

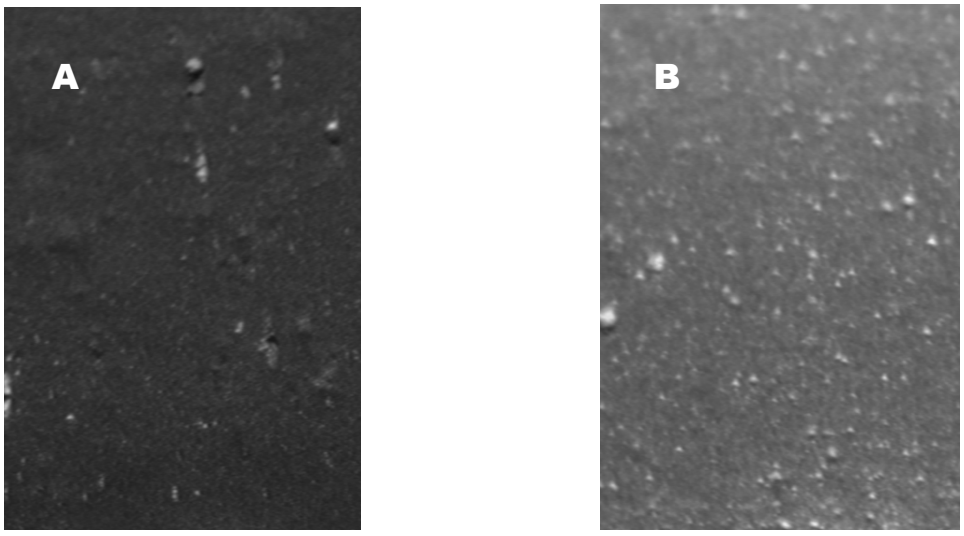

Fig. 5.10-(A) Organoclay-carbon black and (B) Organoclay-silica filler dispersion

5.2.3 Rheometric Properties

All the nanocomposites showed scorch safety 2.0 ± 0.5 and optimum cure time 5.6 ± 0.75 minutes. The rheometric modulus increases with increasing dosages of carbon black or silica filler in the nanocomposites as shown in Table 5.7. All organoclay-carbon black nanocomposites have similar optimum cure time (Tc_{90}) and Tc_{90} of all organoclay-silica nanocomposites are close to each other.

Table 5.7-Compound rheometric properties (MDR 150°C/30 minutes)

	Min torque dN.m	Max torque dN.m	Ts2 Minutes	Tc90 Minutes
NM-7	***2.82***	***7.43***	***2.82***	***5.68***
NC-10	2.20	8.38	2.20	4.72
NC-15	2.13	9.09	2.13	4.70
NC-20	2.07	9.98	2.07	4.77
NS-10	2.78	8.18	2.78	5.53
NS-15	3.02	8.66	3.02	5.95
NS-20	3.03	9.48	3.03	6.12

5.2.4 Mechanical Properties

The nanocomposite NM-7 showed excellent tensile strength and was close to Control compounds but hardness and 100% modulus were much lower than the Control compounds. These mechanical properties required for tire tread application could not be achieved by organoclay filler alone. Therefore, nanocomposites based on dual filler system comprising with organoclay-carbon black and organoclay-silica were developed. In dual filler system, 10, 15 and 20 phr of carbon black or silica were added along with 5 phr of organoclay. In NR/BR blend 7 phr organoclay was found to be optimum and offered the best properties, however in case of carbon black or silica filler, optimum properties observed in the range of 50 to 60 phr, hence 1 phr organoclay loading is approximately equivalent to 8-10 phr loading of carbon black or silica filler. It was observed that with an increased dosage of the second filler (carbon black or silica)

mechanical properties of the nanocomposite improved substantially. The properties of nanocomposite developed with 5 phr organoclay and 20 phr carbon black or silica were close to the properties range of TBR tire tread compound as reported in Smithers report (Tire Analysis, TBR for emerging growth markets", Smithers Scientific Services, 2001, 2008).

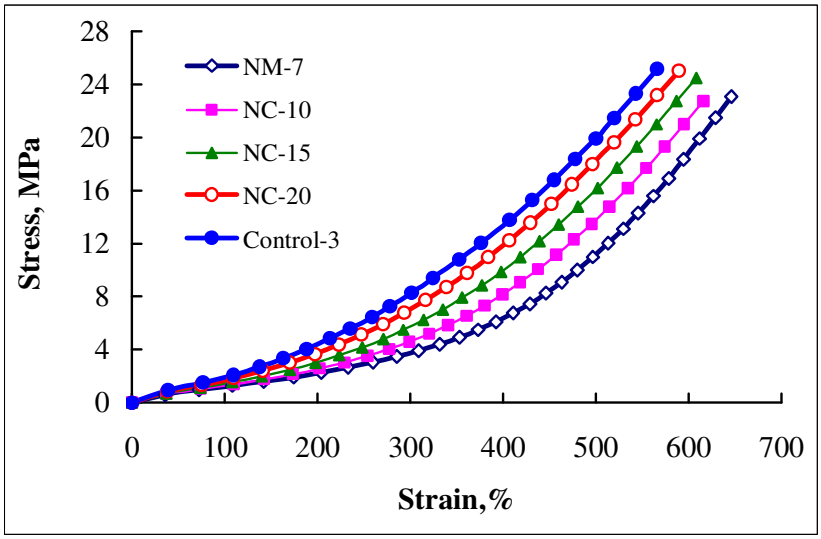

Fig. 5.11- Stress-strain properties of Control-3, organoclay and organoclay –carbon black dual filler nanocomposites

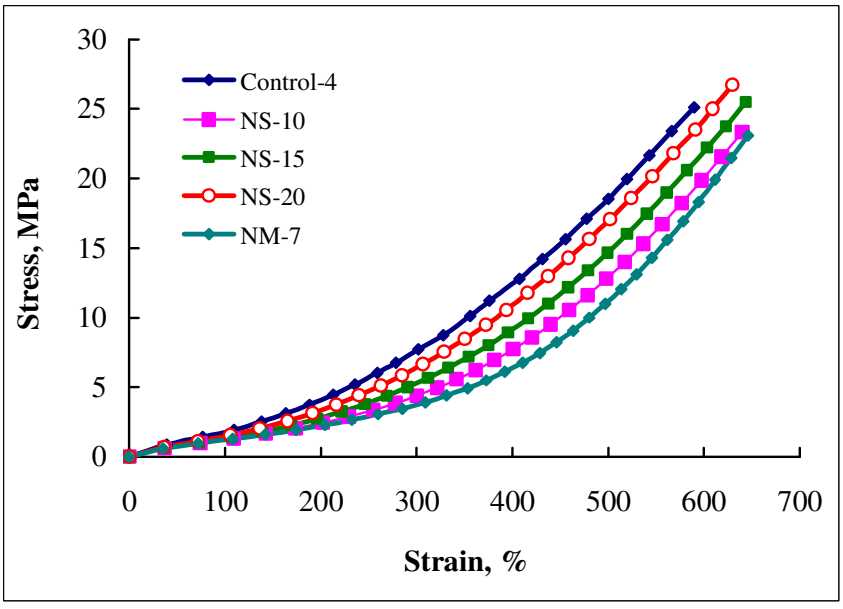

Fig. 5.12- Stress-strain properties: Control-4, organoclay and organoclay –silica dual filler nanocomposites

Stress strain curves of nanocomposite based on NR/BR with organoclay-carbon black and organoclay-silica are shown in Fig. 5.11 and 5.12 respectively along with Control compounds. The stress- strain properties of NC-20 is very close to Control-3 which has 50 phr carbon black filler. Similarly, NS-20 showed similar stress-strain properties to Control-4 which has 50 phr silica filler. Hence with much lower volume fractions of filler in the dual filler nanocomposites, properties similar to 45 to 50 phr carbon black or silica are obtained.

The reinforcement obtained from organoclay depends on two factor (a) loading of filler and (b) extent of intercalation and exfoliation of organoclay in the rubber matrix. During mixing, higher the shear force better is the filler dispersion. Incorporation of silica or carbon black in addition to organoclay generates much more shear force than organoclay alone and hence as a result highly exfoliated nanocomposite is formed. The increase of carbon black or silica filler increases the viscosity of rubber which generates greater shear force during mixing and processing. The excellent mechanical properties obtained using dual filler nanocomposites are to these aspects. Beside mechanical properties, other performance properties like tear strength, abrasion loss and heat build up of all the nanocomposites were also within the target limits of truck bus radial tread compound as shown in Table 5.8.

Table 5.8-Mechanical properties of nanocomposites

Properties	Typical range	NM-7	Control-3	NC-20	Control-4	NS-20
Hardness, Shore A	60 - 70	58	66	64	64	62
100% Modulus, MPa	1.5 - 2.5	1.26	1.82	1.72	1.62	1.50
300% Modulus, MPa	6.0 - 10.0	3.87	9.16	7.10	8.32	6.39
Tensile Strength, MPa	22.0 min	24.7	23.2	25.8	24.9	28.0
Elongation at Break, %	420 min	665	554	651	596	646
Tear Strength, N/mm	65 - 110	39.1	81.0	38.5	107.0	70.1
DIN Abrasion Loss, mm^3	70 - 110	180	88.0	94.0	99.0	106.0
Heat Build Up (ΔT), ^oC	20 - 30	12	28.0	18.0	26.0	16.0
Breaking Energy, $J/m^2 \times 10^4$	-	123.7	129.9	136.4	146.2	155.7

5.2.5 Viscoelastic Properties

Viscoelastic properties of nanocomposites were determined by dynamic mechanical measurement in shear mode and presented in Fig.5.13 to Fig. 5.15. Different dynamic properties such as storage modulus (G'), loss modulus (G''), Tan δ have a great influence on viscoelastic behaviors of the compounds and their performance during applications.

Rolling resistance is related to the hysteresis behavior of compounds. Hysteresis loss is greatly influenced by filler-filler interaction. Higher is the filler-filler interaction, higher will be the hysteresis loss. Tan δ, which is the ratio of loss modulus to storage modulus of the compound, represents the hysteresis loss of the compound. In a tire tread compound, Tan δ at 60°C represents tire rolling resistance and lower is the value; lower will be the rolling resistance. Filler-filler interaction is accounted by measuring the difference in shear modulus (ΔG) at very low strain (G_0 ~ 0.1%) and very high strain ($G\infty$ ~ 100%) i.e. $\Delta G = G_0 - G\infty$. At low strain strong filler aggregates gives very high modulus and modulus starts decreasing as the filler aggregates break down when strain level increases. This behavior was first investigated by Payne (1965) and is known as Payne's effect.

Strong filler network results in big difference between low strain modulus and high strain modulus between as observed during strain sweep experiment. Higher filler-filler interaction leads higher reduction of modulus and thus indicates higher Payne's effect. For the reduction of rolling resistance of tread compounds, magnitude of Payne's effect at 60°C has to be brought down as higher Payne's effect is associated with higher Tan $\delta_{max.}$ Dual filler nanocomposites has much lower Payne's effect in comparison with carbon black and silica based commercial tread compounds (Control-3 and Control-4) as shown in the Fig. 5.13 and Fig.5.14 respectively as well as in Table 5.9 and these are due to lower volume fraction (lower dosages) of filler and greater filler-polymer interaction compared to the commercial tread compounds. In strain sweep, Tan δ values show a maxima when filler aggregates breaks which is seen in Fig. 5.15. Higher Tan δ_{max} also indicates higher hysteresis loss in the compounds and higher rolling resistance in tire. Nanocomposites with organoclay-carbon black dual fillers showed higher Payne's effect than the corresponding organoclay-silica dual filler. This is attributed to the presence of silane coupling agent which react with hydroxyl group of silica and breaks the strong filler network thereby reducing the filler-filler interaction remarkably.

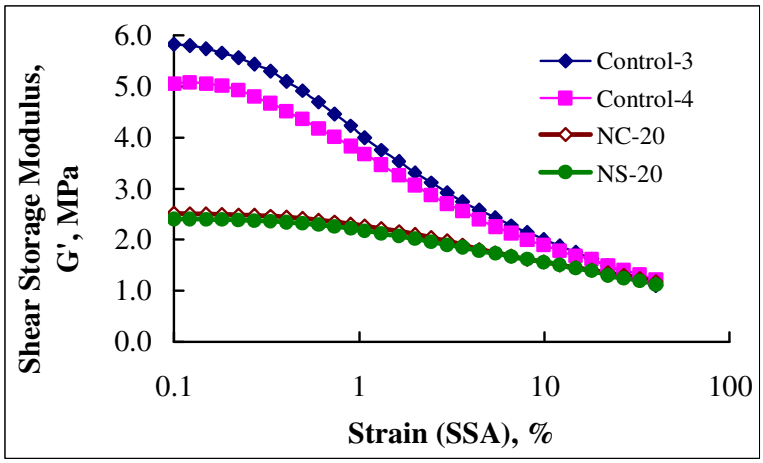

Fig. 5.13- Shear storage modulus versus strain at 60°C

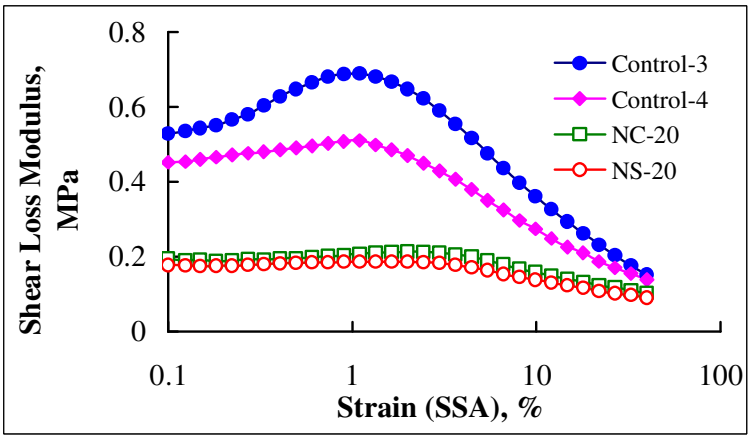

Fig. 5.14- Shear loss modulus versus strain at 60°C

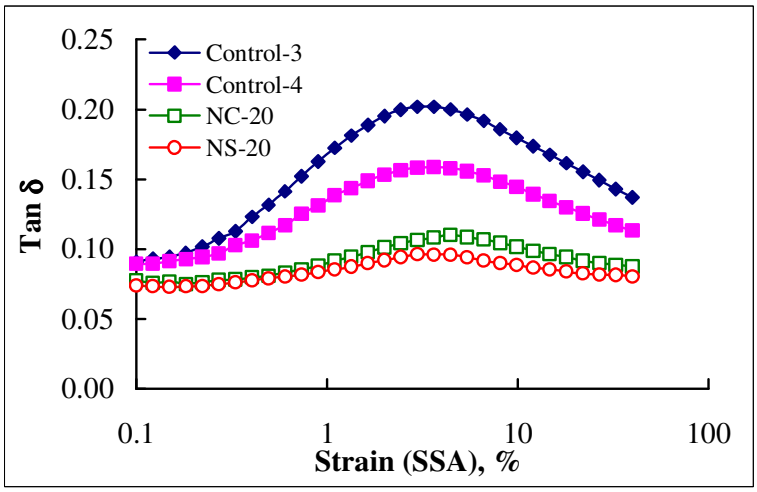

Fig. 5.15- Tan δ versus strain at 60°C

It was observed that organoclay-carbon black dual filler nanocomposite (NC-20) has 72% lower Payne's effect which leads to the reduction of 45% Tan δ_{max} values compared to carbon black based commercial tread compound (Control-3). Similarly organoclay -silica dual filler nanocomposite (NS-20) showed 68% lower Payne's effect and 40% lower Tan δ_{max} comparison with silica based commercial tread compound (Control-4). All nanocomposite based tread compounds showed much lower Tan δ values at 60°C when compared with Control compounds as shown in Fig. 5.15; hence these will have much lower rolling resistance in tire.

Table 5.9-Payne's effect

	Shear Modulus at Low Strain, Go (MPa)	Shear Modulus at very high Strain, G∞ (MPa)	Payne' Effect, ΔG, (MPa) [ΔG= Go- G∞]	Loss Modulus, G'' (MPa)	Tan δmax
Control-3	5.83	1.10	4.73	0.689	0.202
NC-20	2.52	1.18	1.34	0.213	0.110
Control-4	5.08	1.21	3.87	0.510	0.159
NS-20	2.40	1.12	1.29	0.186	0.096

5.2.6 X-Ray Diffraction (XRD) Study

The X-ray diffraction patterns were determined for organoclay, organoclay nanocomposites, and nanocomposites with dual filler system. X-ray diffraction peaks at 2θ angles and corresponding d-spacing of organoclay, clay nanocomposite and dual filler nanocomposites are presented in Table 5.10 and Fig. 5.16.

Diffraction peaks at low 2θ angles and reduction of peaks at higher 2θ angles in the nanocomposite revealed that d-spacing between silicates layers increased in the nanocomposite materials. The d_{001}-spacing increased to 3.88 nm in nanocomposite (NM-7) from 3.12 nm in organoclay and it was further increased to 4.0 nm in organoclay-carbon black dual filler based nanocomposite (NC—20). The dual filler based nanocomposite (NC—20) showed much higher d_{001}-spacing compared to organoclay nanocomposite. The increase of d_{001}-spacing in nanocomposite indicates that the layer silicate structure of organoclay gets expanded. Incorporation of carbon black further expanded the layer silicate structure and improved the dispersion as well as distribution of organoclay and resulted in better intercalated/exfoliated structure and resulted in excellent mechanical properties of the nanocomposites.

Similar to carbon black, incorporation of silica filler also improved the dispersion as well as distribution of organoclay and resulted in much better exfoliated structure than that observed for organoclay – carbon black that was evident from much higher d_{001}-spacing and absence of peaks at higher angle. Organoclay has crystalline structure whereas rubber is amorphous in nature thus incorporation of organoclay in rubber imparts an element of crystallinity in the nanocomposites. The crystallinity in the nanocomposite decreases as intercalation and exfoliation of organoclay increases. Hence, with completely exfoliated structure of the organoclay in the nanocomposite, the matrix will be close to amorphous. Highly exfoliated structure of organoclay in dual filler system reduces the crystallinity compared to organoclay alone and this was observed in XRD studies.

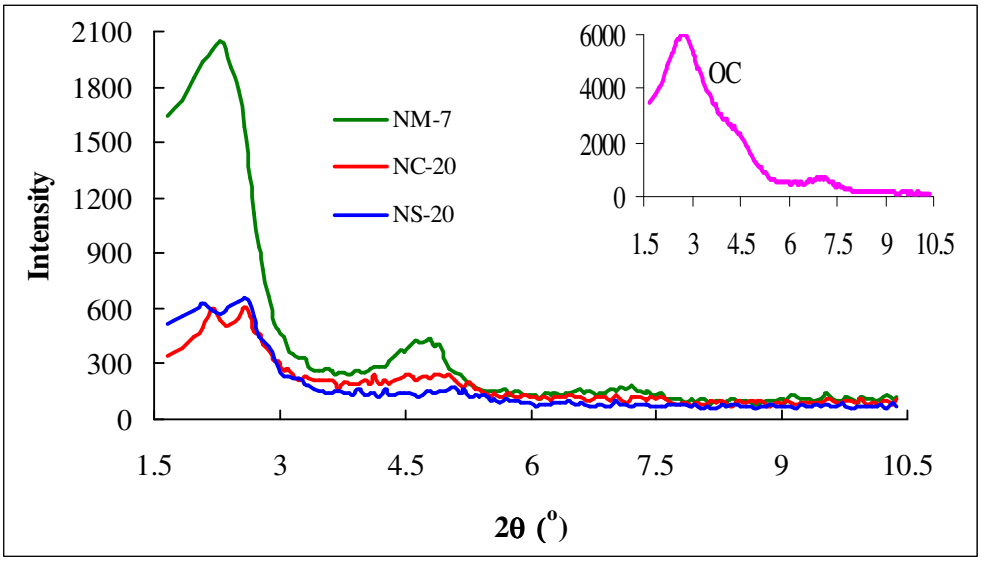

Fig. 5.16- XRD of organoclay and dual filler nanocomposites

Table 5.10-d-spacing (nm) in XRD study

Organoclay OC		Nanocomposite NM-7		Organoclay-carbon black nanocomposite NC-20		Organoclay-silica nanocomposite NS-20	
Angle 2θ	d-spacing (nm)	Angle 2θ	d-spacing (nm)	Angle 2θ	d-spacing (nm)	Angle 2θ	d-spacing (nm)
2.81	3.15	2.28	3.88	2.2	4.00	2.075	4.26
4.37	2.02	4.75	1.86	2.58	3.40	2.62	3.37
7.25	1.22	7.19	1.23				

5.2.7 Transmission Electron Microscopy (TEM) Study

The filler dispersion in the nanocomposites was studied by transmission electron microscopy (TEM). TEM images were taken at different magnifications from 0.5 microns to 50 nm. The exfoliated morphology of organoclay in the nanocomposite (NM-7) is presented in Fig. 5.17.

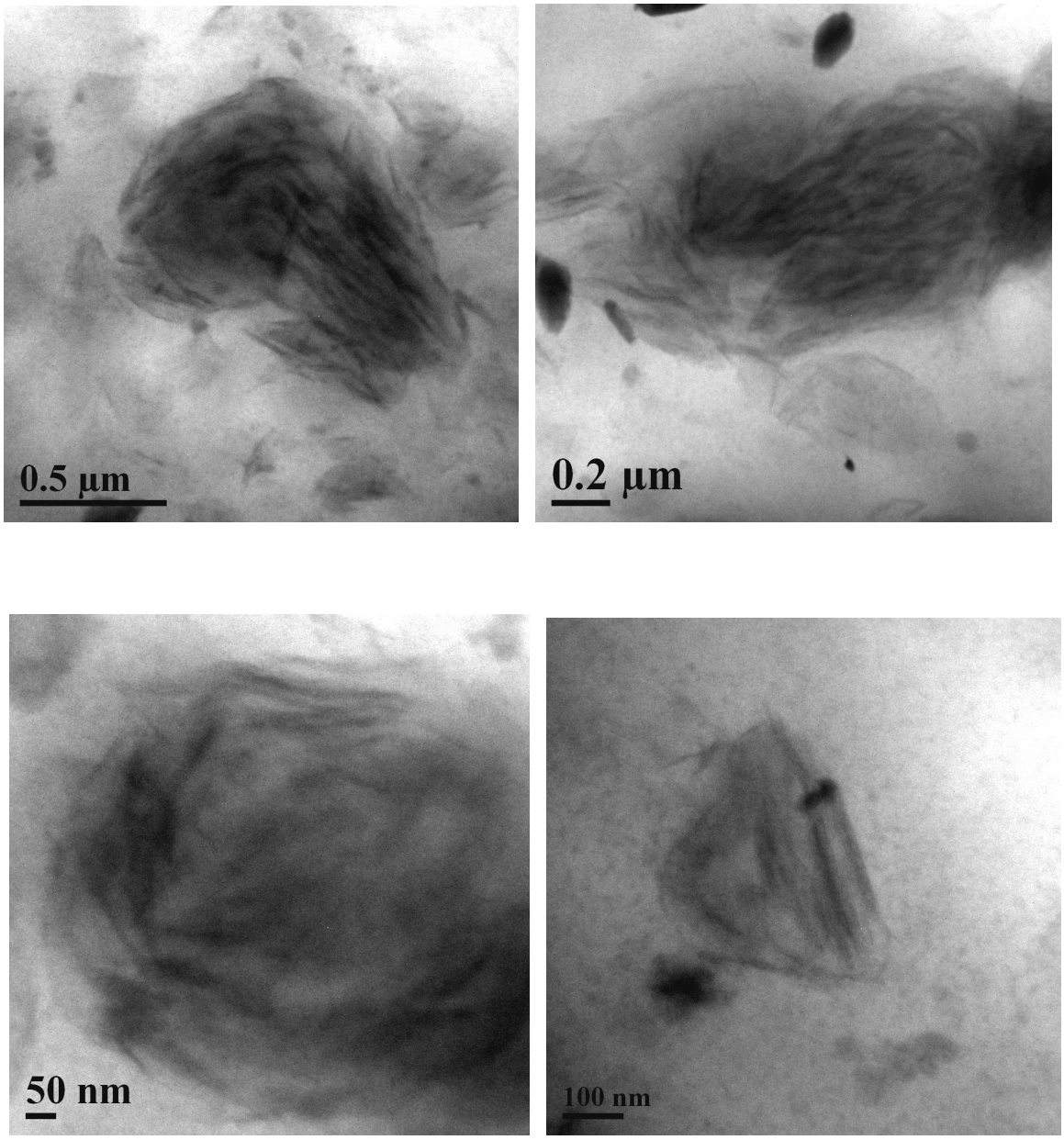

Fig. 5.17- TEM images of NR/BR organoclay nanocomposites (NM-7)

TEM images of organoclay-carbon black dual filler nanocomposite (NC-20) are presented in Fig. 5.18. Highly exfoliated structure of organoclay was observed in the NR/BR rubber matrix. In organoclay-carbon black dual filler system the TEM images of NC-20 showed a large extent of exfoliation of the organoclay, which appear to have a fiber like structure in the image whereas carbon black particles have a spherical shape and are darker in color. The distribution of both organoclay and carbon black are very fine in the nanocomposite material as seen in Fig. 5.18.

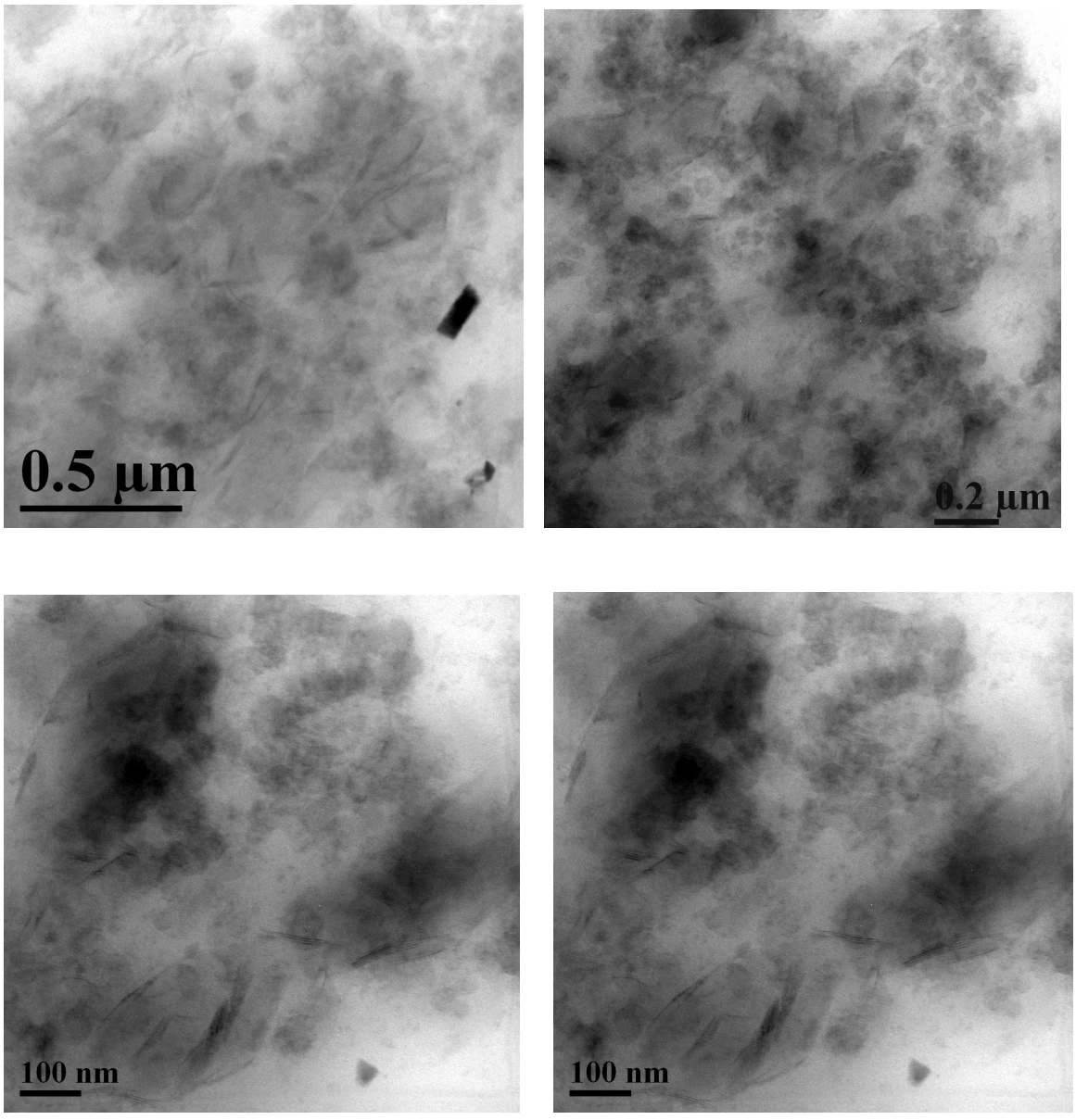

Fig. 5.18- TEM images of NR/BR organoclay-carbon black nanocomposites (NC 20)

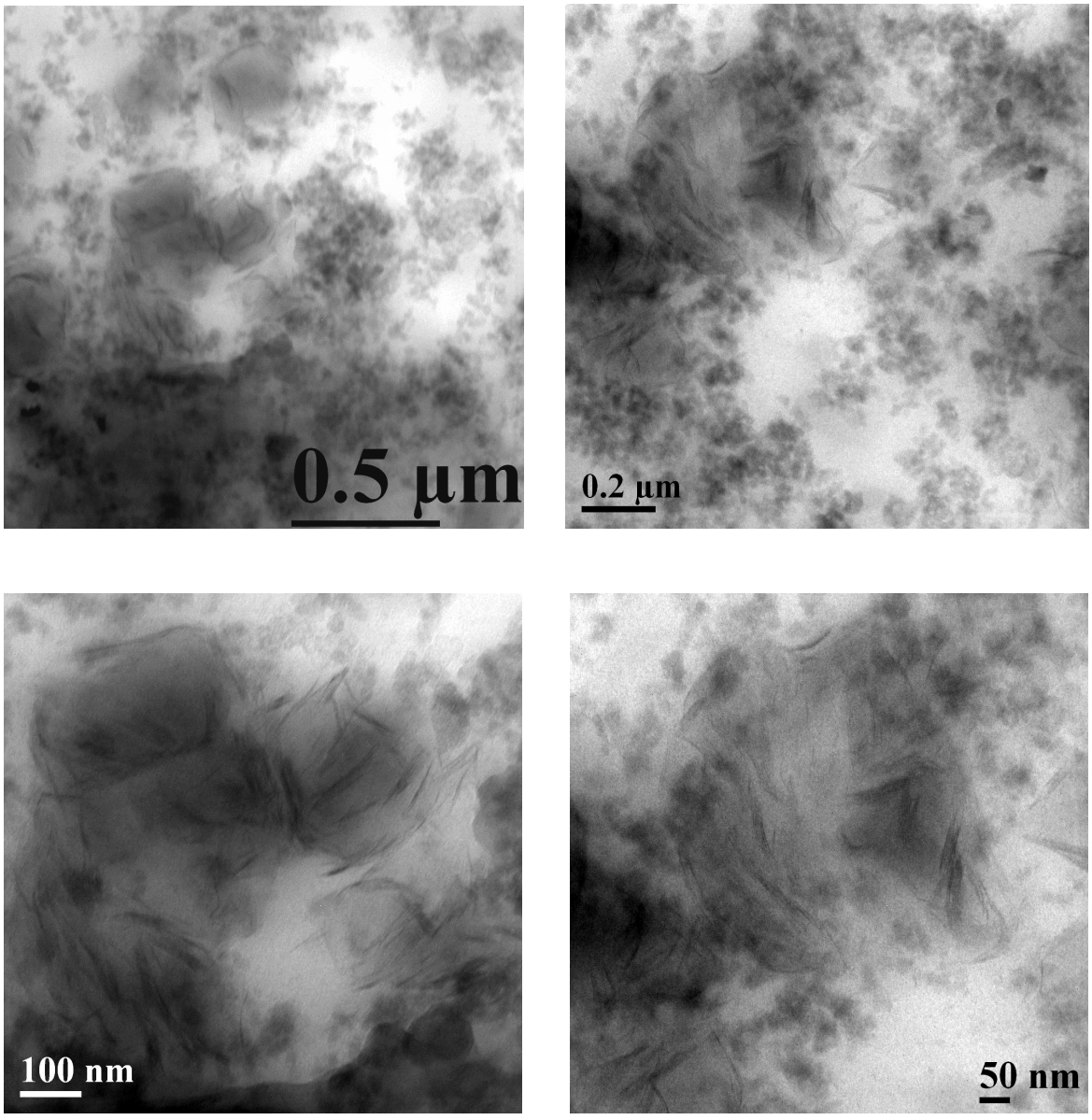

Fig. 5.19- TEM images of NR/BR organoclay-silica nanocomposites (NS 20)

TEM images of nanocomposites (NS-20) with organoclay-silica dual filler system showed a large extent of exfoliation of the organoclay mixed with some intercalated structure, which appear to be a fiber like in nature as seen from the image. Uniform distribution of organoclay and silica are observed in the NR/BR rubber matrix shown in Fig. 5.19. Presence of silane further enhanced the exfoliation of organoclay in organoclay-silica dual filler nanocomposite since it reacts with surface hydroxyl group of silica and organoclay as well thereby enhancing filler-polymer interaction.

Much better exfoliation of the organoclay was observed in both organoclay-carbon black and organoclay-silica dual filler systems compared to organoclay alone. This is attributed to the higher shear force generated during mixing in the presence of carbon black or silica filler in the matrix that resulted in greater exfoliation of organoclay, thereby providing superior reinforcement and excellent mechanical properties.

5.2.8 Conclusions

Nanocomposites based on NR/BR blends with organoclay showed excellent improvement of mechanical properties (Table 5.3 to 5.5) when compared with gum vulcanizate for example in the nanocomposite having NR/BR 70:30 and 7 phr organoclay there was 93 % enhancement in 300% modulus; 68% in Tensile strength; 47% in tear strength and 136% in Breaking Energy.

In spite of remarkable improvement of the above mentioned properties, organoclay nanocomposite did not fully meet the requirements of TBR tread compounds because for TBR tire tread applications, hardness, low strain modulus as well as abrasion resistance are very important. To meet these requirements, nanocomposites based on NR/BR blend were developed with organoclay-carbon black and organoclay-silica dual filler systems. The dual filler nanocomposites showed excellent mechanical properties which are comparable to commercial tread (Control) compounds and also fulfilled the requirements of Hardness, Modulus, Abrasion resistance and Tear strength for tread application. They meet the target performance range for TBR tread compounds.

Tan δ at 60^{o}C indicates lower rolling resistance of the compound and lower the value lower is the rolling resistance. The reduction organoclay-carbon black nanocomposite (NC-20) had 45% less Tan δ_{max} compared to Control-3. Similar reduction of Tan δ_{max} (40%) was observed in organoclay-silica nanocomposite (NS-20) in comparison with Control-4. This clearly shows dual filler nanocomposite (NC-20 and NS-20) will give much lower rolling resistance in tire without sacrificing other performance parameters like mechanical properties, tear properties, wear properties and traction. This investigation revealed the potential of nanocomposites which in future could be used as TBR tire tread to reduce rolling resistance and improve fuel economy in commercial automotive transport.

CHAPTER 6

ROLLING RESISTANCE SIMULATION OF TIRES USING STATIC FINITE ELEMENT ANALYSIS

Tire rolling resistance is a key performance index in the tire industry that addresses the tire quality parameters as well as environmental concern. Reduction of tire rolling resistance is a major technical challenge so as to reduce the fuel consumption. Rolling resistance of tires could be reduced by changing the compound formulation as well as the tire design.

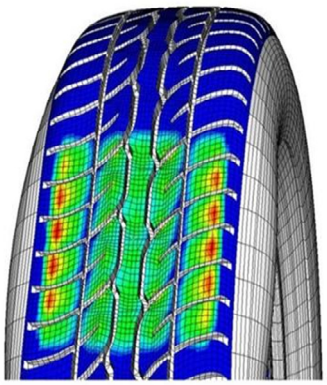

Fig. 6.1: Simulated PCR tire foot print

With the development of tire mechanics and computational technology, tire deformation, rolling resistance, and temperature distribution under roiling conditions could be predicted with a fair amount of accuracy using the finite element analysis (FEA). Commercial software's for the prediction of the tire rolling resistance that arises from the non linear viscoelastic characteristics of rubber are yet to be developed.

This Chapter gives a brief description of elastic tire simulation using Abaqus software that can analyze the tire deformation, stress, and strain under the static inflation and footprint load conditions, emphasizing the tire material hysteresis loss. A finite element program has been developed that uses non linear viscoelastic property of rubber and predicts the tire rolling resistance and temperature distribution. Rolling resistance of PCR and TBR tires with nanocomposite based tread were predicted using this investigation.

6.1 ELASTIC TIRE SIMULATION USING FEA

The whole work was done in three major steps;

I. Elastic tire simulation was carried out using commercial finite element code Abaqus. The simulation includes several steps like (a) FE tire model generation, (b) Material parameter identification, (c) Material modeling and (d) Steady Sate Rolling Simulation
II. Energy dissipation and rolling resistance were evaluated by using internally developed code. The code extracts the strain energy results of the model and the same is post processed with viscous material data. The dissipation energy is calculated based on Equ. 6.1 by taking the product of elastic strain energy and the loss tangent of materials. Computation of tire rolling resistance of both PCR and TBR tires with respective Control compounds and nanocomposites developed for their respective tread applications.
III. Measurement of rolling resistance of tires with Control compounds in In-door Drum type Pulley wheel testing equipment and validation of simulation results of tires with Control compounds against experimentally determined values.

6.1.1 FE Model Generation

The first step is to import tire geometry prepared in Auto CAD to Abaqus CAE and make partition of each tire component as shown in Figure 6.2 and 6.3. A half axi-symmetric tire model was used for 2D analysis. The tire cross section contains different rubber compounds and reinforcing materials. The fabric and steel cords were meshed with SFMGAX1 elements with twist degrees of freedom. The rubber matrix was modeled with hybrid elements like CGAX4H and CGAX3H with twist. The bead was modeled with CGAX4 elements with twist. The symmetric model generation capability was used to create a full 3-d model by revolving the axisymmetric mesh about a prescribed axis. Symmetric results transfer functionality was used to transfer the solution from the axisymmetric model onto the full 3-D model generated by Symmetric Model Generation. The transferred solution acts as the base state for the footprint loading.

6.1.2 Material Properties

A tire usually consists of several rubber components, in addition to several cords and rubber composites. In PCR tire four different types of materials are used and these are rubber compounds, textile fabrics, steel cords and bead wire whereas in TBR tire three types of materials are used such as Rubber compounds, Steel cords and Bead wires. Elastic tire simulation requires uni-axial stress-strain properties of rubber compounds, reinforcing material like Polyester and Nylon fabric and Steel cord. For bead wire elastic modulus and Poisson's ration is need.

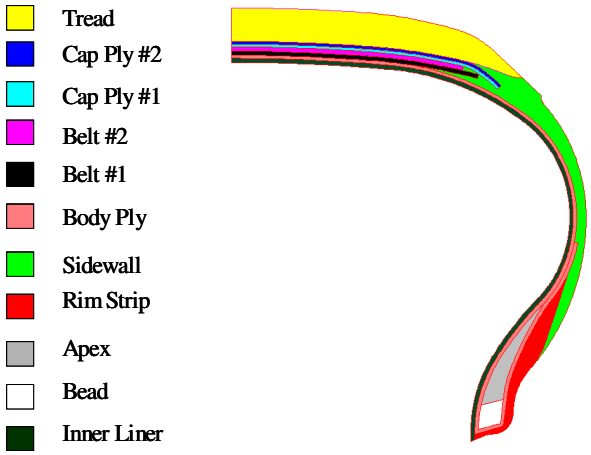

Fig. 6.2- PCR tire geometry: half tire cross section

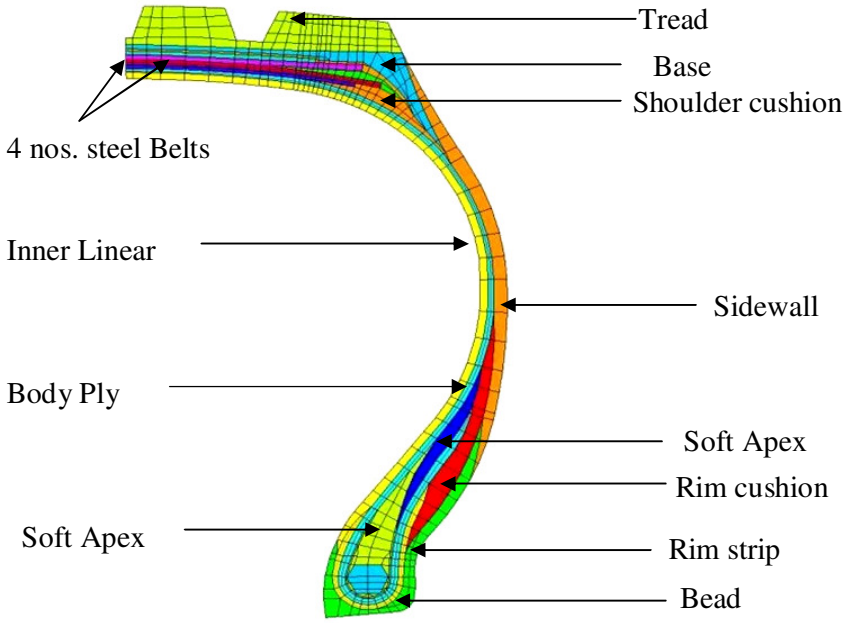

Fig. 6.3- TBR tire geometry: half tire cross section

6.1.3 Material modeling

FE analyses of rubber components need a constitutive model to represent the stress-strain relationship of the material. In commercial code, several material models are available to describe the mechanical behaviour of rubber. The choice of material model depends on several factors like strain range, complexity of loading condition and availability of experimental data. According to external loading, each tire component exhibits considerably distinguished deformation response. Rubber displays large non linear deformation and almost incompressible response, while steel and fabric cords resist most tension as well as compression loads and consequently produce small strain. Generally hyper-elastic material models are used for to describe high deformation. Therefore, Yeoh's hyperelastic material model was chosen for rubber materials and Marlow model for reinforcements such as fabric and steel cords. Bead was modeled as a elastic material.

Yeoh's model is capable of predicting stress-strain behaviour in different deformation modes from data obtained in one simple deformation mode like uniaxial tension.The strain energy function of Yeoh's model is expressed as

$$W= C_{10}(I_1-3) + C_{20}(I_1-3)^2 + C_{30}(I_1-3)^3 \quad \ldots\ldots\ldots\ldots\ldots\ldots\ldots\ldots\ldots\ldots \quad (6.1)$$

The uni-axial stress-strain equation in terms of strain invariant (I) and principle stretch (λ) expresses as;

$$\sigma /(\lambda - \lambda^{-1}) = 2C_{10} + 4C_{20}(I_1-3) + 6C_{30}(I_1-3)^2 \quad \ldots\ldots\ldots\ldots\ldots\ldots\ldots\ldots\ldots\ldots \quad (6.2)$$

Where σ is the nominal stress and I_1 is the first strain invariant

Hyper-elastic material models for rubber and fabric are shown in Fig.6.4 and Fig. 6.5 respectively. Steel cords reinforcements is represented by Marlow model implemented in Abaqus uses first strain invariant only and capture the behaviour of experimental data obtained from uni-axial tension and compression test very close as shown in Fig. 6.6.

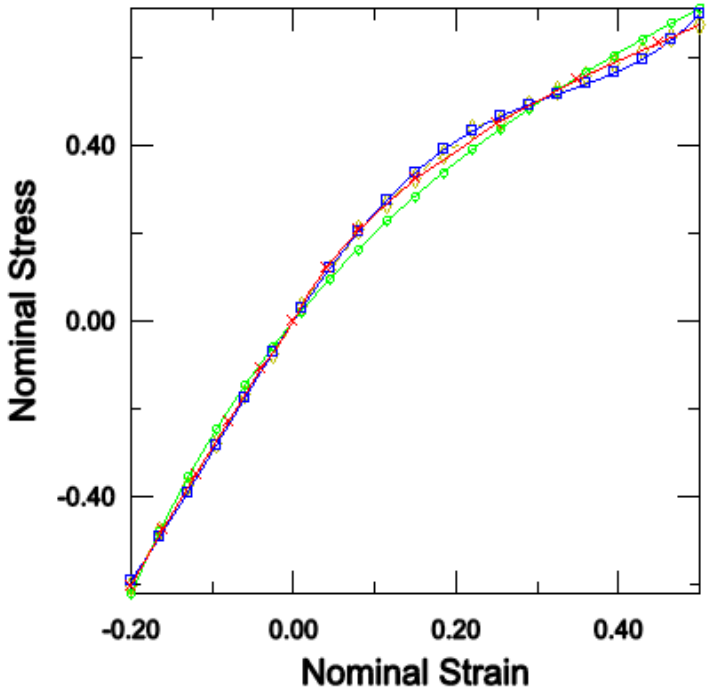

Fig. 6.4- Hyper-elastic material models for NR/BR dual filler (organoclay-carbon black) nanocomposite

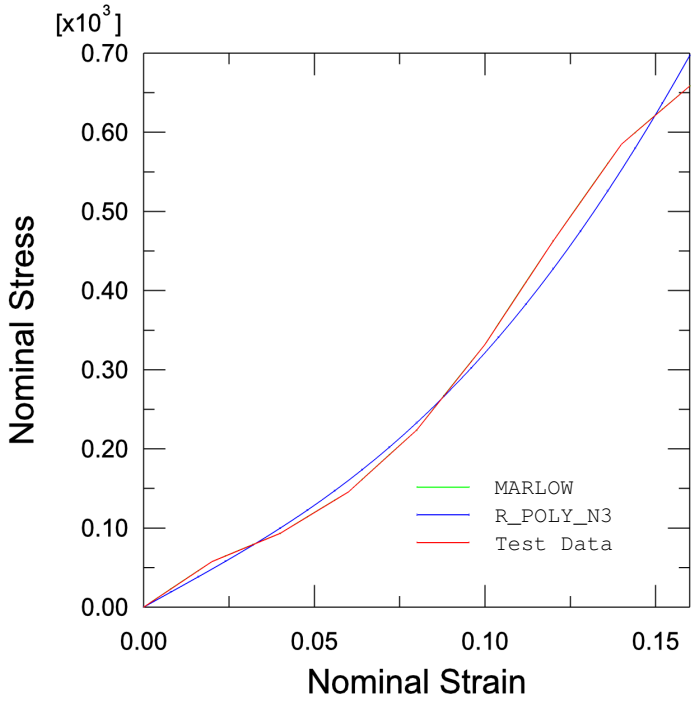

Fig. 6.5- Marlow's model for Nylon 66 tire cord

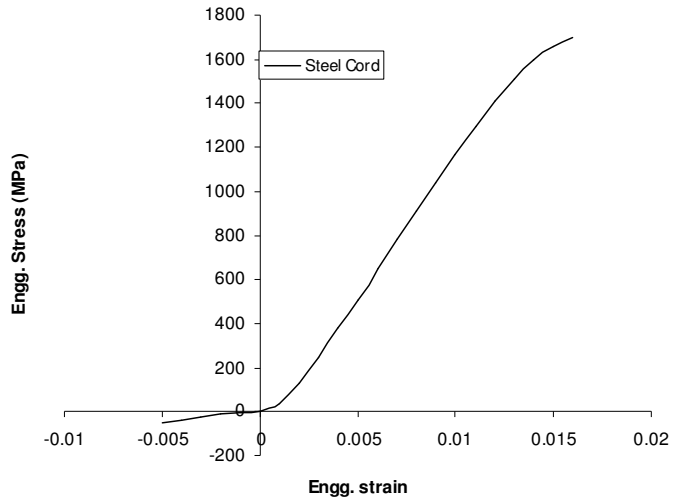

Fig. 6.6-Marlow's material model for steel cord reinforcement

6.1.4 Steady Sate Rolling Simulation

The whole analysis was carried out in three steps (a) 2D axisymmetric analysis (b) 3D footprint loading and (c) Steady state rolling analysis with full 3D tire model.

6.2 ROLLING RESISTANCE SOFTWARE DEVELOPMENT

6.2.1 Introduction

One of most practical way to predict rolling resistance of tires using standard finite element analysis was adopted in this investigation. A rolling resistance software code was developed keeping focus on three requirements: (1) easy input data preparation, (2) shorter computation time, and (3) adequate accuracy.

The method implements a steady state rolling simulation (3D non linear elastic analysis using Abaqus software). The strain energy and principal strains thus obtained, together with the loss factors (Tan δ) of the materials determined separately in the laboratory, are used to estimate the energy dissipation of a rolling tire through post processing.

6.2.2 Prediction of tire rolling resistance and temperature distributions using standard FEA (Fig. 6.7).

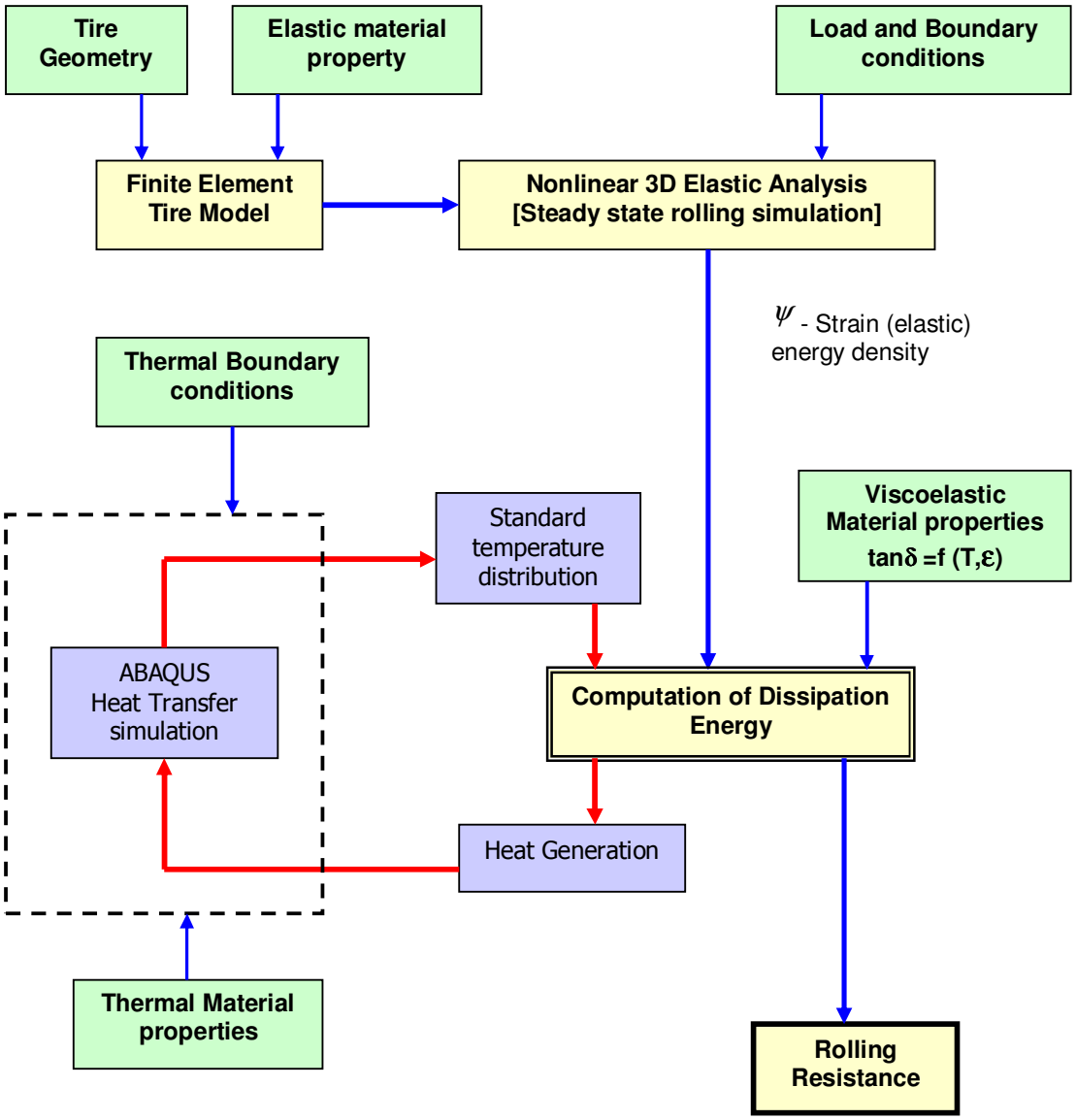

Fig. 6.7- Flow diagram of prediction of tire rolling resistance using FEA

This is a semi coupled thermo-mechanical method where the loss properties are updated as a function of strain and temperature. This simulation tool can be used for studying the relationship between compound and design variables and the rolling resistance of tires.

Elastic materials do not show any dissipation and hence elastic tire simulation does not provide any energy dissipation. Dissipation was computed in post-processing using loss material properties. Dissipation (Loss) can be described by so-called Tan δ quantity which is a ratio of loss modulus (dissipated energy) to storage modulus (elastic energy) in a harmonic loading.

The post processing approach was adopted in this investigation to calculate the energy dissipation, since the alternative approach based on non-linear steady state viscoelastic simulation requires extensive computation. The non-linear viscoelastic behavior was incorporated by providing strain and temperature dependent dynamic viscoelastic properties of rubber. In this study only hysteresis losses of rubber components were considered. The hysteresis loss of fabric was neglected because they were very small compared to rubber.

6.2.3 The methodology used in RR code development

Pure elastic simulation was carried out using standard finite element method. Both Static as well as steady state rolling tire simulation can be used in this investigation. In this procedure, tire is adaptively discretised along the circumference (Fig. 6.8a) in such a way that footprint area has finer mesh and mesh remains stationary and tire revolves during rolling simulation. Tire cross section is also discretised into elements (Fig. 6.8b) and every element represents a ring along the circumference as shown if Fig. 6.8c.

Every element is determined by a number of material points called integration points and the dissipated energy was evaluated at the integration points. Integration of dissipated energy is was multiplied with material volume and summed over integration point of all elements to obtain total dissipation. The dissipation depends on the amplitude of the strain energy density induced by a harmonic loading. In tire, the loading of a material point is non harmonic so it has to be replaced by a set of harmonic functions because Tan δ quantity which is used to get dissipation energy is measured in harmonic loading (Fig. 6.9).

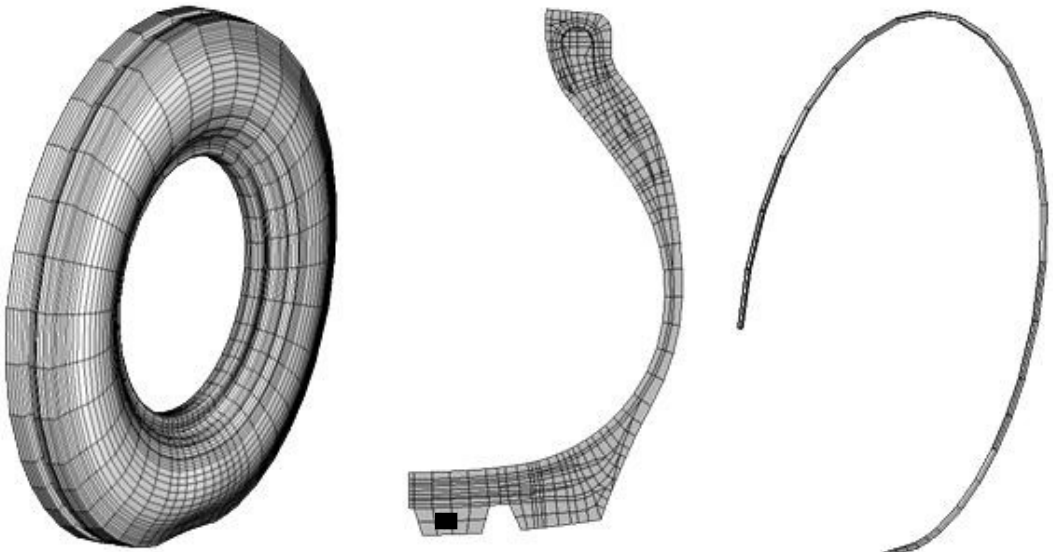

(a) (b) (c)

Fig. 6.8- Tire cross section and elemental ring along the circumference

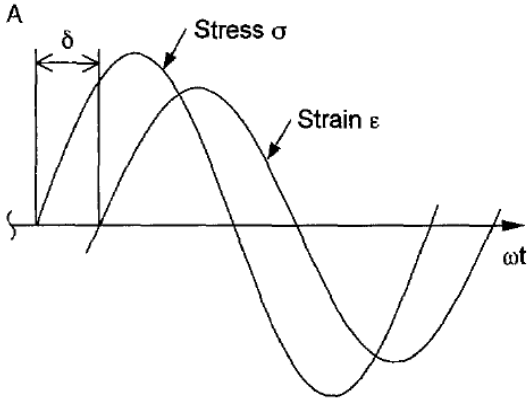

Fig. 6.9- Stress-strain relationship of viscoelastic materials under cyclic loading-phase lag between stress and strain

Non-harmonic function can be composed from a number of harmonic functions (trigonometric interpolation) using Fourier-Series transformation. However, data has to fulfil several requirements like data has to be equidistant; number of data points has to correlate with the number of series, etc. Due to the given adaptive discretisation along the circumference, the data has to be converted to fulfil these requirements. With increasing n, frequency increases and

amplitude decreases and solution of dissipation converged. The conversion of non-harmonic to harmonic function using Fourier Transform is shown is Fig. 6.10.

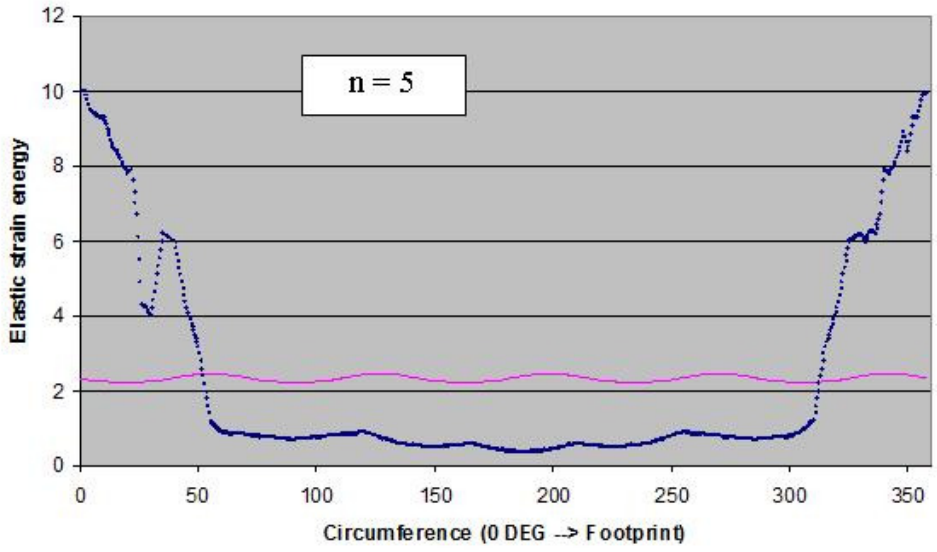

Fig. 6.10- Transformation of Non harmonic to harmonic function using Fourier Series

6.2.4 Computation of energy dissipation and rolling resistance

The total energy loss per one tire revolution is calculated by summation over the circumferential rings of the rubber as per the Equ. 6.1.

$$\psi^{diss} = \sum_{i=1}^{\infty} i 2\pi \psi_i Tan\delta_i \quad \text{..... (6.1)}$$

Where, Ψ – *Strain (elastic) energy*

Ψ^{diss} – *Dissipated energy in one full rotation*

$Tan\ \delta$ = *Loss Modulus (E'')/Storage Modulus (E')*

Rolling resistance was computed by dividing the total dissipated energy in one revolution by the distance travelled in one revolution using Equ. 6.2.

$$F_{RR} = -\psi^{diss} / 2\pi r \quad \text{..... (6.2)}$$

Where, F_{RR} *- Rolling Resistance*

$2\pi r$ *- Circumferential length*

6.2.5 Temperature equation

Rubber shows strong visco-elastic effects during cyclic deformation. Visco-elastic properties can by described with a combination of springs and dashpots as represented by Maxwell-element (Fig. 6.11). Response of the rubber material depends on the strain rate experienced by it.

Elastic materials do not show any dissipation and hence elastic tire simulation does not provide any energy dissipation. Dissipation (Loss) can be described by so-called Tan δ quantity which is a ratio of loss modulus (dissipated energy) to storage modulus (elastic energy) in a harmonic loading (Equ. 6.3). Hysteresis loop of rubber is shown in Fig. 6.12

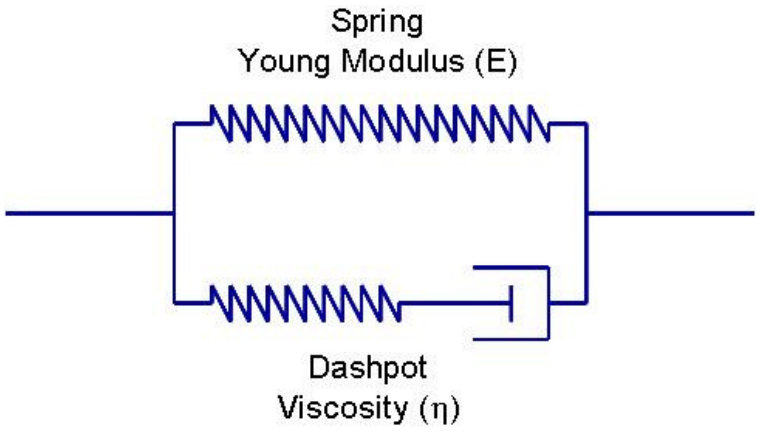

Fig. 6.11- Maxwell model: rubber is represented by spring and dashpot

Dependency of Tan δ on strain is very strong and greatly influences simulation results. Temperature also has a strong influence and it has to be considered. No significant dependency on frequency in the working range was observed.

$$Tan\delta = \frac{E''}{E'} = \frac{\psi^{diss}}{\psi} \quad \text{..... (6.3)}$$

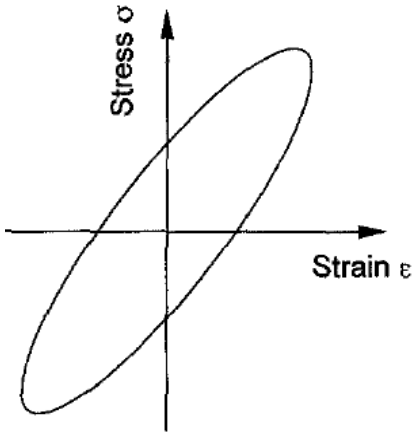

Fig. 6.12- Hysteresis loop of viscoelastic materials under cyclic loading.

A "Loss energy-Strain-Temperature" Equation was developed to capture the combined effect of strain and temperature on Tan δ (loss) is presented in Equ. 6.4.

$$\mathbf{Tan\ \delta_{i(Ts)} = Tan\ \delta_{i(To)}\ e^{-\xi\ (Ts-To)}} \quad \text{..... (6.4)}$$

Where,

ξ = - [Tm/Ts {Ln (Tan $\delta_{i(Tm)}$/Tan $\delta_{i(To)}$)}]/(Tm-To)

To and Tm – Two reference temperatures

Ts –working temperatures

ξ– factor

Tan $\delta_{i(To)}$, Tan $\delta_{i(Tm)}$ and Tan $\delta_{i(Ts)}$ --- Tan gent delta values at temp To, Tm and Ts

The strain sweep (Strain versus Tan δ) starting from 0.1% to 40% single strain amplitude (SSA) was carried out at two reference temperatures To (30^{o}C) and Tm (100^{o}C) using dynamic mechanical analyzer. The strain sweep (Strain versus Tan δ) curve at Ts (50^{o}C) was created using Equation 6.4 and compared with strain sweep curve determined experimentally at 50^{o}C. The strain sweep curve (strain versus Tan δ) predicted from the Equ.6.4 are similar to the

experimentally determined strain sweep curve and this showed very good correlation between experimental and predicted data as shown in Fig. 6.13.

To evaluate the energy dissipation at any integration point in a tire cross section, loss energy at that particular strain and temperature is required and to calculate the Loss energy, Tan δ at the same conditions is required. The measurement of Tan δ at any strain and temperature is not physically possible but with the help of Equ. 6.4, this could be predicted conveniently with reasonable accuracy.

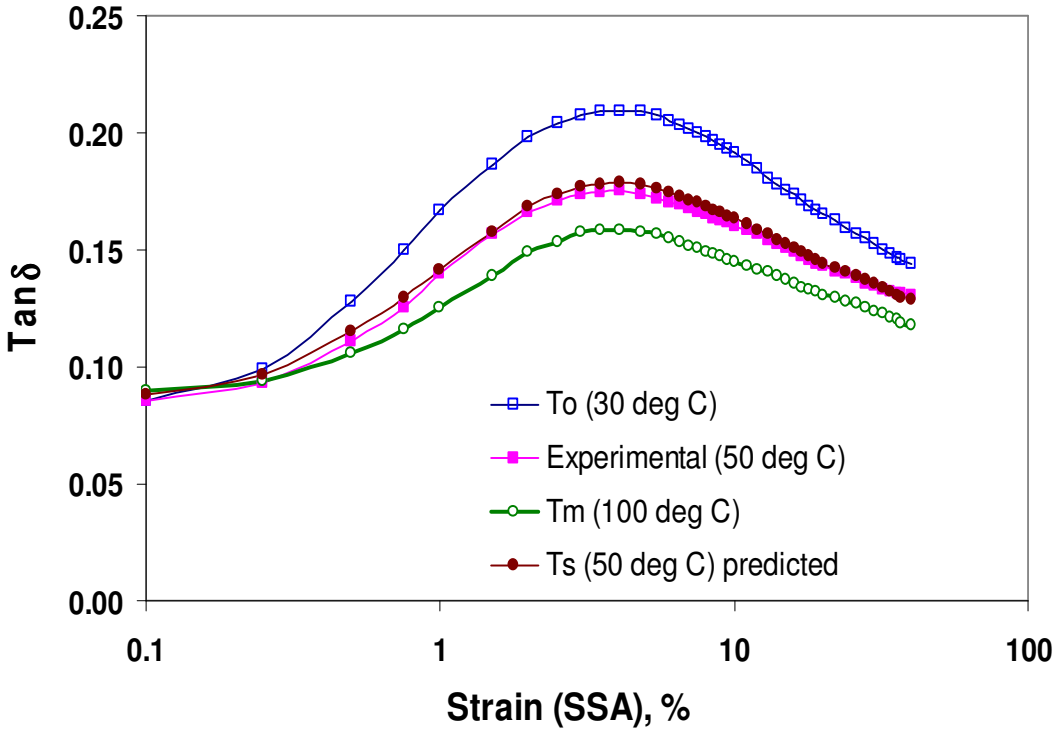

Fig. 6.13- Strain versus Tan δ at 10 Hz

6.2.6 Temperature distribution in a tire

The temperature distribution was done using standard ABAQUS heat transfer simulation. Tire was divided into finite elements and the material was evaluated at every integration points in the elements. In tire, dissipated energy acts as a heat source and to evaluate tire temperature. thermal conductivity of materials and heat transfer film coefficients are required. Heat capacity is not needed due to the stationary characteristic of the problem. The red colour indicates maximum temperature (~150^{o}C) followed by yellow, green, sky and blue colour.

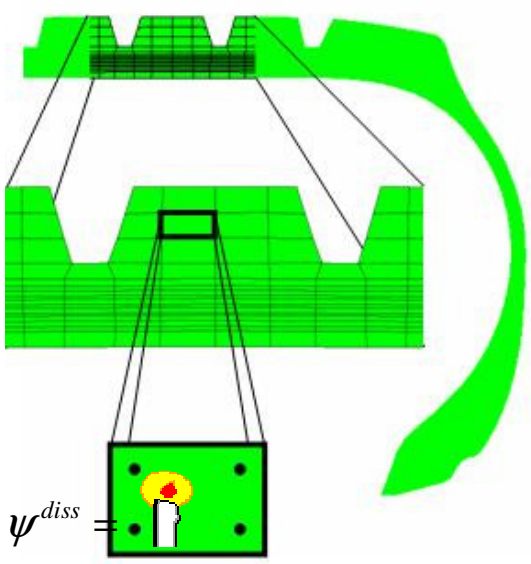

Fig. 6.14- Element and integration points in a PCR tire cross-section

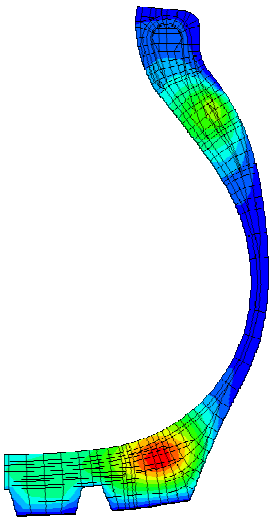

Fig. 6.15- Temperature distribution in a TBR tire cross-section

Using this rolling resistance code developed with FEA on Abaqus platform the rolling resistances were predicted with appropriate inputs of material properties and other constitutive equations and models discussed in this chapter. The results obtained are elaborated in the next Chapter

CHAPTER 7

PREDICTION OF ROLLING RESISTANCE OF PCR AND TBR TIRES WITH NANOCOMPOSITE TREADS USING FINITE ELEMENT SIMULATION

At a constant speed of 100 km/h a passenger car needs ~50% of its fuel to overcome rolling resistance and the rest of the fuel is used to overcome air drag whereas at a constant speed of 80 km/h a truck needs ~40% of his fuel to overcome rolling resistance. This indicates the importance of tire rolling resistance on fuel consumption. Tire rolling resistance is greatly influenced by viscoelastic behaviour of rubber. Approximate 90% of tire rolling loss may be attributed to hysteresis loss of rubber components and tread rubber alone is responsible for ~40% (Willet 1973, 1974). The different rubber components have its own contribution for tire rolling resistance; tread rubber is a major contributor followed by inner liner and apex in passenger car tires.

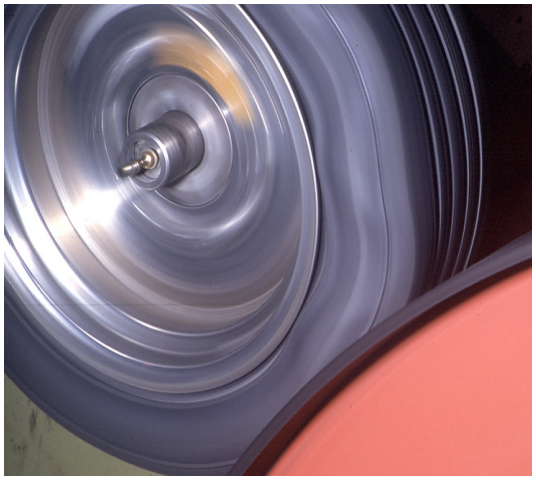

Fig. 7.1- TBR tire RR measurement

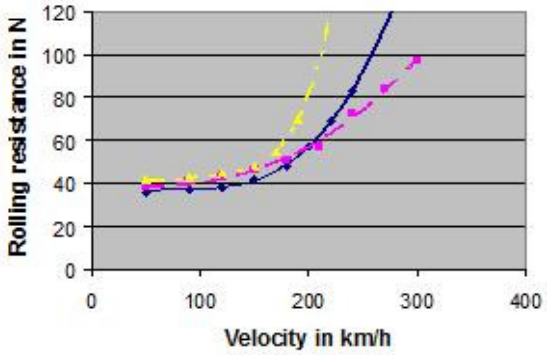

Fig.7.2- PCR tire Speed versus RR

Fig. 7.1 shows the measurement of rolling resistance of TBR tire on rotating drum. At higher speed, tire has higher rolling resistance as shown in Fig. 7.2.

Nanocomposites based on 70/30: SBR/BR blend and dual filler systems were developed for PCR tread application. These nanocomposites show much lower Tan δ at 60°C indicative of low tire rolling resistance when compared with commercial PCR tread compound (Control-1 and Control-2). Similarly nanocomposites based on 70/30: NR/BR have been developed for TBR tread application which also show much lower Tan δ at 60°C when compared with commercial TBR tread compounds (Control-3 and Control-4). The Tan δ at 60°C provides qualitative indication on compound rolling resistance but do not give any quantitative information on rolling resistance in tire. The rolling resistance of nanocomposite tread compounds in the tire could be predicted by using finite element simulation as described in Chapter 6.

7.1 INVESTIGATIONS ON ROLLING RESISTANCE OF NANOCOMPOSITE BASED PASSENGER CAR RADIAL TIRE TREAD COMPOUNDS USING FE SIMULATION TECHNIQUE

Tire rolling resistance is very important parameter in passenger car tire as it is responsible for 25% fuel consumption at average speed of 60 kmph. Lower rolling resistance saves a lot of fuel and protects the environment by lowering greenhouse gas emission. European Union has introduced strict norms for tire rolling resistance with effect from 2012. To meet the regulation, further reduction of rolling resistance through innovative tread compound is the need of the hour.

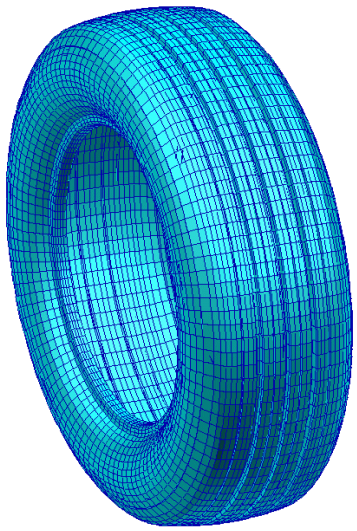

Fig. 7.3- PCR tire model with meshing

To achieve these requirements, nanocomposites based on 70/30: SBR/BR with organoclay-carbon black and organoclay-silica dual filler system were developed. In this investigation commercial carbon black based tread (Control-1) compounds and silica based tread (Control-2) were taken for reference. Tires with Control compounds as well as with nanocomposites were simulated and tire rolling resistances were computed. Rolling resistance of organoclay-carbon

black (SC-25 and FC-25) nanocomposites were compared with Control-1 and organoclay -Silica nanocomposites (SS-25 and FS-25) with Control-2.

7.1.1 Mechanical properties

The mechanical properties like hardness, modulus, tensile strength and elongation at break of the nanocomposites are presented in Table 7.1. The typical range of mechanical properties of passenger car tire tread compounds are also listed in the same Table. Mechanical properties of all the nanocomposites were within the typical performance range of passenger car tread compound. The improvement of properties with dual filler system is much more when compared to the individual filler contribution. Dual fillers had synergistic effect in the nanocomposite which resulted in better exfoliation of organoclay, thereby providing superior reinforcement and excellent mechanical properties.

Table 7.1-Mechanical properties of nanocomposites

Compound Reference	100% Modulus (MPa)	Tensile Strength (MPa)	Elongation at Break (%)	Hardness (Shore A)
Target→	**(1.5 – 2.5)**	**12.5 min**	**350 min**	**(60 – 70)**
Control-1	***1.96***	***18.9***	***510***	***66***
SC 25	**1.77**	**14.5**	**483**	**62**
FC 25	**1.80**	**14.8**	**460**	**62**
Control-2	***1.85***	***19.1***	***500***	***65***
SS25	**1.61**	**14.0**	**484**	**62**
FS 25	**1.60**	**13.0**	**452**	**61**

7.1.2 Hyper-elastic material properties

Hyper-elasticity is used to model a material the exhibits nonlinear, but reversible, stress strain behavior even at high strains. Properties of rubber material are;

a) large deformation, finite strains
b) Incompressible/ nearly incompressible
c) Final deformation state doesn't depend on load path, load-history
d) Isotropic

Most material models in commercially available finite element analysis codes are designed to describe only a subset of the structural properties of rubber. Stress-strain curves obtained from experiments done at different mode of deformation such as uni-axial, pure shear and bi-axial are fitted to calibrate the material model. The conditions, under which the stress-strain curves are created, are not defined by the material model. Hyper-elastic material properties of Control compounds and nanocomposites are shown in Fig. 7.4.

Hyper-elastic material properties have a great influence on FE elastic simulation results. Control compound had higher stiffness compared to all nanocomposites, however Control-1(CB tread) is stiffer than Control-2 (Silica tread). Lower stiffness of nanocomposites is due to much lower loading of fillers. Organoclay - carbon black nanocomposites (SC-25 and FC-25) showed slightly higher stiffness than organoclay-silica nanocomposites as observed in hyper-elastic stress-strain behaviour. The experimental stress-strain data was fitted in Yeoh's material model implemented in "***Abaqus software"*** and hyper-elastic material constants for all the compounds were determined as shown in Table 7.2.

Table 7.2-Yeoh's hyperelastic material constant

	C10	**C20**	**C30**	**D1**
Control-1	0.6541	-0.5738	0.5102	0.0308
SC-25	0.6201	-0.5973	0.5028	0.0325
FC-20	0.5836	-0.5040	0.3994	0.0345
Control-2	0.8202	-0.8605	0.6972	0.0245
SS-25	0.5252	-0.4247	0.3360	0.0383
FS-25	0.5410	-0.3932	0.2970	0.0372

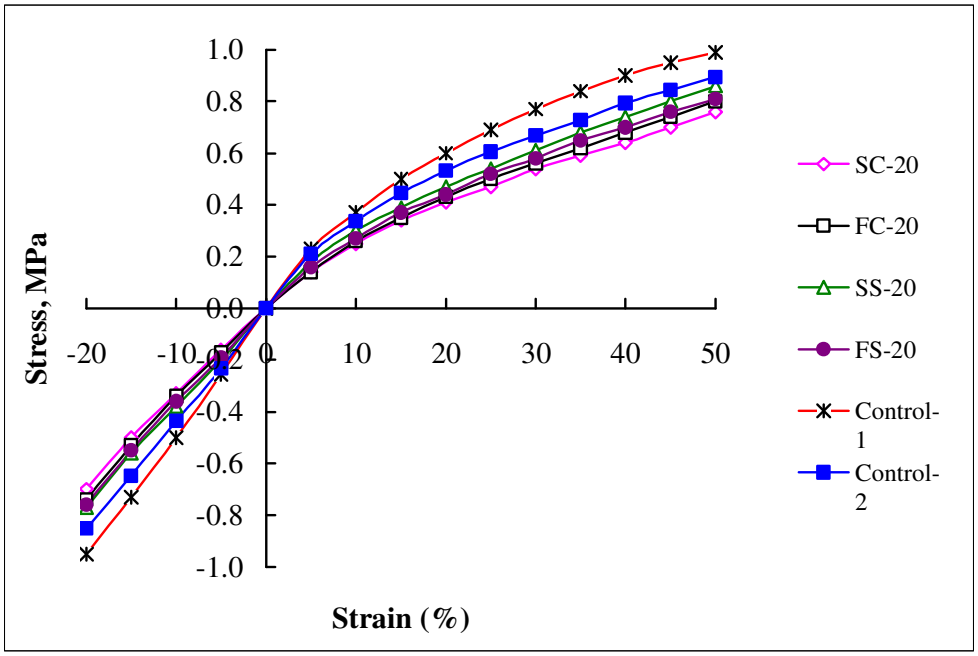

Fig. 7.4- Hyperelastic stress-strain properties of nanocomposites and Control compounds

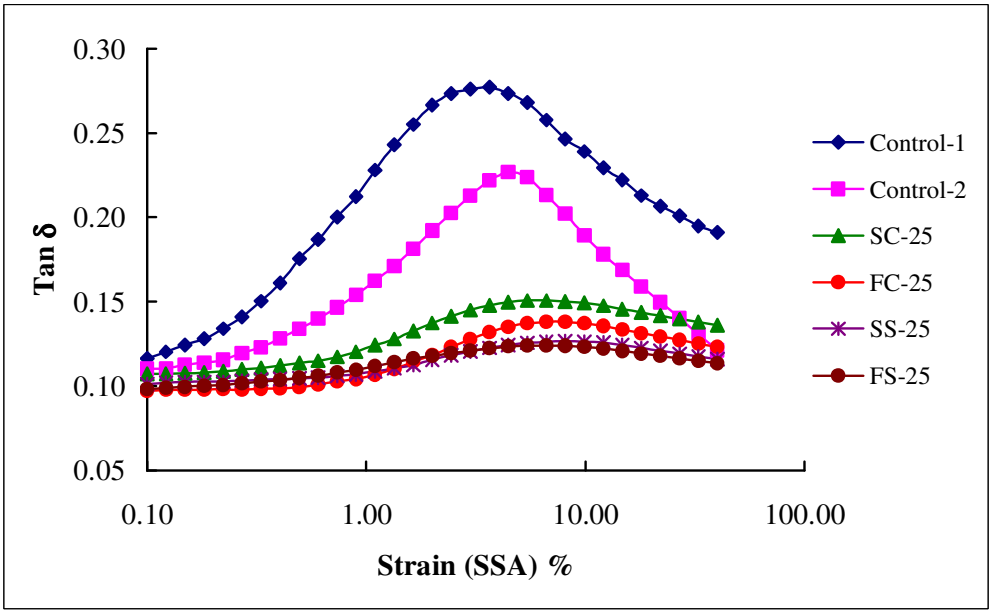

Fig. 7.5- Tan δ versus strain at 10 Hz and 60°C

7.1.3 Viscoelastic Material Properties

During strain sweep, nanocomposites showed much lower Tan δmax compared to the corresponding Control compounds as shown in Fig. 7.5. This behaviour was attributed to lower Filler-filler interaction (Payne's effect) in nanocomposites compared to the respective Control compounds with conventional fillers like carbon black and silica.

7.1.4 Computation of Rolling Resistance

The passenger car radial tires; 205/60R15 and 155/70R14 were investigated for rolling resistance. Rolling resistance of both the tires with carbon black and silica tread were measured in Drum type RR testing equipment and are shown in Table 7.3.

Table 7.3-Rolling resistance of tire with Control compounds at RR M/c.

Tire Size	Load (N)	Pressure (kPa)	Average Rolling Resistance (N)	
			Control- 1	Control- 2
205/60R15	6033	240	52.9	45.6
155/70R14	2827	240	30.7	23.6

Finite element simulation was carried out with both the tire 205/60R15 and 155/70R14. The 2D simulated tires cross-section and foot print of 205/60R15 are presented in Fig. 7.6 and 7.7.

Two Control compounds (Control-1 and Control-2) and four different nanocomposite treads SC-25 and FC-25 (organoclay-carbon black nanocomposites with 70/30, SSBR/BR and FSSBR/BR blends respectively) and FC-25 and FS-25 (organoclay-silica nanocomposite with 70/30, SSBR/BR and FSSBR/BR blends respectively) were used as tread compounds in tire. Rolling resistance of all the compounds were computed through simulation using *RR Code* and presented in Table 7.4 and 7.5.

The reductions of RR of nanocomposites of SC-25 and FC-25 against Control-1 were 21% and 24.9% respectively. Nanocomposite FC-25 (functional Solution SBR) showed more improvement in rolling resistance than nanocomposite SC-25 (Solution SBR). Similarly, the

reductions of rolling resistance of nanocomposites of SS-25 and FS-25 against Control-2 were 17.1% and 18.9% respectively. Nanocomposite FS-25 (functional solution SBR) showed more improvement in rolling resistance than nanocomposite SS-25 (solution SBR).

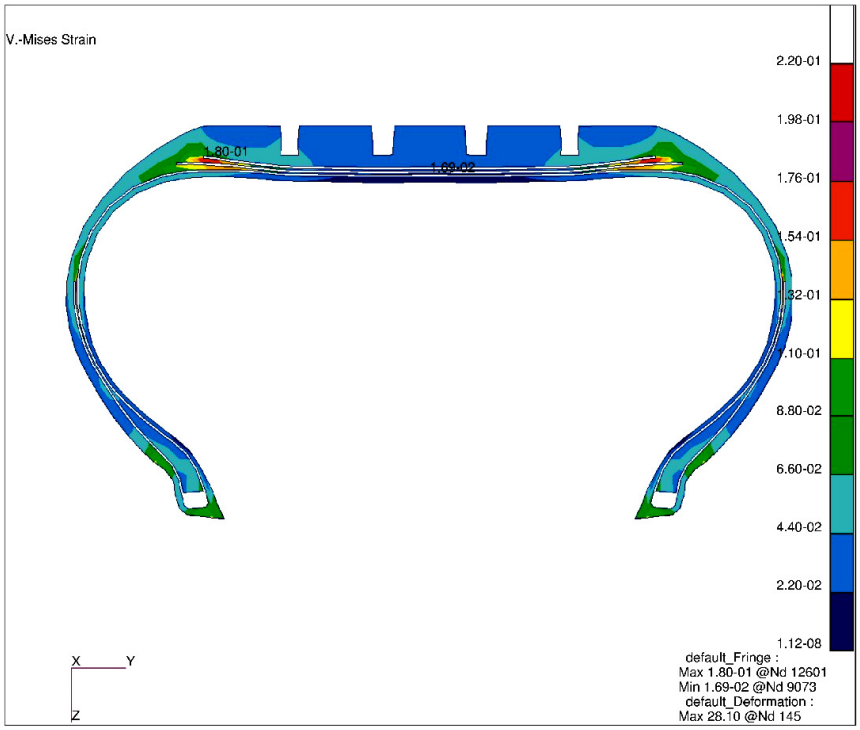

Fig. 7.6- 2D Finite element tire (205/65R15) cross section

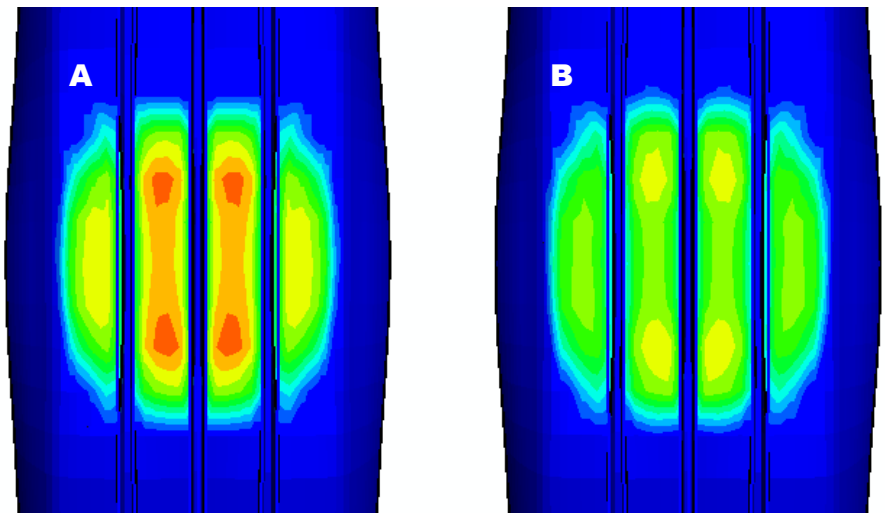

Fig. 7.7- Footprint of PCR tire (A) with silica based commercial tread compound (Control-1) and (B) with organoclay-silica dual filler nanocomposite (SS-25) tread compound

Table 7.4-Rolling resistance by simulation of organoclay –carbon black nanocomposites and Control-1

	Tire Size: 205/60R15			Tire Size: 155/70R14		
	Dissipated Energy (J)	Rolling Resistance (N)	% Reduction	Dissipated Energy (J)	Rolling Resistance (N)	% Reduction
Control 1	98.6	49.7		58.3	29.4	
SC-25	79.8	40.3	19.1	46.2	23.3	21.0
FC-25	75.7	38.2	23.2	43.8	22.1	24.9

Table 7.5-Rolling resistance by simulation of organoclay -silica nanocomposites and Control-2

	Tire Size: 205/60R15			Tire Size: 155/70R14		
	Dissipated Energy (J)	Rolling Resistance (N)	% Reduction	Dissipated Energy (J)	Rolling Resistance (N)	% Reduction
Control 2	88.9	44.8		45.0	22.7	
SS-25	73.9	37.3	16.8	37.3	18.8	17.1
FS-25	72.7	36.7	18.2	36.1	18.2	19.8

This investigation revealed that reduction of rolling resistance was more in case of organoclay – carbon black nanocomposites compared to organoclay-Silica nanocomposites from their respectively Control compounds. Filler-filler interaction (Payne's effect) in silica/silane system is less compared to carbon black with equal filler dosages in the compound. Replacement of equal amount carbon black or silica by small quantity of organoclay from their respective compound would lead to more reduction in Payne's effect in carbon black compound than silica

compound. Higher reduction of rolling resistance in organoclay –carbon black nanocomposite from Control-1 could be attributed to higher reduction of filler-filler interaction in this compared to organoclay -silica nanocomposite.

7.1.5 Conclusions

- Prediction of rolling resistance using finite element analysis is a very useful technique which is less expensive and fast and does not require any test tire. This simulation technique would be very useful to improve compound formulations as well as tire design in terms of rolling resistance in the design stage.

- In organoclay –carbon black nanocomposites (SC-25 and FC-32) the average reduction of rolling resistance was ~22% compared to carbon black based commercial passenger car tread compound (Control-1).

- Similarly ~18% reduction of rolling resistance was observed in organoclay-silica nanocomposites (SS-25 and FS-25) over silica based commercial passenger car tread compound (Control-2).

- The difference in rolling resistance between measured and simulated values of Control compounds is attributed to the difference in parameters such as aerodynamic drag, hysteresis loss of reinforcement and environmental conditions which were not incorporated in simulation. Approximately 90% correlation between measured and simulated values is observed which is reasonably precise from simulation perspective.

- 20% reduction in rolling resistance saves 5% fuel consumption, hence PCR having 18 to 22% less rolling resistance with tread compound with nanocomposite in comparison commercial PCR tread would save around 5% fuel from being consumed.

7.2 INVESTIGATIONS ON ROLLING RESISTANCE OF NANOCOMPOSITE BASED TRUCK BUS RADIAL TIRE TREAD COMPOUNDS USING FE SIMULATION TECHNIQUE

At a constant speed of 80 km/h a truck needs ~40% of its fuel to overcome rolling resistance and rest 60% is consumed to overcome aerodynamic drag. Energy efficient tires having 20% less rolling resistance in comparison to conventional tires reduces the fuel consumption by ~5%. Improvement of 10 % rolling resistance will lead to ≈ 2 g/km less CO_2 emission

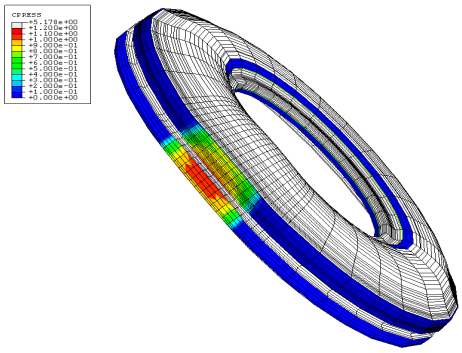

Fig. 7.8- Simulated TBR half tire model

To fulfill the requirements, nanocomposites based on 70/30: NR/BR blends with organoclay-carbon black and organoclay-silica dual filler system were developed. In this investigation commercial carbon black based TBR tread (Control-3) compounds and silica based tread (Control-2) were taken for reference. Tires with Control compounds as well as with nanocomposites were simulated and tire rolling resistances were computed. Rolling resistance of organoclay-carbon black nanocomposite (NC-20) was compared with Control-1 and organoclay-silica nanocomposite (NS-20) with Control-2.

7.2.1 Mechanical properties

The mechanical properties of tire tread rubber like hardness, modulus, tensile strength and elongation at break are critical for tire performance. Beside mechanical properties, abrasion loss, tear properties, hysteresis loss and dynamic properties play vital role in determining tire performances such as tire wear, durability, traction and rolling resistance. The performance properties of nanocomposite treads; NC-20 and NS-20 were compared with respective carbon black tread (Control-3) and silica tread (Control-4) as shown in Table 7.6. The typical range of commercial truck bus radial tread compound properties are also included in Table-7.4 for comparison purpose.

Table 7.6-Mechanical properties of nanocomposites

Properties	Typical range	Control-3	NC-20	Control-4	NS-20
Hardness, Shore A	60 - 70	66	64	64	62
100% Modulus, MPa	1.5 - 2.5	1.82	1.72	1.62	1.50
300% Modulus, MPa	6.0 - 10.0	9.16	7.10	8.32	6.39
Tensile Strength, MPa	22.0 min	23.2	25.8	24.9	28.0
Elongation at Break, %	420 min	554	651	596	646
Tear Strength, N/mm	65 - 110	81.0	68.5	107.0	70.1
Abrasion Loss, mm^3	70 - 110	88.0	94.0	99.0	106.0
Heat Build Up (ΔT), ^oC	20 - 30	28.0	18.0	26.0	16.0

Mechanical properties of the nanocomposite tread NC-20 are close to Control-3 and are well within the typical range of TBR commercial tread compounds. The nanocomposite tread NC-20 showed slightly lower hardness, modulus and tear strength than Control-3 but higher tensile strength, elongation at break and much lower heat build up indicate much lower hysteresis loss. The abrasion loss of NC-20 is slightly higher than Control-3 which indicates slightly lower mileage from nanocomposite tread. Nanocomposite tread NS-20 also exhibited the similar trend in properties like NC-20 when compared to Control-4. Lower modulus could be explained by the lower loading of filler in nanocomposite tread than carbon black and silica tread. Higher tensile strength in the nanocomposite is due to higher reinforcement and less hindrance in strain induced crystallization when stretch during tensile test.

7.2.2 Hyper-elastic material properties

For tire elastic simulation, hyperelastic material properties of rubber is required in finite element model. The material properties have a great influence on simulation results. Nanocomposite based tread compound NC-20 showed slightly lower stiffness both in tension and compression

mode than Control-3. Similarly, NS-20 organoclay-silica dual filler nanocomposite also showed slightly lower stiffness than Control-4. The lower stiffness of nanocomposite tread compounds is due to the presence of lower volume fraction of filler (25 phr) compared to carbon black or silica treads having 50 phr filler loading. Hyperelastic stress-strain properties of Control compounds and nanocomposites are shown in Fig. 7.9

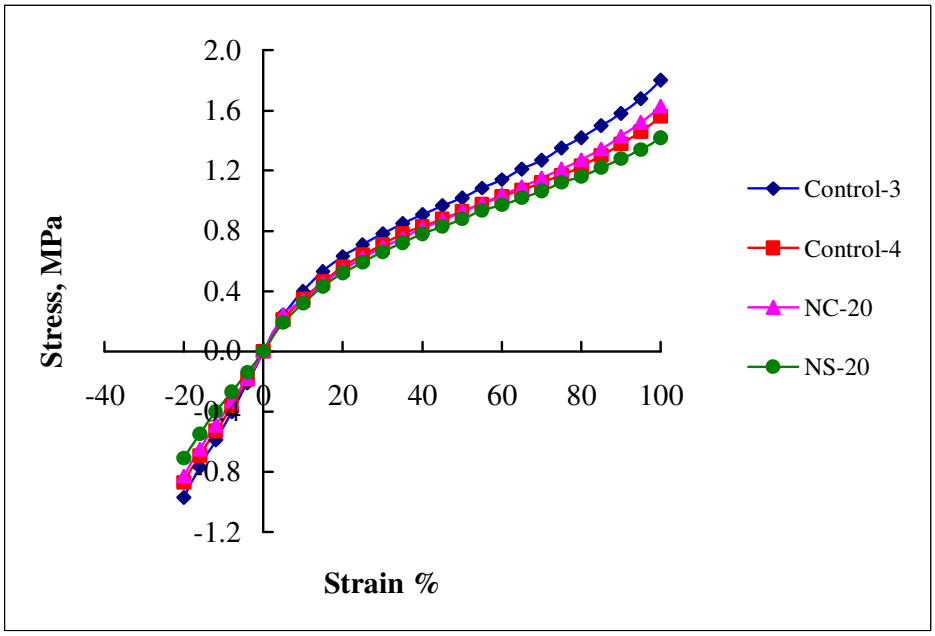

Fig.7.9- Hyperelastic properties of TBR tread rubber compounds

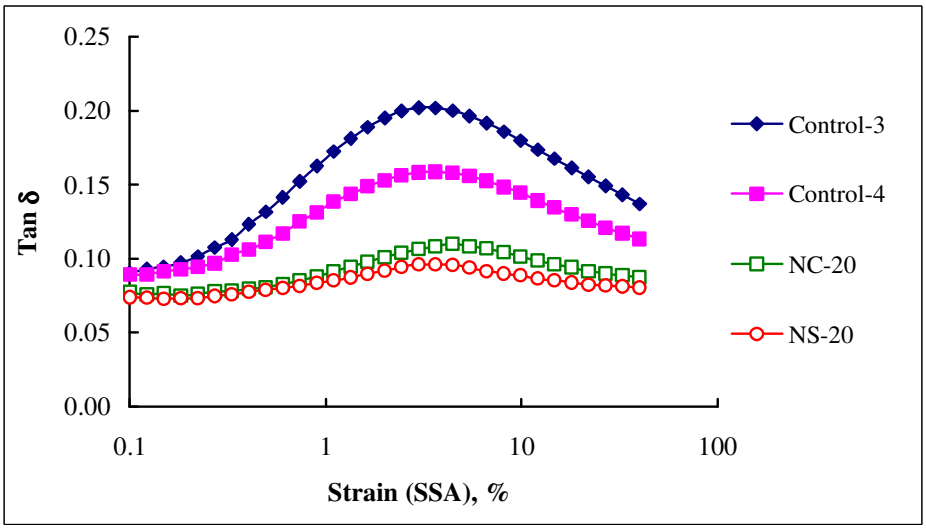

Fig. 7.10: Tan δ versus strain (SSA) at 60°C.

7.2.3 Viscoelastic material properties

The rolling resistance of tire originates from the energy dissipation which is the product of elastic strain energy density and viscoelastic properties of rubber (Tan δ). The Tan δ at any strain and temperature is required to evaluate the energy dissipation (hysteresis loss).

Nanocomposites showed much lower Tan δ values as observed during strain sweep in comparison with Control compounds as shown in Fig. 7.10. The high Tan δ values in Control tread compounds indicate much higher hysteresis losses than tire with nanocomposite treads. This behaviour is attributed to lower volume fraction of filler present in the nanocomposite compared with the Control tread compounds.

7.2.4 Computation of rolling resistance

Simulation is an effective tool to predict the rolling resistance of tire in design stage, using simulation techniques one can study the effect of new compounds and different design aspects on tire rolling resistance. Rolling resistance of three different sizes of tires such as 10.00R20 and two low aspect ratio tires 295/80R22.5 and 315/80R22.5 with commercial carbon tread compound (Control-3) were experimentally measured using drum type rolling resistance testing equipment as shown is Table 7.7.

Table 7.7-Rolling resistance of tire with Control-3 compound measured at pulley wheel machine

	10.00R20	295/80R22.5	315/80R22.5
Rolling Resistance, N	181.05	222.13	236.2

These three tires with Control tread compounds were modeled using finite element simulation techniques and their rolling resistances were evaluated using ***"RR Code".*** The simulated values correlated well with the measured values and approached to 94% of the measured value in 10R20, 92% in 295/80R22.5 and 91% 315 80 R 22.5 as shown in Fig. 7.11. The difference between measured and simulated values is attributed to the difference in parameters such as aerodynamic drag, hysteresis loss of reinforcement, etc. that are not accounted in simulation.

Interestingly the footprint shape of 10.00R20 real tire and simulated one appear very similar as observed in Fig. 7.12.

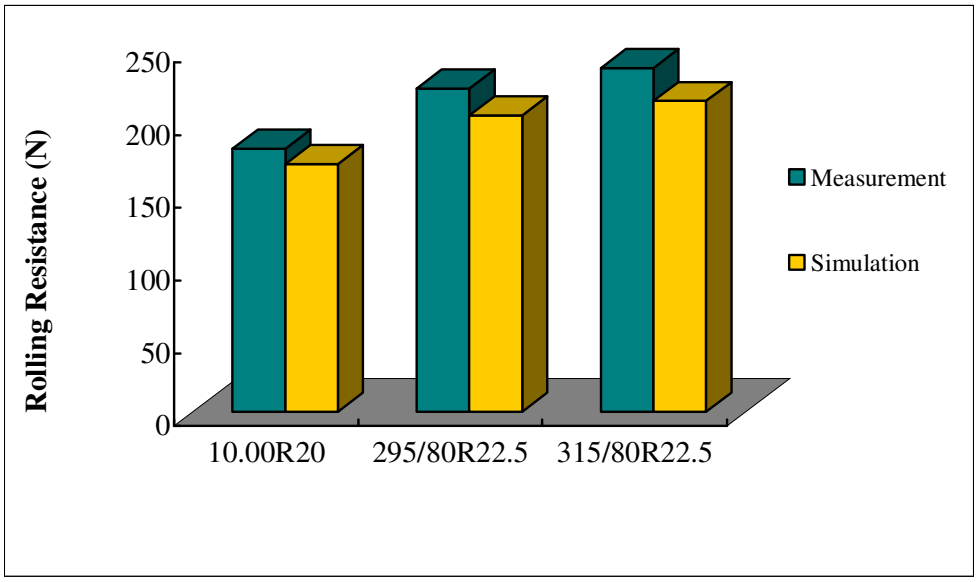

Fig. 7.11- RR results- measurement versus simulation

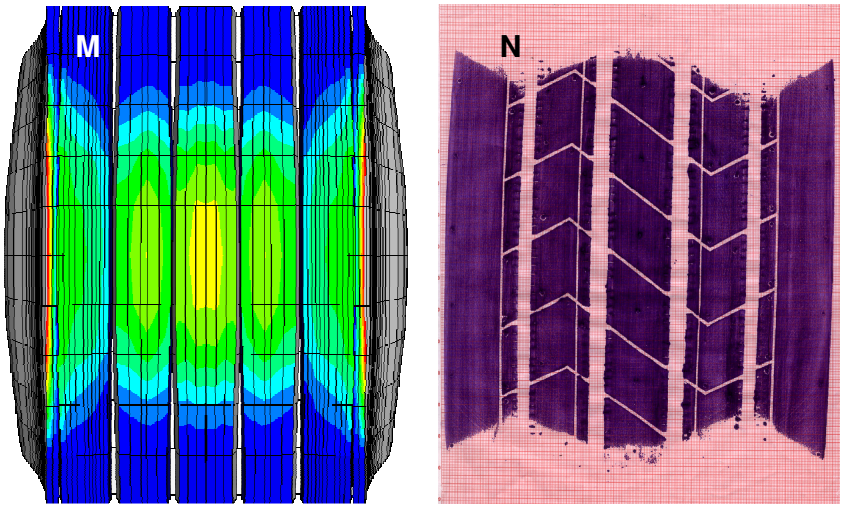

Fig. 7.12- Footprint of 10.00 R20 TBR tire with commercial carbon black tread (M) simulated footprint and (N) measured footprint

All three tires, 10.00R20, 295/80R22.5 and 315 80 R 22.5 with nanocomposite treads (NC-20 and NS-20) were simulated and their rolling resistances were evaluated using ***"RR Code".*** Finite element simulation of all three TBR tires with nanocomposite tread compounds, such as NC-20

and NS-20 were carried out and the rolling resistances were computed using *"RR Code"*. Simulated 2D cross section of 10.00R20 (full section) and 295/80R22.5 (half section) truck bus radial tire with nanocomposite tread (NC-20) are shown in Fig.7.13 and 7.14 respectively.

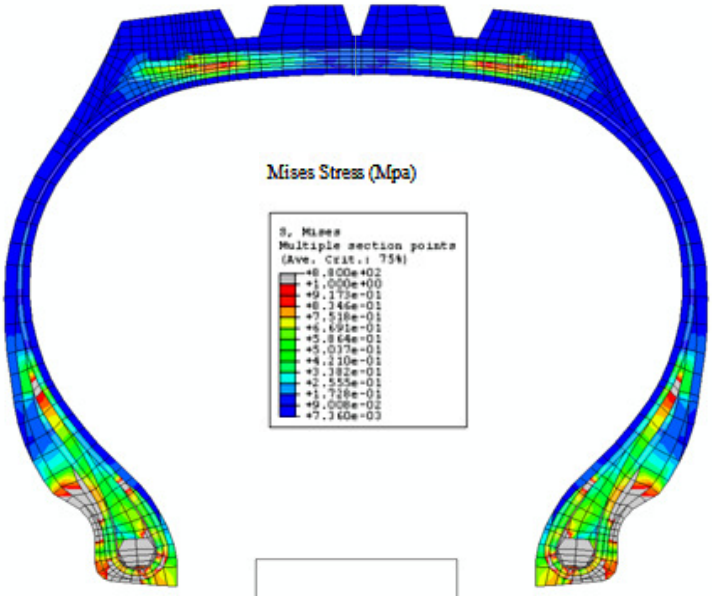

Fig. 7.13- TBR tire (10.00R20) 2D full tire cross section

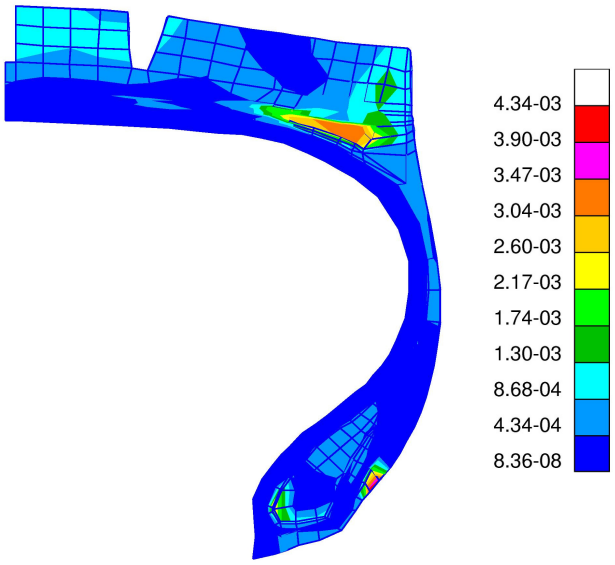

Fig. 7.14- TBR tire (295/80R22.5) 2D half tire cross section

The simulated foot print of 295/80R22.5 TBR tire with commercial carbon black tread (Control-3) and with organoclay-carbon black nanocomposite tread (NC-20) are shown in Fig. 7.15.

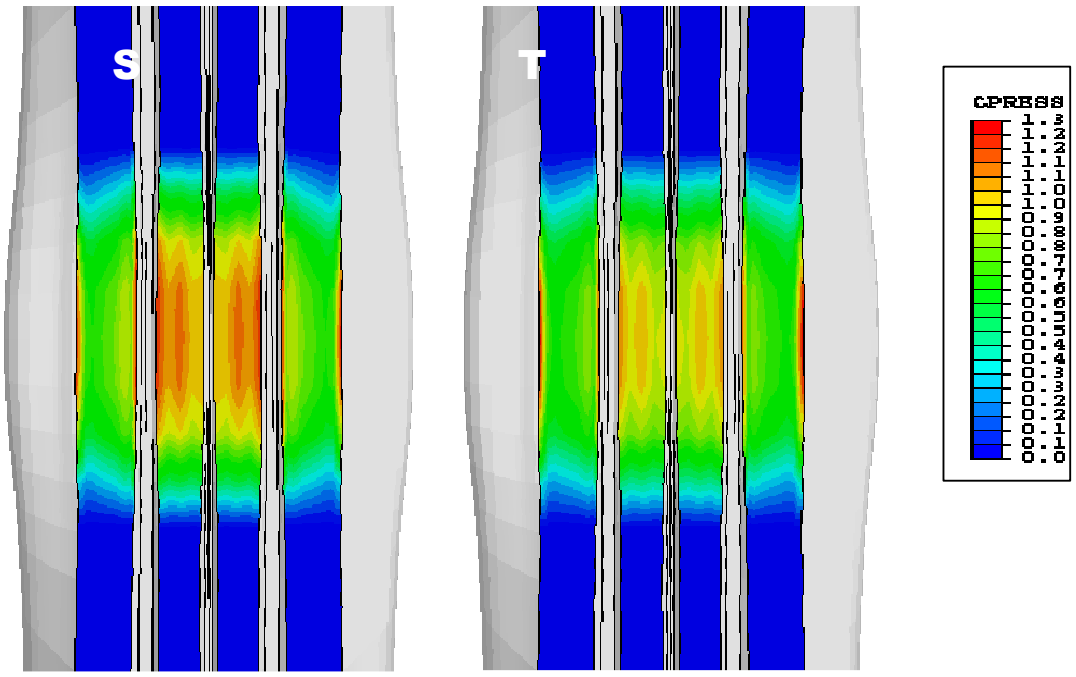

Fig. 7.15- Footprint of 295/80R22.5 TBR tire (S) with commercial carbon black tread, Control-3 and (T) with organoclay-carbon black nanocomposite tread, NC-20.

The rolling resistances of all three tires with organoclay-carbon black nanocomposite tread (NC-20) were compared with corresponding sizes of tires with commercial carbon black tread (Control-3). The nanocomposite tread showed much lower RR values than their corresponding carbon black counter parts for all three tire sizes. In organoclay-carbon black nanocomposite tread (NC-20), improvement of rolling resistance compared to commercial carbon black tread (Control-3) in 10.00R20, 295/80R22.5 and 315 80 R 22.5 are ***37.1, 34.4 and 32.8%*** respectively as shown in Fig. 7.16 and Table 7.6 to Fig. 7.8.

Similarly, the rolling resistances of all three tires with organoclay-Silica nanocomposite tread (NS-20) were compared with corresponding sizes having silica tread (Control-4). The nanocomposite tread showed much lower values than the corresponding Silica counter part in all three sizes. In organoclay-carbon black nanocomposite tread (NS-20), improvement of rolling

resistance compared to commercial silica tread (Control-4) in 10.00R20, 295/80R22.5 and 315 80 R 22.5 are ***35.2, 32.8 and 34.4 %*** respectively as shown in Fig. 7.17 and Table 7.6 to Fig. 7.8.

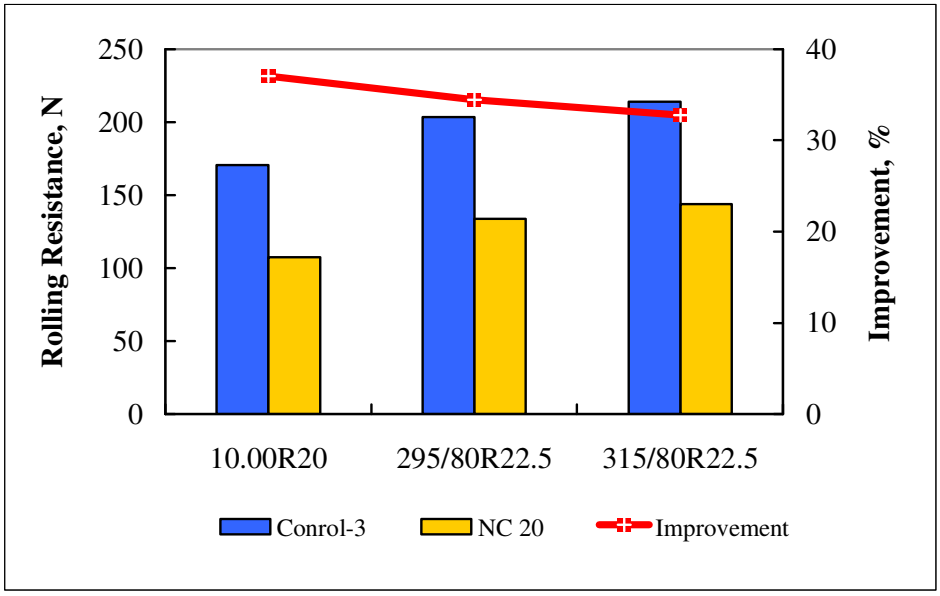

Fig. 7.16- RR results: organoclay-carbon black nanocomposite

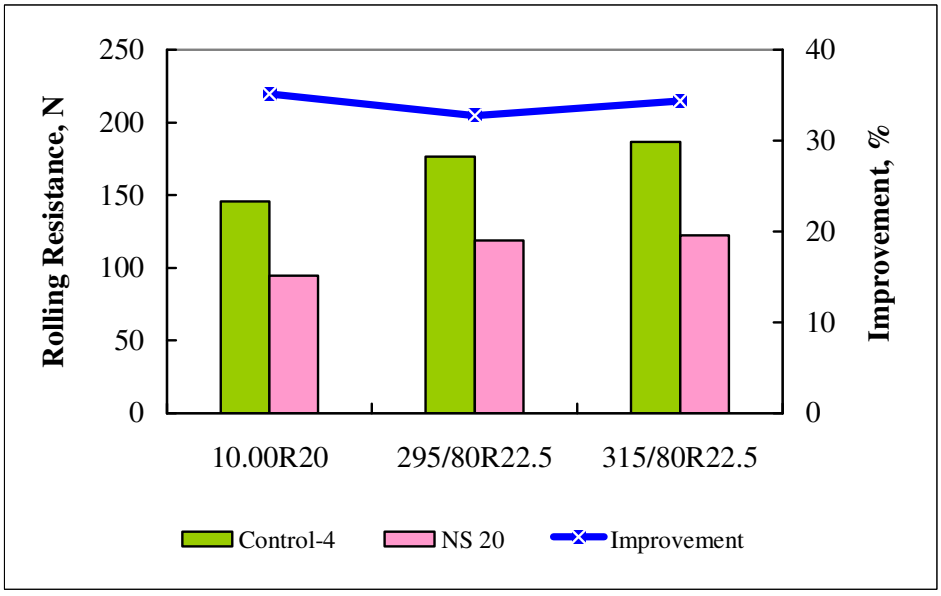

Fig. 7.17- RR results: organoclay-silica nanocomposite

Organoclay-carbon black and organoclay-silica dual filler nanocomposites have shown 32 to 37 % lower rolling resistance than commercially used carbon black and silica treads. Hence introduction of dual filler nanocomposite treads in truck bus radial tire would lead to ~8 to 9 % saving of precious fuel and would reduce environmental pollution. The rolling resistance of the nanocomposites and Control compounds for all three tires are presented in Table 7.8 to 7.10.

Table 7.8-Rolling resistance of 10.00R20 TBR tire predicted by simulation

		Dissipated Energy, N-mm	Rolling Resistance N	Percentage Improvement
10.00R20	Control-3	568443.0	170.4	
	NC 20	357779.2	107.2	37.1
	Control-4	486556.0	145.8	
	NS 20	315381.0	94.5	35.2

Table 7.9-Rolling resistance of 295/80R22.5 TBR tire predicted by simulation

		Dissipated Energy, N-mm	Rolling Resistance, N	Percentage Improvement
295 80 R 22.5	Control-3	679972.0	203.6	
	NC 20	446697.3	133.5	34.4
	Control-4	590998.8	176.6	
	NS 20	397164.3	118.7	32.8

Table 7.10-Rolling resistance of 315/80R22.5 TBR tire predicted by simulation

		Test Load N	Dissipated Energy, N-mm	Rolling Resistance, N	Percentage Improvement
315/80R22.5	Control-3	3403	737380.0	213.8	
	NC 20	3403	498761.2	143.8	32.8
	Control-4	3403	644333.2	186.7	
	NS 20	3403	422480.8	122.5	34.4

Future work would focus on further improvement of clay dispersion in NR/BR blend in industrial mixer and aim to produce tire for indoor endurance and outdoor road tests such as durability, mileage, traction, rolling resistance and fuel efficiency.

7.2.5 Conclusions

The performance properties of nanocomposite treads; NC-20 and NS-20 were compared with respective commercial carbon black tread (Control-3) and silica tread (Control-4). Mechanical properties such as hardness, modulus, tensile strength and elongation at break and critical performance properties like tire wear, durability, traction and rolling resistance of nanocomposites, NC-20 and NS-20 are comparable to their respective Control compounds and are well within the typical performance range.

In hyperelastic material characterization, nanocomposite based tread compounds NC-20 and NS-20 showed slightly lower stiffness both in tension and compression mode than respective Control compounds and this is due to the lower volume fraction (lower phr) of filler in nanocomposites.

Nanocomposites shows much lower Tan δ_{max} values as observed in dynamic mechanical study (strain sweep) in comparison with respective Control compounds. The much higher Tan δ value of Control tread compounds give higher hysteresis loss leads to higher rolling resistance in tire during rolling.

Rolling resistance of all three tires; 10.00R20, 295/80R22.5 and 315/80R22.5 with commercial carbon black tread (Control-3) and silica tread (Control-4) were experimentally measured in the drum type rolling resistance testing equipment as well as computed through finite element simulation using ***RR Code*.** The correlation between measurement and simulation were 94% in 10.00R20, 92% in 295/80R22.5 and 91% in 315/80R22.5. In general more than 90% correlation between simulation and measurement is considered to be very good.

The rolling resistances of all three tires with organoclay-carbon black nanocomposite tread (NC-20) show much lower rolling resistance when compared with their corresponding counter part with commercial carbon black tread (Control-3). The improvement of 37.1% rolling resistance

is the highest in 10.00R20 followed by 295/80R22.5 where it is 34.4% and 315/80R22.5 is also very close having value of 32.8%.

Similarly, the improvement of rolling resistances of 10.00R20, 295/80R22.5 and 315 80 R 22.5 tire with organoclay-silica nanocomposite tread (NS-20) when compared with their corresponding sizes with commercial silica tread (Control-4) are 35.2%, 32.8% and 34.4% respectively. In both the cases, the maximum improvement is observed in 10.00R20, however, improvement in 295/80R22.5 and 315/80R22.5 are very close.

In TBR tire average reduction of rolling resistance with nanocomposite tread is ~34.5% which would save ~ 8.6% fuel consumption and reduce environmental pollution. Introduction of silica filler in place of carbon black ~5% reduction of rolling resistance has been achieved. Therefore, dual filler nanocomposites are the future tread compound for extremely low rolling resistance highly fuel efficient truck bus radial (TBR) tire.

CHAPTER 8

SUMMARY AND CONCLUSIONS

8.1 INTRODUCTION

Vehicles are ubiquitous to modern civilization without them civilization would almost come to stand still, tire are perhaps the most important components of vehicles. In road transport vehicle is powered by petroleum fractions (petrol / Diesel / CNG) that exhaust CO_2 which is perhaps the most singular green house gas responsible for global warming. One of the major concerns of civilization is CO_2 emission. Higher is the fuel consumption more is the emission.

Tire rolling resistance plays an important role in fuel consumption. 20% reduction of tire rolling resistance can save 5% fuel. In the last 20 years, reduction of 20% tire rolling resistance was achieved by the introduction of silica technology. Ever since the introduction of the low rolling resistance tire "green" tire, silica is being used more and more as reinforcing filler in tire applications. Silica when compared to carbon black strongly reduces the rolling resistance of a tire, which in turn leads to a lower fuel consumption of the automobile.

To meet the requirements of European Union (EU) regulation on tire labeling by 2012, silica technology is not enough to meet the target and new technologies are the need of the day.

This investigation was undertaken to make an attempt to address these pressing issues. In this investigation composites based on nano clay (organoclay) were formulated and their efficiency was tested as true tread material for both passenger car radial (PCR) and truck bus radial (TBR) tires. The significant findings and conclusions are listed below sequentially.

8.2 PREPARATION AND CHARACTERIZATION OF NANOCOMPOSITES BASED ON ORGANOCLAY AND BLENDS OF DIFFERENT TYPES OF SBR WITH BR

i. Organoclay has poor dispersibility in SBR/BR rubbers hence a compatibilizer XNBR was required to be used for appropriate dispersion of the filler.

ii. The mechanical and dynamic mechanical properties of the investigated rubber nanocomposites improved as the carboxyl content in XNBR increased.

iii. Among the three mixing techniques used in this investigation internal mixing resulted in the best properties. Moreover, this method is very convenient for industrial applications. The solution method provided better properties than 2 roll mill mixing but removal of solvent was difficult, time consuming and therefore not feasible for industrial applications where as, mixing of clay in 2 roll mill was quite difficult.

iv. For SBR/BR=70/30 blends, the optimum dosages of organoclay and XNBR were found to be 6 and 10 phr respectively.

v. Among three types of SBR investigated, ESBR showed the best mechanical properties followed by SSBR and FSSBR.

vi. All SBR nanocomposites showed slightly lower glass transition temperature and lower Tan δ values at Tg compared to their corresponding gum counter parts in dynamic mechanical testing.

vii. TEM images of SBR nanocomposites prepared by all three mixing technique exhibited mixed intercalated and exfoliated structure of layer silicate in the matrix; however internal mixer showed the best exfoliated morphology.

viii. XRD investigations also supported the intercalated and exfoliated morphology of nanocomposite which was evidenced by the increase of d-spacing of layer silicate and reduction of peaks intensity.

ix. Although organoclay nanocomposite showed excellent mechanical properties but hardness, modulus and other performance properties such as abrasion resistance, tear strength were not sufficient for tire tread application. Further research is required in this field to improve these properties.

8.3 DEVELOPMENT AND CHARACTERIZATION OF HIGH PERFORMANCE NANOCOMPOSITES BASED ON DUAL FILLER SYSTEM AND BLENDS OF DIFFERENT TYPES OF SBR WITH BR

i. Nanocomposites based on SBR/BR blends with organoclay showed remarkable improvement in mechanical properties like hardness, modulus, tensile strength, elongation at break, breaking energy and tear strength compared to gum vulcanizate.

ii. To meet the requirements of tire tread, nanocomposites were developed with organoclay-carbon black and organoclay-silica dual filler systems based on SBR/BR blend using 7% carboxylated nitrile rubber (XNBR) as compatibilizer.

iii. The dual filler nanocomposites showed excellent mechanical properties and are well within the target performance range of passenger car radial tire tread compounds. These blend with dual filler system nanocomposites also fulfilled the requirement of abrasion properties; wet traction and dry traction which are very important for PCR tread application.

iv. Since nanocomposites contain much lower dosage of filler, they show lower hysteresis loss which was reflected in lower Tan δ values at 60^{o}C.

v. Nanocomposite based passenger car tread compounds showed lower rolling resistance without sacrificing other performance parameters like mechanical properties, tear properties, wear properties, wet traction and dry traction.

vi. The properties achieved by dual filler nanocomposites with reasonably small amount of the filler content are close to commercial tread compounds that are highly loaded with fillers.

vii. This investigation revealed the potential of nanocomposites could be used as high performance passenger car radial tread to reduce rolling resistance and improve fuel economy in automotive transport.

6.1 PREPARATION AND CHARACTERIZATION OF NANOCOMPOSITES BASED ON NR/BR BLENDS AND ORGANOCLAY.

Investigations on nanocomposites of NR/BR (70/30) with organoclay (Closite®15A) using XNBR as a compatibiliser reveals the following:

i. NR/BR blends are usually used to formulate TBR tire tread compounds. It was observed that using organoclay as the filler all mechanical properties like modulus, tensile strength and elongation at break increased as the carboxyl content of XNBR increased from NB1(1% carboxyllation) to NB7 (7% carboxyllation). As carboxyl % in XNBR increases, the surface energy of the rubber increases which leads to higher interfacial interaction between filler and polymer (Das *et al*, 2008).

ii. The mixing technique used also influences the organoclay dispersion and ultimately the mechanical properties. Internal mixer lead to the best clay dispersion and mechanical property enhancement followed by solution mixing and 2 roll mill. The mixing temperature (140^{o}C) and high shear force in internal mixer has influence on the filler-polymer interaction which may be the reason for better clay dispersion and properties of nanocomposite compared to solution and 2 roll mill mixing.

iii. The NR/BR-organoclay nanocomposite with 7 phr organoclay was found optimum as it exhibited the best physical properties like hardness, modulus, tensile strength, elongation at break and dynamic mechanical properties. The XRD study of the same nanocomposite reveals the silicate layers were expanded. TEM image also shows the intercalated and exfoliated morphology of the nanocomposite.

iv. The strong interfacial interaction between highly polar XNBR and organoclay played an important role in clay dispersion with in the rubber matrix. Strong interaction between carboxyl group and polar organoclay formed a thermodynamically stable composite and help clay dispersion when mixed with rubber.

8.5 DEVELOPMENT AND CHARACTERIZATION OF HIGH PERFORMANCE NANOCOMPOSITES BASED ON NR/BR BLENDS AND DUAL FILLER SYSTEM

i. Nanocomposites based on NR/BR blends with organoclay showed excellent improvement of mechanical properties when compared with gum vulcanizate for example in the nanocomposite having NR/BR 70:30 and 7 phr organoclay there was 93 % enhancement in 300% modulus; 68% in Tensile strength; 47% in tear strength and 136% in Breaking Energy.

ii. In spite of remarkable improvement of the above mentioned properties, organoclay nanocomposite did not fully meet the requirements of TBR tread compounds because for TBR tire tread applications, hardness, low strain modulus as well as abrasion resistance are very important.

iii. To meet these requirements, nanocomposites based on NR/BR blend were developed with organoclay-carbon black and organoclay-silica dual filler systems. The dual filler nanocomposites showed excellent mechanical properties which are comparable to commercial tread (Control) compounds and also fulfilled the requirements of Hardness, Modulus, Abrasion resistance and Tear strength for tread application. They meet the target performance range for TBR tread compounds.

iv. Tan δ at 60^{o}C indicates lower rolling resistance of the compound and lower the value lower is the rolling resistance. The reduction organoclay-carbon black nanocomposite (NC-20) had 45% less Tan δ_{max} compared to Control-3. Similar reduction of Tan δ_{max} (40%) was observed in organoclay-silica nanocomposite (NS-20) in comparison with Control-4. This clearly shows dual filler nanocomposite (NC-20 and NS-20) will give much lower rolling resistance in tire without sacrificing other performance parameters like mechanical properties, tear properties, wear properties and traction.

v. This investigation revealed the potential of nanocomposites which in future could be used as TBR tire tread to reduce rolling resistance and improve fuel economy in commercial automotive transport.

8.6 ROLLING RESISTANCE SIMULATION OF TIRES USING STATIC FINITE ELEMENT ANALYSIS

i. To investigate tire rolling with the help finite element analysis, a rolling resistance software "*RR code*" was developed and validated with standard tire. One of most practical way to predict rolling resistance of tires using standard finite element analysis was adopted in this investigation. A rolling resistance software "*RR code*" was developed keeping focus on three requirements: (1) easy input data preparation, (2) shorter computation time, and (3) adequate accuracy.

ii. The method implements a steady state rolling simulation (3D non linear elastic analysis using Abaqus software) first and then the strain energy and principal strains thus obtained, together with the loss factors (Tanδ) of the materials determined separately in the laboratory, are used to estimate the energy dissipation of a rolling tire through post processing. In this method loss properties are updated as a function of strain and temperature. Elastic tire simulation was carried out using commercial finite element code Abaqus. The simulation includes several steps like (a) FE tire model generation, (b) Material parameter identification, (c) Material modeling and (d) Steady state rolling simulation

iii. A temperature equation was developed to capture non linear behaviour of Tan δ with variation of dynamic strain and temperature. This equation updates Tan δ value at any strain and temperature during computation of dissipation energy through iterative process. This simulation tool can be used for studying the relationship between compound and design variables and the rolling resistance of tires.

iv. As loss energy representing tire rolling resistance is temperature depended and during service tire gets heated due to conversion of loss energy into heat and reaches a steady state, hence tire temperature distribution in tire to be captured to get accurate rolling resistance value. The temperature distribution in the tire was simulated using standard ABAQUS heat transfer simulation.

8.7 INVESTIGATIONS ON ROLLING RESISTANCE OF NANOCOMPOSITE BASED PASSENGER CAR RADIAL TIRE TREAD COMPOUNDS USING FE SIMULATION TECHNIQUE

i. Prediction of rolling resistance using finite element analysis is a very useful technique which is less expensive and fast and does not require any test tire. This simulation technique would be very useful to improve compound formulations as well as tire design in terms of rolling resistance in the design stage.

ii. In organoclay –carbon black nanocomposites (SC-25 and FC-32) the average reduction of rolling resistance was ~22% compared to carbon black based commercial passenger car tread compound (Control-1).

iii. Similarly ~18% reduction of rolling resistance was observed in organoclay-silica nanocomposites (SS-25 and FS-25) over silica based commercial passenger car tread compound (Control-2).

iv. The difference in rolling resistance between measured and simulated values of Control compounds is attributed to the difference in parameters such as aerodynamic drag, hysteresis loss of reinforcement and environmental conditions which were not incorporated in simulation. Approximately 90% correlation between measured and simulated values is observed which is reasonably precise from simulation perspective.

v. 20% reduction in rolling resistance saves 5% fuel consumption, hence PCR having 18 to 22% less rolling resistance with tread compound with nanocomposite in comparison commercial PCR tread would save around 5% fuel from being consumed.

8.2 INVESTIGATIONS ON ROLLING RESISTANCE OF NANOCOMPOSITE BASED TRUCK BUS RADIAL TIRE TREAD COMPOUNDS USING FE SIMULATION TECHNIQUE

i. Rolling resistance of all three tires; 10.00R20, 295/80R22.5 and 315/80R22.5 with commercial carbon black tread (Control-3) and silica tread (Control-4) were experimentally measured in the drum type rolling resistance testing equipment as well as computed through finite element simulation using *RR Code*. The correlation between measurement and simulation were 94% in 10.00R20, 92% in 295/80R22.5 and 91% in

315/80R22.5. In general more than 90% correlation between simulation and measurement is considered to be very good.

ii. The rolling resistances of all three tires with organoclay-carbon black nanocomposite tread (NC-20) show much lower rolling resistance when compared with their corresponding counter part with commercial carbon black tread (Control-3). The improvement of 37.1% rolling resistance is the highest in 10.00R20 followed by 295/80R22.5 where it is 34.4% and 315/80R22.5 is also very close having value of 32.8%.

iii. Similarly, the improvement of rolling resistances of 10.00R20, 295/80R22.5 and 315 80 R 22.5 tire with organoclay-silica nanocomposite tread (NS-20) when compared with their corresponding sizes with commercial silica tread (Control-4) are 35.2%, 32.8% and 34.4% respectively. In both the cases, the maximum improvement is observed in 10.00R20, however, improvement in 295/80R22.5 and 315/80R22.5 are very close.

iv. In TBR tire average reduction of rolling resistance with nanocomposite tread is ~34.5% which would save ~ 8.6% fuel consumption and reduce environmental pollution. Introduction of silica filler in place of carbon black ~5% reduction of rolling resistance has been achieved. Therefore, dual filler nanocomposites are the future tread compound for extremely low rolling resistance highly fuel efficient truck bus radial (TBR) tire.

The primary objective of development of nanocomposites that can match the prevalent tire tread compounds in term of physical properties while returning much lower rolling resistance without sacrificing other requirements viz. Wet traction, Dry traction, Wear, etc was made. The nanocomposites used as tread show ~20% less rolling resistance in PCR tire which accounts for 5% saving in fuel consumption and ~35% lower in TBR tire which also accounts for ~8.5% fuel saving and reduction of CO_2 emission to save environment.

The secondary objective of prediction of rolling resistance during the design stage through finite element simulation was also made. The good correlation ~90 - 95% was observed between measured and simulated rolling resistance. Using simulations, rolling resistances of tire tread with nanocomposites were predicted with reasonably good accuracy.

8.9 FUTURE WORK

One of the main goals in this project was to develop low rolling resistance passenger car tire tread with SBR/BR-dual filler nanocomposite and truck bus radial tire tread with NR/BR-dual filler nanocomposites. With the newly developed nanocomposite ~ 20-25% reduction of RR in PCR tire and ~30-35% in TBR tire was observed with the help of simulation. However there is ample scope to continue this work further. Some aspects that may be addressed in future are;

i. Produce tire with nanocomposite tread and carry out the indoor testing like endurance, rolling resistance, force and moment and wear characteristics. Presently very high cost of nanoclay is one of the major concerns for its commercial application in tire. In future price of nanoclay may decrease and can find its application in low rolling resistance tire production.
ii. Modification of clay so that no compatibilizer is required especially in SBR
iii. Modification of rubber to have better compatibility with nanoclay
iv. Direct mixing of nanoclay along with conventional filler like carbon black and silica in industrial Banbury mixer.
v. Study of mixing conditions like temperature, rotor speed and mixing time on clay-rubber interaction and investigation of clay exfoliation by TEM and XRD.

This work is the beginning of new era to develop extremely low rolling resistance PCR and TBR tire to reduce CO_2 emission and save precious fuel as well as environmental damage.

REFERENCES

- Abe A, Kamergawa T, Nakajima Y. Optimum young modulus distribution in tire design. Tire Sci. Technol.1996; 24 (3):204.
- Abaqus. Example Problem manual, Version 6.7, Volume II. 2006; Other Application and Analysis, Tire Analysis, Section; 3.1.1 to 3.1.3, Simulia, Providence Rhode Island, USA.
- Abaqus. Analysis user's manual, Version 6.7, Volume III. 2006; Materials, Simulia, Providence Rhode Island, USA.
- Ahmed MB, Darroudi M, Shameli K. Antibacterial effect of synthesized Silver/Monmorillonite Nanocomposites by UV-irradiation Method. Res. J. Biol. Sci. 2009; 4(9): 1056-1060.
- Alexandre M, Dubois P. Polymer layered silicate nanocomposites: Preparation, properties and uses of a new class of materials. Mater. Sci. Eng. 2000; 28: 1-63.
- Ansarifar A, Nijhawan R, Nanapoolsin T, Song M. Reinforcing effect of silica and silane fillers on the properties of some natural rubber vulcanizates. Rubber Chem. Technol. 2003; 76:1290.
- Arroyo M, Lopez-Manchado M, Herrero B. Organo-montmorillonite as Substitute of Carbon Black in Natural Rubber Compounds. Polymer. 2003; 44:2447-2453.
- Bandyopadhyay S, Giannelis E, Hsieh A. Thermal and Thermo-Mechanical Properties of PMMA Nanocomposites. Polym. Mater. Sci. & Eng. 2000; 82: 208-209.
- Bharadwaj R. Modeling the Barrier Properties of Polymer-Layered Silicate Nanocomposites. Macromolecules. 2001; 34: 9189-9192.
- Blume A. Analytical Properties of Silica - a Key for Understanding Silica Reinforcement. Paper No. 73 presented at a meeting of ACS, Rubber Division, Chicago, IL, 1999.
- Blow CM. Rubber Technology and Manufacture, Butterworths, London, 1971.
- Boyce M, Sheng N, Parks D. Micro/Nanoscale Modeling of Anisotropic Mechanical Properties of Polymer Nano-Clay Composites. Polymeric Materials Sci. and Eng. 2002; 86, 425-426.
- Bridgestone environmental report, Tokyo, Japan, Bridgestone 2002; 14: 12.

REFERENCES

- Brinke AT. Silica Reinforced Tyre Rubbers, mechanistic aspects of the role of coupling agents. University of Twente, Ph.D. Thesis, 2002.
- Carrado KA. Synthetic organo-and polymer-clays: preparation, characterization and materials applications. Appl. Clay Sci. 2000; 17: 1–23.
- Carrado K. Polymer-Clay Nanocomposites. Advanced Polymeric Materials. Shonaike G, and Advani S (Eds). CRC Press. Boca Raton. 2003; 349-396.
- Chen G, Chen X, Lin Z, Ye W, Yao K. Preparation and Properties of PMMA/Clay Nanocomposite, J. Mat. Sci. 1999; Letters, 18: 1761-1763.
- Clark SK. Mechanics of Pneumatic Tires, Office of Vehicle Systems Research, Institute for Applied Technology and National Bureau of Standards, Washington, 1971; 596–597.
- Costa FR, Goad MH, Wagenknecht U, Heinrich G. Layered double hydroxides: noble materials for the development of multi-functional nanohybrids Polymer. 2005; 46: 4447.
- Das A, Jurk R, Stöckelhuber KW, Engelhardt T, Fritzsche J, Klüppel M. Nanoalloy based on clays: intercalated-exfoliated layered silicate in high performance elastomer. J. Macromol. Sci. Pure Appl. Chem. 2008; 45:144–50.
- Dick J (Ed.), Rubber Technology Compounding and Testing Performance, Hanser Gardner Publications, 2001.
- Donnet JB, Bansal R, Wang MJ (Eds.). Carbon Black Science and Technology, Marcel Dekker, Inc. New York, 1993.
- Ebbott TG, Hohman RL, Jeusette JP, Kerchman V. Tire temperature and rolling resistance prediction with finite element analysis. Tire Sci. Technol. 1999; 27:2–21.
- Eitzman D, Melkote R, Cussler E. Barrier Membranes with Tipped Impermeable Flakes. AIChE Journal. 1996; 42:2-9.
- Fro¨hlich J, Niedermeier W, Luginsland HD. The effect of filler–filler and filler–elastomer interaction on rubber reinforcement. Composites: Part A. 2005; 36 : 449–460.
- Frogley MD, Ravich D, Wagner HD. Mechanical properties of carbon nanoparticle-reinforced elastomers. Compos. Sci. Technol. 2003; 63:1647–54.
- Freund B, Niedermeier W. Novel Rubber nanocomposite with Adaptable Mechanical properties, Kautsch. Gummi Kunstst. 1998; 51: 444.

REFERENCES

- Fu X. Synthesis and characterization of polymer-layered silicate nanocomposites. Case Western Reserve University, Ph.D. Thesis, 2001.
- Fu X, Qutubuddin S. Synthesis of polystyrene-clay nanocomposites. Mater. Lett. 2000; 42: 12-15.
- Ganter M, Gronski W, Semke H, Zlig T, Thomann C, Muhlhaupt R. Surface-Compatibilized Layered Silicates. A Novel Class of Nanofillers for Rubbers with Improved Mechanical Properties. Kautsch. Gummi Kunstst. 2001; 54**:** 166-171.
- Ganter M, Gronski W, Reichert P, Muhlhaupt R. Rubber Nanocomposite: Morphology and Mechanical Properties of BR and SBR Vulcanizates Reiforced by Organophilic Layered Silicates. Rubber Chem. Technol. 2001; 74**:**221-235.
- Gehman SD. Material characteristics in mechanics of pneumatic tires. S.K. Clark (Ed.), Mechanics of Pneumatic Tires, Office of Vehicle Systems Research, Institute for Applied Technology and National Bureau of Standards, US Department of Commerce, Washington, 1971: 1–40.
- Ghosh S, Sengupta RA, and Henrich G. High performance nanocomposite based on organoclay and blends of different types of SBR with BR. Kautsch. Gummi Kunstst. 2011; 48-54.
- Ghosh S, Sengupta RA, and Henrich G. Investigations on Rolling Resistance of Nanocomposite based Passenger Car Radial Tyre Tread Compounds using Simulation Technique. Tire Sci. Technol. 2011 (DOI).
- Giannelis E. Polymer Layered Silicate Nanocomposites. Adv. Mater. 1996; 8: 29-35.
- Glaeser K-P (Dr.- Ing). Rolling resistance of Tyre on Road Surface-procedure to measure Tyre Rolling Resistance. Federal Highway Research Institute; Energy Efficient Tires, IEA, Paris, 15.Nov.-16.Nov. 2005.
- Grosch KA, The Rolling Resistance, Wear and Traction Properties of Tread Compounds.Rubber Chem. Technol. 1996: 69:495.
- Hasegawa N, Okamoto H, Usuki A. Preparation and properties of ethylene propylene rubber (EPR)-clay nanocomposites based on maleic anhydride-modified EPR and organophilic clay. J. Appl. Polym. Sci. 2004; 93:758–764.
- Hofmann W. Rubber Technology Handbook. Hanser/Gardner, Munich, 1996.

REFERENCES

- Huber G, Vilgis TA. Universal Properties of filled rubbers, Mechanism for reinforcement on different length scales. Kautsch. Gummi Kunstst. 1999; 52:102-107.
- Jia QX, Wu YP, Xiang P, Ye X, Wang YQ, Zhang LQ. Combined effect of nano-clay and nano-carbon black on properties of NR nanocomposites. Polym. Compos. 2005;13:709–19.
- Joly S, Garnaud G, Ollitrault R, Bokobza L, Mark J. Organically Modified Layered Silicates as Reinforcing Fillers for Natural Rubber. Chem. Mater. 2002; 14: 4202-4208.
- Kim J, Oh T, Lee D. Preparation and characteristics of nitrile rubber (NBR) nanocomposites based on organophilic layered clay. Polym. Int. 2003; 52: 1058.
- Kim W, Kim SK, Kang JH, Cheo Y, Chang YW. Structure and properties of the organoclay filled NR/BR nanocomposites. Macromol. Res. 2006;14:187–193.
- Kojima Y, Fukumori K, Usuki A, Okada A, Kurauchi T. Gas Permeabilities in Rubber-Clay Hybrid. J. Mater. Sci. Lett. 1993:12, 889-890.
- Kobayashi Y, Fukuda M, Takagi A, Kanetsuki M, Matsuzawa F, Kabe K. Technique for Estimating Tire Rolling Resistance Using Finite Element Method. SAE, Japan, 1987:No. 35:140-146.
- Konishi Y, Cakmak M. Nanoparticle induced network self-assembly in polymer–carbon black composites. Polymer 2006;47: 5371–91.
- Kumar C, Karger-Kocsis J. Curing and Mechanical Behavior of Carboxilated NBR Containing Hygrothermally Decomposed Polyurethane. Eur. Polym. J. 2002; 38, 2231-2237.
- Lange H (Dr.). Consumer can safely save. Continental AG, 2011. www.conti-online.com
- Lan T, Pinnavaia TJ, Clay Reinforced Epoxy Nanocomposites. Chem. Mater. 1994; 6:2216-2219.
- Lopez-Manchado M, Arroyo M, Herrero B, Biagiotti J. Vulcanization Kinetics of Natural Rubber-Organoclay nanocomposites. J. Appl. Polym. Sci. 2003; 89:1-15.
- Lou AYC. Relationship of Tire Rolling Resistance to the Viscoelastic Properties of the Tread Rubber, Tire Sci. Technol. 1978; 6 (3) :176-188.
- Luchini JR, Peters JM, Arthur RH. Tire Rolling Computation with the Finite EIement Method. Tire Sci. Technol. 1994; 22(4):206-222.

REFERENCES

- Magaraphan R, Thaijaroen W. Lim-Ochakun R. Structure and Properties of Natural Rubber and Modified Montmorillonite Nanocomposites. Rubber Chem. Technol. 2003; 76:406-418.
- Mark JE. Science and Technology of Rubber. Academic Press, San Diego, 1994.
- Medalia A. Morphology of aggregates: Effective volume of aggregates of carbon black from electron microscopy; Application to vehicle absorption and to die swell of filled rubber, J. Colloid. Interface Sci. 1971; 36:173-190.
- Meneghetti PC. Synthesis and Properties of Rubber-Clay nanocomposites. Ph.D thesis, Case Western Reserve University, 2005.
- Messersmith PB, Giannelis EP. Synthesis and Characterization of Layer Silicate-Epoxy Nanocomposites. Chem. Mater., 1996; 6**:** 1719-1725.
- Mingyi L, Zang W, Shan W, Zhang YJ. Structure and properties of polybutadiene/ montmorillonite nanocomposites prepared by in situpolymerization. Appl Polym Sci 2006; 99:3615–21.
- Mousa A, Karger-Kocsis J. Rheological and Thermodynamical Behavior of Styrene/Butadiene Rubber-Organoclay Nanocomposites. Macromol. Mater. Eng., 2001; 286: 260-266.
- Nakajimi Y, Kadowaki H, Kamegawa T, Abe A, New tire design procedure based on optimization technique. 1966; SAE paper No.960997.
- Nah C, Ryu HJ, Kim WD, Chang YW. Preparation and properties of acrylonitrile butadiene copolymer hybrid nanocomposites with organoclays, Polym. Int'l. 2003:52**:**1359–1364.
- Nielsen L. Models for the Permeability of Filled Polymer Systems. J. Macromol. Sci., Chem. 1967; A1**:**929-941.
- Okamoto M, Morita S, Taguchi H, Kim, YH, Kotaka T. Tateyama H. Synthesis and Structure of Smetic Clay/Poly(Methyl Methacrylate) and Clay/Polystyrene Nanocomposite via in situ Intercalative Polymerization. Polymer. 2000; 41:3887-3890.
- Payne AR, Kraus G (Ed). Reinforcement of Elastomers. Interscience Publishers, New York, 1965.
- Payne AR, Whittaker R. Low strain dynamic properties of filled rubbers. Rubber Chem. Technol. 1971; 44: 440-478.

- Payne AR, Whittaker R. Low strain dynamic properties of filled rubbers. Rubber Chem. Technol. 1971; 44: 440-478.
- Park HC, Youn SK. Song TS, Kim NJ. Analysis of Temperature Distribution in a Rolling Tire Due to Strain Energy Dissipation. Tire Sci. Technol. 1997; 25(3) :214-228.
- Pillai PS, Fielding-Russell GS. Tire rolling resistance from whole tire hysteresis ratio", Rubber Chem. Technol.1992; 65(2) :444-452.
- Plueddemann EP. Silane coupling agents. Plenum Press, New york, 1991.
- Qutubuddin S, Fu X. Polymer-Clay Nanocomposites: Synthesis and Properties. Nano-Surface Chemistry, Rosoff M (Ed.), Marcel Dekker, 2001; 653-673.
- Ray S, Okamoto M. Polymer/layered silicate nanocomposites: a review from preparation to processing. Prog. Polym. Sci. 2003; 28:1539-1641.
- Sadhu S, Bhowmick A. Effect of Chain Length of Amine and Nature and Loading of Clay on Styrene-Butadiene Rubber-Clay Nanocomposites. Rubber Chemistry and Technology. 2003; 76: 860-875.
- Schon F, Thomann R, Gronski W. Shear Conntrolled Morphology of Rubber/Organoclay Nanocomposite and Dynamic Mechanical Analysis. Macromol. Symp. 2002; 189:105-110.
- Schon F, Gronski W, Filler Networking of Silica and Organoclay in Rubber Composites: Reinforcement and Dynamic-Mechanical Properties. Kautsch. Gummi Kunstst. 2003; 56166-171.
- Shia D, Hui C, Burnside S, Giannelis E. An Interface Model for the Prediction of Young's Modulus of Layered Silicate-Elastomer Nanocomposites. Polymer Composites, 1998; 19: 608-617.
- Shida Z, Koishi M, Kogure T, Kabe K. A Rolling Resistance Simulation of Tires Using Static Finite Element Analysis. Tire Sci. Technol.1999; 27(2) :84-105.
- Shah RK, Kim DH, Paul DR. Morphology and properties of nanocomposites formed from ethylene/methacrylic acid copolymers and organoclays. Polymer, 2007; 48: 1047-1057.
- Stöckelhuber KW, Das A, Jurk R, Heinrich G. Contribution of physico-chemical properties of interfaces on dispersibility, adhesion and flocculation of filler particles in rubber. Polymer. 2010; 51:1954-1963.

- Stretz HA, Paul DR, Li R, Keskkula H, Cassidy PE. Intercalation and exfoliation relationships in melt-processed poly (styrene-co acrylonitrile)/montmorillonite nanocomposites. Polymer, 2005; 46: 2621-2637.
- Theng BKG. Formation and properties of clay-polymer complexes. Elsevier, New York, 1979.
- Theng BKG. The Chemistry of Clays-Organic Reactions. Wiley, New York, 1974.
- Tire Analysis.195/65R15-Ecofriendly, Energy Saving passenger tire-European Tire Analysis Report.2009-1; Smithers Scientific Services, Inc. Akron, Ohio, USA.
- Tire Analysis. 175/65R14 82T-PCR for emerging growth market report 2004-1. Smithers Scientific Services, Inc. Akron, Ohio, USA.
- Tire Analysis. 295/80R22.5-TBR for emerging growth market report.2008-1; Smithers Scientific Services, Inc. Akron, Ohio, USA.
- Tire Analysis, 10.00R20-TBR for emerging growth markets report 2001; Smithers Scientific Services, Inc. Akron, Ohio, USA.
- Tyres-online: The Benefits of Silica in Tyre Design-A Revolution in Tyre Technology. www.tires-online.co.uk/technology/silica.asp
- Usuki A, Kawasumi M, Kojima Y, Okada A, Fukushima Y, Kurachi T, Kamigaito O. Synthesis of Nylon 6-Clay Hybrid. J. Mater. Res. 1993; 8(5):1179-1184.
- Usuki A, Kawasumi M, Kojima Y, Okada A, Kurauchi T, Kamigaito O. Swelling behavior of montmorillonite cation exchanged for ω-amino acids by ε-caprolactam, J. Mater. Res. 1993; 8:1174–1178.
- Usuki A, Tukigase M. Preparation and properties of EPDM-clay hybrids. Polymer, 2002; 43:2185-2189.
- Van AG. Diffusion in Elastomers. Rubber Chem. Technol. 1964; 37: 1065-1152.
- Varghese S, Karger-Kocsis J. Natural rubber-based nanocomposites by latex compounding with layered silicates. Polymer, 2003; 44: 4921-4927.
- Varghese S, Karger-Kocsis J. Melt-Compounded Natural Rubber Nanocomposites with Pristine and Organophilic Layered Silicates of Natural and Synthetic Origin. J. Appl. Polym. Sci. 2004; 91: 813-819.

- Vaia RA, Ishii H, Giannelis EP. Synthesis and Properties of Two Dimensional Nanostructures by Direct Intercalation of Polymer Melts in Layered Silicates. Chem. Mater., 1993; 5**:**1694-1696.
- Vaia R, Sauer B, Tse OK, Giannelis E. Relaxation of Confined Chains in Polymer Nanocomposites: Glass Transition Properties of Poly(ethylene oxide) Intercalated in Montmorillonite. J. Polym. Sci. Phys. Ed. 1997; 35**:**59-67.
- Wang M-J. Effect of Polymer-Filler and Filler-Filler Interactions on Dynamic Properties of Filled Vulcanizates. Rubber Chem. Technol. 1998; 71:520-588.
- Wang MJ. The Role of Filler Networking in Dynamic Properties of Filler Rubber. Rubber Chem. Technol. 1999; 72:430-448.
- Wang Y, Zhang, Tang C, Yu D. Preparation and Characterization of Rubber-Clay Nanocomposites. J. Appl. Polym. Sci. 2000; 78: 1879-1883.
- Wang SH, Peng Z. Zhang L, Zhang YX. Structure and properties of BR/organomontmorillonite nano composites, Symposium of International Rubber Conference 2004, Beijing, China, Volume B: 257–263.
- Wang YQ, Zhang HF, Wu YP, Wang J, Zhang LQ. Structure and properties of strain crystallized rubber-clay nanocomposites by co-coagulating the rubber latex and clay aqueous suspension, Symposium of International Rubber Conference, Beijing, China. 2004; Volume B: 420–425.
- Warholic TC. Tire Rolling Loss Prediction from the Finite Element Analysis of a Statically Loaded Tire. M.S.E. Thesis, 1987: University of Akron.
- Willett PR, Hysteresis loss in rolling tire. Rubber Chem. Technol. 1973; 45:425.
- Willett PR. Variation of tire hysteretic loss due to tire design. Rubber Chem. Technol. 1974; 47:118.
- White JL. Rubber Processing: technology, materials, and principles. Hanser, Munich, 1995.
- Wolff S, Wang M-J. Physical properties of vulcanizate and shift factors," Kautsch. Gummi Kunstst. 1994; 47:17-25.
- Wu Y, Jia Q, Yu D, Zhang L. Structure and Properties of Nitrile Rubber (NBR)-clay nanocomposites by co-coagulating NBR latex and clay aqueous suspension. J. Appl. Polym. Sci. 2003; 89:3855-3858.

REFERENCES

- Xu, S. and Boyd S. Cationic Surfactant Adsorption by Swelling and Non swelling Layer Silicates. Langmuir. 1995;11:2508-2514.
- Yano K, Usuki A, Okada A. Synthesis and Properties of Polyimide-clay Hybrid Films. J. Polym. Sci. A: Polym. Chem. 1997; 35**:**2289-2294.
- Zanzig D J, Sandstrom PH, Crawford MJ, Verthe JJA, Losey CA. Silica Reinforced Tyre Rubbers. The Goodyear Tire & Rubber Company.1994.
- Zhang L, Wang Y, Wang Y, Sui Y, Yu D. Morphology and Mechanical Properties of Clay/Styrene Butadiene Rubber Nanocomposites, J. Appl. Polym. Sci. 2000; 78:1873-1878.
- Zheng H, Zhang Y, Peng Z, Zhang Y. Influence of the clay modification and compatibilizer on the structure and mechanical properties of ethylene-propylene-diene rubber/montmorillonite composites. J. Appl. Polym. Sci. 2004; 92:638–646.
- Zidelkheir B, Abdelgoad M, Effect of surfactant agent upon the structure of montmorillonite X-ray diffraction and thermal analysis. J. Therm. Anal. Calorimetry, 2008; 94: 181-187.